June 2014

STRATIGRAPHIC FRAMEWORK AND QUATERNARY PALEOLIMNOLOGY OF THE LAKE TURKANA RIFT, KENYA

Amy Morrissey
Syracuse University

Dissertation abstract

Lake sediments are some of the best archives of continental climate change, particularly in the tropics. This study is focused on three ~10m sediment cores and high-resolution seismic reflection data from Lake Turkana in northern Kenya. Lake Turkana is the world's largest desert lake and the largest lake in the Eastern Branch of the East African Rift System. It is situated at ~2 °N at 360 m elevation and is ~250 km long and ~30 km wide with a mean depth of 35 m. The lake surface receives less than 200 mm yr^{-1} of rainfall during the twice-annual passing of the Intertropical Convergence Zone via Indian Ocean-derived moisture, and evaporation is >2300 mm yr^{-1}. This study is the first to quantify the climate and deepwater limnologic changes that have occurred in the area during the African Humid Period (AHP) and since the Last Glacial Maximum.

A 20-kyr, multiproxy lake level history was derived from ~1100 km of CHIRP seismic reflection data, in conjunction with gamma ray bulk density, magnetic susceptibility, total organic carbon, total inorganic carbon, core lithology, and scanning XRF data from sediment cores that were chronologically constrained by radiocarbon dates. Two desiccation events occurred at 18.5 and 17 ka when the lake was at least 100 m lower than today, as evidenced by basin-wide, high-amplitude reflections correlated to sand intervals in the sediment cores. Lake level rose abruptly at ~11 ka as interpreted from an increase in organic carbon content and abrupt shift to silt and clay-sized sediment, after which Lake Turkana overflowed into the White Nile River System. AHP highstand conditions lasted until ~5 ka when the lake became a closed basin. The loss of Lake Turkana as a White Nile input likely had significant implications for nascent communities living along the Nile. Lake level has fluctuated but remained at a moderate lowstand since its mid-Holocene closure.

An easterly shift of moisture derived from the Congo Basin has been proposed as an additional moisture source for environments in East Africa during the AHP, as evidenced by an expanding number of hydrogen isotope records from lake basins in East Africa. To determine if Atlantic-derived moisture reached Lake Turkana in the past via the Congo Basin, compound specific (C_{28} *n*-alkanoic acids) hydrogen isotopes (δD_{wax}) were measured from the composite sediment core record from Lake Turkana.

The record revealed that δD_{wax} values were depleted by more than -60‰ during the AHP. δD_{wax} depletion occurs abruptly at 13.7 ka and is sustained throughout the AHP, and values gradually become more enriched after 7 ka. This depletion suggests that Congo-derived moisture had a significant influence on Turkana precipitation during the AHP, but depletion of that magnitude cannot be explained solely by a change in moisture source. In addition to the source effect, a possible vegetation effect was quantified using stable carbon isotopes of leaf waxes, and the amount effect was estimated using modern Kenyan amount effect coupled with a published basin fill model. It was determined that vegetation can account for up to -17‰, and amount effect estimations range from -17‰ to - 24‰ of the total AHP depletion. After accounting for these effects, precipitation during the AHP is depleted relative to a 100% increase in precipitation amount, which we suggest is driven by an influx of moisture derived from the Congo Basin. Our calculations suggest that at least 45% of the moisture supplied during the AHP was Congo-derived.

The precipitation-evaporation balance of a lake system is closely related to its heat budget. To quantify changes in temperature through the onset and termination of the AHP, the paleotemperature proxy called TEX_{86} was used to generate a 14-kyr record of lake

surface temperatures for Lake Turkana. This proxy has successfully reconstructed regional and high-latitude paleotemperatures in other large African lakes.

TEX_{86} temperatures from 14 to 0.4 ka are highly variable and range from 24.3 °C to 28.6 °C with a mean of 25.9 °C. There is a long-term trend within the temperature record that follows mean northern hemisphere peak summer insolation, and a mean temperature of 26.2 °C during the early Holocene decreases to 25.7 °C during the late Holocene. A century-scale fluctuation of ~1 °C persists throughout most of the record which appears to be related to lake mixing processes that overprint the regional climate signal based on fluctuations in metal ratios. While this reduced sensitivity of the TEX_{86} proxy was an unexpected result from this analysis, it has shown that this proxy may have limitations in its application to well-mixed, tropical, arid-land lake systems. Despite high-frequency variation, TEX_{86} temperatures remain close to the mean for the duration of the record, which is attributed to the evaporation response of this lake system.

STRATIGRAPHIC FRAMEWORK AND QUATERNARY PALEOLIMNOLOGY OF THE LAKE TURKANA RIFT, KENYA

by

Amy Morrissey

B.S., 2009, Geological Sciences University of Missouri, Columbia, Missouri
B.A., 2009, Anthropology University of Missouri, Columbia, Missouri

DISSERTATION

Submitted in partial fulfillment of the requirements for the degree of Doctor of Philosophy in Earth Sciences

Syracuse University
June 2014

Acknowledgements

This work could not have been accomplished without the support and guidance of Chris Scholz, my advisor, to whom I am grateful for bringing me to this program and encouraging me to stick around for a few extra years to see what else I could learn about Lake Turkana. I also appreciate the guidance from and accommodation by Jim Russell and Bruce Wilkinson and the rest of my committee.

I would like to thank my parents and my sister for being patient and supportive from halfway across the country, and Joe from halfway across the Pacific Ocean. I would like to thank Pete and Jacki, both of whom have been nothing but helpful for the last five years. The rest of the members of the Department of Earth Sciences have also played necessary roles in my completion of this degree.

Most of all I want to thank the friends that I have made while being in Syracuse. They have acted as my family and have encouraged me without obligation throughout this entire process. Alina, Aaron, Joe, Melissa, Jen, Matt, AnneMarie, and Ed, I truly cannot thank you enough.

Table of Contents

List of Figures:

CHAPTER 1:

CHAPTER 2:

CHAPTER 3:

List of Tables

CHAPTER 1:

CHAPTER 2:

CHAPTER 3:

Preface

East Africa is one of the most climatically diverse regions in the world. The influence of moisture sources and precipitation delivery systems have shifted through time due to changes in orbital parameters and the accompanying climatic feedbacks. Lake Turkana is a unique study area in that it is at one of the lowest inland elevations on the African continent. Its degree of aridity results in quick changes in precipitation and temperature. Lake Turkana is also part of the Nile River drainage when the lake is at highstand, and likely played an important role in both historic and prehistoric times for nascent communities and animal populations in the Nile Valley.

This project was designed to determine timing of transitions between humid versus arid climates in the late Quaternary of East Africa as well as changes in temperature as derived from the sediment record and proxies generated therein. The work was divided into three parts:

Chapter 1: Stratigraphic framework and lake level change in Lake Turkana over the last 20 ka. This chapter set the groundwork and sedimentological basis for the rest of the project. Seismic sequences were developed and analyzed in conjunction with Kullenberg sediment cores to develop a lake level history and general climatic context for Lake Turkana since the Last Glacial Maximum.

Published as: Morrissey, A. and Scholz, C.A., 2014, Paleohydrology of Lake Turkana and its influence on the Nile River system: Palaeogeography, Palaeoclimatology, Palaeogeography, v. 403, p. 88-100.

Chapter 2: Paleoprecipitation analysis as derived from compound-specific hydrogen isotopes of leaf waxes through the African Humid Period. A δD_{wax} record was generated from sediment cores to determine both amount and sources changes in precipitation through time.

> *To be submitted as:* Morrissey, A., Scholz, C.A. and Russell, J.M., Late Quaternary atmospheric circulation over the Turkana Rift, East Africa to *Earth and Planetary Science Letters.*

Chapter 3: Temperature variation was analyzed using a high-level organic carbon lake surface paleotemperature proxy called TEX_{86}. Lake surface temperature is sensitive to the ambient air temperature and changes in relative humidity. This record gives insight into local temperature shifts in response to insolation and atmospheric changes over time.

> *To be submitted as:* Morrissey, A., Scholz, C.A., and Russell, J.M., TEX_{86} paleotemperature proxy application at the world's largest desert lake, Lake Turkana, Kenya to the appropriate journal.

Chapter 1:

Paleohydrology of Lake Turkana and its influence on the Nile River System

Amy Morrissey[1,*] and Christopher A. Scholz[1]

[1]Department of Earth Sciences, Syracuse University, Syracuse, New York, 13244, USA

*corresponding author: Amy Morrissey, Dept. of Earth Sciences, Syracuse University, 204 Heroy Geology Laboratory, Syracuse, New York, 13244, USA, +1-315-443-4334, E-mail address: amorriss@syr.edu

Abstract

The detailed paleohydrological record of Lake Turkana, the largest lake in the eastern branch of the East African Rift, is necessary for determining the connectivity between adjacent watersheds in tropical Africa. The migration of both the Intertropical Convergence Zone (ITCZ) and the Congo Air Boundary (CAB) constrain rainfall amount and duration for most of East Africa. Lake Turkana, in northern Kenya, is the world's largest desert lake and experiences two ITCZ-associated rainy seasons annually, with cumulative rainfall of ~200 mm/yr. Evidence from new continuous, high-fidelity sediment core records and high-resolution CHIRP seismic reflection data suggests Lake Turkana received enough rainfall during the African Humid Period (AHP) to fill the lake to its sill (100 m above current lake level) and spilled over into the White Nile River system. An atmospheric configuration with an eastward-shifted CAB over the Turkana region and the northern Kenya Rift is invoked as an additional source of rainfall for the catchment. This configuration began abruptly at ~11 ka and lasted until ~5 ka when Lake Turkana became a closed basin and was cut off from the White Nile. Prior to the AHP, Lake Turkana

experienced at least two desiccation events following the Last Glacial Maximum at 18.5 and 17 ka when the lake was at least 100 m lower than modern, as evidenced by basin-wide, high-amplitude reflections and ^{14}C-dated shallow water facies in sediment cores. Lake level fluctuations generally follow trends in mean solar insolation, however the onset of lake level extremes are much more abrupt than rates of insolation change. Lake Turkana's location in relation to atmospheric convergence and dynamic rainfall patterns makes it susceptible to extreme climate change over relatively short timescales.

1 Introduction

Solar insolation change and the Intertropical Convergence Zone (ITCZ) migration are commonly invoked as causes for changes in amount and geographical distribution of rainfall in tropical climate on orbital timescales (Trauth et al., 2001). More abrupt climate shifts may be associated with sea surface temperature (SST) variability and vegetation feedbacks (deMenocal et al., 2000; Camberlin et al., 2001; Castañeda et al., 2009; Verschuren et al., 2009; Tierney et al., 2009, 2011a, 2011b, 2013). These different influences are more or less important depending on the geography and the latitudinal position of a study area (Fig. 1). This study presents multiproxy paleoclimate data from Lake Turkana, the world's largest desert lake and an area that until now contributed only limited information from continuous offshore records on the late Quaternary climate history of tropical Africa. Data presented here constrain high and low lake level extremes associated with changes in the ITCZ and SSTs through time in the Turkana region, and provide insight into African paleoclimate patterns and atmospheric circulation since the Last Glacial Maximum (LGM).

This study extends and refines the record of climate variability and lake level change in the Turkana catchment of tropical East Africa to at least 20 ka. Lake Turkana's extreme desert environment, limited outcrops, and rapid sedimentation rates limited the length and fidelity of late Quaternary paleolimnologic records in past studies (e.g. Butzer et al., 1972; Owen et al., 1982; Halfman and Johnson, 1988; Halfman et al., 1992, 1994; Ricketts and Johnson, 1996; Garcin et al., 2012). The continuous deepwater sediment core and high-resolution seismic records presented here provide a more detailed paleohydrologic record of the Turkana basin that extends further back in time than previous studies (Fig. 2).

The aridity established in parts of East Africa during peak glaciation (Gasse, 2000) continued intermittently through the latest Pleistocene until it slowly gave way to a wetter environment beginning ~12 ka BP. More favorable conditions lasted until the mid-Holocene. This interval when moist conditions prevailed in much of northern hemisphere tropical Africa is commonly referred to as the African Humid Period (AHP)(e.g. Ritchie et al., 1985; deMenocal et al., 2000; Castañeda et al., 2009). This study demonstrates that Lake Turkana experienced more humid conditions and a higher lake level for several thousand years during the AHP, and it provides new constraints on the timing and rates of onset and demise of this climatic optimum.

The watersheds of large lakes commonly span several degrees of latitude, and accordingly, long-term lake level records integrate climate processes across space. Thus, the impact of hydrological connectivity of climate-sensitive lake basins between adjacent watersheds through time is not always taken into consideration in paleoclimate reconstructions. Rainfall throughout East Africa is associated with the migration of enhanced equatorial convection (the ITCZ) that moves several degrees of latitude both north and south of the equator on both seasonal (Fig. 1) and longer timescales. Changes in evaporation associated with vegetation cover and catchment size can exacerbate or inhibit lake level changes during periods of aridity and high humidity (Castañeda et al., 2009; Lyons et al., 2011). Reconstructed water level records from lakes across the region display consequential, sometimes drastic, lake level fluctuations over just a few centuries (Lamb et al., 2007; Garcin et al., 2009; Verschuren et al., 2009; Lyons et al., 2011), leading to opening and closing of adjacent lake systems.

The amount and distribution of water across the African continent controls the dispersal of human populations (Gasse, 2000). Overflow conditions for Lake Turkana provide an additional input into the Nile system (Hopson, 1982; Johnson et al., 1987), which affected the annual flow dynamics of the Nile and likely impacted nascent communities living near the river in the mid- to late-Holocene. The hydrologic closure of Lake Turkana into the Nile River in the mid Holocene reduced Nile flow and likely had negative societal ramifications for groups of people living near the Nile River in Predynastic Egypt (Stanley et al., 2003; Williams et al., 2006; Williams, 2009). The Nile River played a critical role in sustaining human communities of northeast Africa for thousands of years and continues to do so today (Butzer, 1976; Nicoll, 2001; Stanley et al., 2003; Williams, 2009). The loss of Lake Turkana outflow and associated aridification of the Nile region likely promoted the consolidation of groups along the Nile River, which led to land cultivation and planned irrigation.

Here we focus on the paleoclimatological factors that impact lake level change in Lake Turkana by analyzing changes in lithology in sediment cores along with correlative high-resolution seismic sequences that provide a detailed record of deepwater lake deposits that have accumulated since the LGM. The objective of this paper is to present a global climate context for a 20 ka paleoclimate record from Lake Turkana in northern Kenya and describe its role in East African hydrology. This continuous record provides a new perspective on Turkana paleoclimate since the LGM that has not yet been discussed in a context of paleohydrological connectivity and associated changes over time.

2 Study area

Lake Turkana is the largest lake in the Eastern Branch of the East African Rift System at 250 km long, ~30 km wide, and with a maximum depth of ~120 m (Fig. 1). It is situated between 2.3° and 4.6° N latitude in the northern Kenya Rift within a depression between the Kenyan and Ethiopian Highlands. The entire water column is well mixed because the mean lake depth is only ~30 m and the area experiences pervasive unidirectional winds from the north with an average speed of 11 ms^{-1} (Lake Turkana Wind Power, 2012), and diurnal winds from the southeast in the South Basin (Hopson, 1982). The lake is slightly saline (2.5 ppt) and mildly alkaline (pH = 9.2)(Yuretich and Cerling, 1983). The Omo River drains the southern part of the Ethiopian highlands (Fig. 1) and provides the lake with 80–90% of its water (Yuretich, 1979; Hopson, 1982;Yuretich and Cerling, 1983). The Kerio and Turkwel Rivers and ephemeral, rainy-season streams provide additional hydrologic inputs.

The sedimentary subbasins of the lake are the result of extension on large half-graben fault systems (Fig. 3) associated with the north-south-striking continental rift (Dunkleman et al., 1988). The lake has three main bathymetric basins, each with volcanic islands near their centers. A broad shield volcano, referred to as “the Barrier” (Brown and Carmichael, 1971; Furman et al., 2004), dams the southernmost margin of the lake. Prior to the eruption of this edifice, Lake Turkana extended farther south into what is now the Suguta Valley (Champion, 1935; Dunkley et al., 1993). The former deep Lake Suguta (Fig. 1) is now the ephemeral Lake Logipi or Suguta Swamp (Garcin et al., 2009; Garcin et al., 2012). Much of the land surrounding the southern part of the lake is covered in intermediate-to-mafic-composition volcanic rocks ranging in age from Miocene to recent;

Teleki's volcano erupted just south of the lake in 1897 (Champion, 1935; Curtis, 1991; Karson and Curtis, 1994).

Past studies characterized sedimentation patterns across the lake as simple basin infill (Yuretich, 1979, 1986; Johnson et al., 1987). Sediment sources to the lake include detrital material from igneous cover and metamorphic basement rocks eroding within the catchment, as well as more limited lacustrine sedimentary rocks deposited during former lake level highstands (Yuretich, 1979, 1986). Authigenic carbonate precipitation is most prevalent in the South Basin, where the influence from the Omo River detrital sediment load is reduced (Yuretich, 1979, 1986; Halfman et al., 1989). Eolian sediment is transported by strong winds, especially in the South Basin. Biogenic material accumulates on the lake floor in the form of amorphous organic matter, diatoms, gastropods, and ostracodes (Hopson, 1982; Halfman et al., 1992). Stromatolites, other microbialites, and carbonate grainstones are present in outcrop adjacent to the southeastern shoreline of the South Basin (Abell et al., 1982; Owen et al., 1982; Hargrave et al., in press).

The lake is hydrologically closed, with the spill point 100 m above the modern lake surface (Garcin et al., 2012). Overfilling of the basin occurred as recently as ~4 ka BP (Halfman et al., 1992; Garcin et al., 2012). At highstand, Lake Turkana's watershed increased the Nile's drainage area by 162,000 km^2 (Fig. 1)(Garcin et al., 2009) by including the southern Ethiopian Highlands and part of the Kenyan Highlands in its catchment. The Nile River watershed presently drains most of northeast Africa north of ~4.5° N and east of ~25° E. Bodies of water within the watershed include Lakes Albert, Victoria, and Edward, which provide most of the river's baseflow due to high year-round rainfall near the equator (Fig. 1). The northern Ethiopian Highlands drain south into Lake Tana and north into the

Atbara River, both of which source the Blue Nile (Lamb et al., 2007; Williams, 2009; Blanchet et al., 2013) and support high flow of the Nile during rainy seasons.

This study focuses on data collected in the southernmost basin of Lake Turkana. The South Basin is an asymmetric half-graben with the main border fault zone on the western side of the basin (Fig. 3). The basement along the border fault is displaced over 1 km, creating a steep lake margin (slopes >35°) adjacent to hills and mountains of the western footwall, which are composed of Precambrian gneissic and schistic basement rock (Ochieng and Kagasi 1988; Dunkleman et al., 1988). The eastern, flexural margin of the basin exhibits a low-relief ramp margin (slopes <5°).

3 Materials and methods

3.1 Seismic methods

Over 1100 km of high-resolution Compressed High Intensity Radar Pulse (CHIRP) 2D seismic reflection data were collected in the South Basin using an EdgeTech 3100P acquisition system with Discover 3100 v 5.23 software. Seismic lines were acquired in an orthogonal grid with a ~2 km line spacing (Fig. 1). CHIRP data were acquired using a swept bandwidth of 4–24 kHz with a dominant frequency near 8 kHz and a sample rate of 0.023 s. The high frequency source yields data with centimeter-scale resolution. The ping rate of the system varies with water depth, but shot spacing is nominally 1 m with a record length of 125 ms. Typical subbottom penetration was ~35 m. A Trimble AgGPS 132 receiver was used to acquire navigation data at a sample rate of once per second. The seismic data were conditioned and processed using ProMAX 2D processing software, and fault and seismic stratigraphic interpretations were carried out using Landmark SeisWorks 2D software.

Additional seismic lines were acquired to extend imaging deeper into the subsurface. A 1 in^3 Bolt 600b airgun was used to acquire approximately 140 km of single-channel airgun seismic reflection data along lines that were coincident with CHIRP profiles (Fig. 1). A GeoAcoustics Geopulse receiver and a Chesapeake Technologies Incorporated SonarWiz 4 acquisition system were used for data collection. The depth of penetration of the airgun data is ~70 m, and data resolution is ~1 m.

3.2 Sediment core acquisition

The paleolimnology of Lake Turkana was reconstructed using data derived from three sediment cores (Figs. 1 and 4). Three cores were collected using a Kullenberg piston coring system. Piston cores, 4P, 14P, and 46P are 9.7, 8.5, and 10.6 m in length, and were recovered from 52, 58, and 56 m water depth, respectively. Both 46P and 4P were collected from the northeastern part of the south basin approximately 6 and 8 km from the current shoreline and 4 km apart (Fig. 1). Core 14P was collected ~28 km to the south of 4P and 4 km west of the current shoreline. During the collection of these cores, the Kullenberg system over penetrated the sediment-water interface; accordingly the piston cores do not preserve the youngest part of the sediment record. This was confirmed by mud on the weight stand after the cores were recovered from the water.

3.2.1 Physical properties and core descriptions

Non-invasive measurements of bulk density and magnetic susceptibility on whole cores were made at Brown University using a GEOTEK MSCL-S whole core scanner. Saturated bulk density from the Gamma Ray Attenuation Porosity Evaluator (GRAPE) and

magnetic susceptibility were recorded at a 1-cm interval. The lithologies of the cores were described immediately after splitting to avoid effects of oxidation and color fading (Figs. 2, 4, and 5).

3.2.2 Sediment Core Geochemistry

The cores were split and subsampled at 8-centimeter intervals. Discrete dry sediment samples were analyzed at Syracuse University for percent total organic carbon (TOC) content by elemental analysis using a COSTECH Elemental Analyzer. The total inorganic carbon (TIC) content was measured by coulometry using a UIC acidifier coupled with a Coulemetrics CO_2 coulometer (Fig. 2).

Scanning X-ray fluorescence for major element chemical analysis was carried out on archive-core halves using a molybdenum-sourced ITRAX scanner. Measurements were taken at a 0.5-centimeter interval at the Large Lakes Observatory at the University of Minnesota–Duluth (Fig. 2). Data was filtered to remove measurements with a mean standard error over 1.5% due to irregularities in core surface profile.

3.2.3 Geochronology Methods

Twenty-four AMS ^{14}C samples of bulk organic matter, bulk carbonate, plant material, or shells were dated to constrain the chronology of the three piston cores (Fig. 6 and Table 1). The flexible Bayesian age-depth program, "Bacon," (Blaauw and Christen, 2011) was used to construct the age models of all three cores. Within this model, the ages were calibrated using the IntCal09 calibration curve.

4 Results

4.1 Basin framework and late Quaternary sediment distribution

High-resolution seismic data show many intrabasinal normal faults across South Basin (Fig. 3) with offsets between 1 and ~8 m on shallow depositional surfaces and on the lake floor. Intrabasinal faults are both synthetic and antithetic to the east-dipping main basin border fault on the western side of the lake. Sediment accumulation patterns indicate growth faulting, with sediment accumulation rates much higher in the open basin and near the border fault compared to the eastern, flexural margin (Figs. 3 and 4). Conformable sedimentary sequences thicken to the west along the border fault. Sediment packages thin considerably and onlap in shallower water (~40 m) along the flexural margin. Many sediment packages along this margin are truncated due to erosion or non-deposition during low lake levels (Fig. 4). A sediment bypass zone exists along an area within 2–3 km of the eastern shore (Fig. 4). In much of this zone, sediment at the sediment-water interface is 5 ka in age or possibly older (geochronology and sequence boundaries discussed in results). Fine-grained sediments only accumulate more than 3 km to the west of the eastern shore, in water depths of ~55 m or more (Fig. 3).

4.2 Seismic stratigraphy and lithologic correlation

4.2.1 Seismic Sequences

The extensive CHIRP seismic data set helps to laterally extend events interpreted from sediment cores across the basin using subsurface stratal geometries. Significant seismic reflections (stratigraphic surfaces) were picked throughout the South Basin

dataset. Letters denote sequence names, and letters advance towards the recent. Sequences outlined below can be seen in Fig. 4 and Table 2.

Sequence A: T9, a high amplitude reflection, is the lower boundary for Sequence A and the lowermost widespread horizon in the CHIRP dataset, and serves as acoustic basement for the late Quaternary record (Fig. 4 and Table 2). T9 is observed on profiles on the eastern side of South Island and is absent in many of the seismic lines in the western part of the basin. The upper boundary of Sequence A is horizon T10, a high-amplitude, laterally continuous reflection present in most seismic lines. Sequence A onlaps along the eastern margin onto an older, high-amplitude reflection. Sequence A between T9 and T10 is characterized by a low-amplitude, nearly transparent package. T10 is relatively shallow on the flexural margin where the sedimentary sequences are condensed and onlap older coarse-grained shoreline deposits (Figs. 3 and 4). Sequence A was not sampled by any of the sediment cores.

Sequence B: Just above T10, a package of low amplitude reflections is present. This sequence lacks internal structure and is thin (< 250 cm) near the eastern shore but expands dramatically in a westerly direction, to a maximum of ~10 m. This package is truncated above by another high amplitude reflection, T11, that also onlaps older, nearshore deposits (Fig. 4). Sequence B was sampled in piston cores, which are described in a subsequent section.

Sequence C: The sequence above T11 is characterized by transparent, low-amplitude reflections that transition upward into higher amplitude, flat-lying reflections. A marker horizon, T11_1a, delineates this transition. This upper part of this sequence displays a reduced amplitude towards T11_1. Surface T11_1 is a subsequence boundary

based on a distinct change in spatial sediment depositional patterns. It is observed between Sequence C and the overlying sequence where sediment shifts from basin-wide deposition to focused deposition in deep water.

Sequence D: The seismic character of Sequence D displays a distinct amplitude and frequency character compared to underlying sequences. This uppermost sequence between T11_1 and T_12 is characterized by low amplitude, low frequency flat-lying reflections. An unconformity is observed within this sequence on several nearshore seismic lines (Fig. 7) and is marked by horizon T11_2. Surface T12 is the uppermost horizon picked and is observed near the top of core 4P, which is described below.

4.2.2 Additional seismic features

In the subsurface data, several progradational packages and distinct changes in slope of lakefloor and subsurface horizons are interpreted as paleodeltas (Fig. 8) or terraces. These features are paleoshoreline indicators that have been buried in the subsurface to depths of several meters. Two sets of these features are seen at two different subsurface depths. The sound source of the CHIRP data is not powerful enough to penetrate into these features, however, the airgun data penetrates into these deposits, and basinward prograding clinoforms are readily observed (Fig. 8). The exact time of formation is not available, but they are associated with lowstands of Lake Turkana before the onset of the AHP and probably developed between 17 and 15 ka.

4.3 Geochronology

The 24 AMS ^{14}C samples from the three cores (Fig. 6 and Table 1) range in age from 19,700 to 860 yr BP. Core 46P is the oldest recovered record and is dated from 19,700 to 5,870 yr BP constrained by 13 AMS ^{14}C dates. Core 14P is 13,480 yr BP at the base and 380 yr BP at the top, based on 6 AMS ^{14}C dates from organic-rich mud. Core 4P is constrained by 4 AMS ^{14}C dates, and has ages of 860 yr BP at the top and 3,730 yr BP at the base. Radiocarbon dates are not corrected for a reservoir effect. The new radiocarbon data reveal similar results for the different materials dated including macrophytes, bulk organic matter or bulk inorganic carbon (Table 1, Fig. 6). We acknowledge that Junginger et al. (2014) established a reservoir effect for Lake Suguta, adjacent to Lake Turkana, however this approach is consistent with other ^{14}C studies from Lake Turkana (e.g. Owen et al., 1982; Halfman and Johnson, 1988; Berke et al., 2012b; Garcin et al., 2012), which do not normalize for reservoir effect in their age models, as old carbon sources in the catchment are relatively minor. Using a radiocarbon date from a living snail, Garcin et al. (2012) determined that the present-day reservoir effect is negligible (~10 yr).

4.4 Core lithostratigraphy, geochemistry, and correlation

The three sediment cores, 46P, 14P, and 4P were correlated using multiple proxies in order to generate a composite paleolimnological record from 20 ka BP to present. Cores 46P and 4P comprise most of the composite record, however a ~1.2 kyr time gap exists between the two cores, and core 14P is used to bridge the time gap, as it overlaps the top of 46P and the base of 4P (Figs. 4 and 5). Both organic and inorganic carbon, XRF-derived Ca counts, magnetic susceptibility, and radiocarbon ages were used for correlation between the three cores used in this study (Fig. 5). The composite record is separated into

sedimentary units. The core lithologies, geochemistry, and geophysical properties are described starting from the bottom of the composite record (Fig. 2).

Unit 1 (19–14 ka): The base of the unit is the oldest sediment analyzed; it is composed of carbonate-rich, green mud interspersed with black sand grains and diatoms and sand lenses spaced 15–20 cm apart (Fig. 2). TIC content ranges from ~0 to ~7% with an average of 1.1 ± 1%, while the TOC ranges from ~1 to ~6%.

Unit 2 (14–11 ka): Sediment is light brown-green mud and lacks laminations or clear bedding. TOC increases up section from ~1 to ~3% and TIC is high but variable with values of 2–4 % (Fig. 2).

Unit 3 (11–4.5 ka): This unit is made up of dark green-gray diatomaceous mud with rare light green laminations that are 3–5 mm thick and occur every 10–15 cm (Fig. 2). TOC values up to 6% are observed with abundant diatoms and extremely low values of TIC (0.3% or less). There is no evidence for bioturbation and little lithologic variation within this unit.

Unit 4 (4.5 – 0.7 ka): This unit is composed of diatomaceous green-brown mud with fine sand intervals with some bedding present (Fig. 2). TIC values for this unit have an average value of 1.9 ± 0.4%, whereas total organic carbon has an average of 1.1 ± 0.3%. TIC and TOC covary within this unit. Scanning XRF elemental analyses show that downcore Ca counts closely track the changes in percent TIC. There are no extremely high or low excursions in any of the proxies measured in this interval. The record is continuous, with no obvious unconformities present in the core or in the nearby seismic sections. Near the middle of this unit there are more occurrences of light tan-brown laminations that are spaced 2–10 cm apart, with rare occurrences of denser, light tan-brown 2–3 cm thick beds.

The upper 300 cm of this unit contains is darker grey-brown mud interbedded with the green-brown mud with decreasing diatoms. The uppermost 0.40 m is green-tan mud with abundant diatoms and rare amorphous organic matter. There are interbeds and laminations of lighter tan mud that are 0.5–2 cm in thickness and 3–5 cm apart, and lighter yellow-tan clay laminations that are 0.3 to 0.5 cm thick and ~10 cm apart and more diatom-rich.

The lithology record has been correlated to the seismic data using variations in density and lithology compared to seismic reflection amplitude and seismic sequence character. Radiocarbon dates from cores provide age constraints for limnological changes interpreted from seismic data (Fig. 6; Table 1). The base of Unit 1 correlates to horizon T10 in seismic reflection data; radiocarbon ages from the lowermost sediment of Unit 1 indicate the T10 horizon is approximately 19 ka in age. T11 correlates with sediment that is dated to be ~17.8 ka. T11_1 correlates to sediment in Unit 4 that is dated at ~4.3 ka. T11_2 has an age of approximately 2.3 ka, based on radiocarbon dates from Unit 5.

5 Discussion

5.1 Lake level indicators from sediment cores and seismic reflection data

Sediment physical properties, geochemical analyses, and observations of stratal terminations and subsurface features were interpreted to produce a lake level record for Lake Turkana (Figs. 2 and 4). Several unconformable surfaces and onlapping sequences (Table 1) are observed in seismic data, and are correlated to changes in core lithology and geochemistry, suggesting regressions and transgressions over the last 20 ka. This record provides insight on local paleohydrological change as well as regional climate processes.

At the base of the composite sediment record (Fig. 2), high TIC (~6%), high calcium counts (near 100,000 counts), high bulk density (~1.6 g cm^{-3}), and the presence of sand suggest that Lake Turkana was smaller in volume and in surface area. Reduced lake volume concentrated dissolved ions, increased authigenic calcite precipitation, and induced the basinward migration of littoral facies. The high-amplitude reflection (T10) that correlates to this sediment interval is widespread throughout the lake, indicating this lowstand event affected the depositional patterns and geochemistry of deep parts of the lake, and was not isolated to nearshore environments. The deepest region where this reflection retains its high-amplitude character is 130 m below current lake level (230 masl). This is interpreted as a lowstand of at least ~110 m below current lake level that extended from ~19 until 18 ka. The South Basin was likely desiccated during this interval. Paleodeltas observed in seismic data are probably associated with this regression as they are coeval with T10, however the sequence of deposition cannot be constrained due to ambiguities within the seismic data. The younger AHP sequences onlap all of these features, indicating the progradational features must all be substantially older than ~12 ka.

Following this lowstand, lake level rose for a short period of time as indicated by an increase in organic carbon, a decrease in saturated bulk density and seismic amplitude as well as an absence of sand in the interval (Fig. 2). The amount of the lake level rise is not precisely constrained, but the core site was likely in several meters of water, and perhaps as high as the modern lake (~360 masl) as indicated by similarities in geochemical measurements to modern samples. This increase in lake level persisted from ~18 until ~17.5 ka which was followed by another lowstand at ~17 ka (Fig. 2), as indicated by an increase in density from the presence of mafic lithic sand grains and an increase in calcite

preservation. This interval correlates to another high amplitude reflection (T11) in the seismic data indicating a lowstand (Figs. 2 and 4). The deepest part of the basin showing this seismic character is ~120 m (240 masl) below the current lake level, which indicates the South Basin was probably desiccated during this interval (~240 masl).

From ~17–13 ka, brown-green mud and clay dominate the lithology. The TIC and TOC values are relatively low in this interval with TIC increasing around 14 ka. This suggests lake level remained low but the lake was not desiccated during this interval, with a possible subsequent decrease between 15 and 14 ka. Above this interval, organic and inorganic carbon, saturated bulk density, seismic character, and sediment type change. The abrupt and substantial increase in organic carbon to nearly 6% and decrease of TIC to 0% suggest that a deep-water environment was established quickly and persisted for several thousand years (Fig. 2). During this period of extremely low inorganic carbon preservation, water column stratification probably developed, resulting in anoxic bottom waters with low pH inhibiting calcite deposition. The seismic data in this interval are characterized by continuous and flat-lying reflections, indicative of an undisturbed, deep-water environment. The sediment is finely laminated with no evidence of bioturbation throughout the interval, indicating bottom water anoxia. These conditions likely persisted from ~12.5 until ~5.0 ka (Fig. 10). The consistent nature of the sediment record indicates high, stable lake level during this period, a deep lake, and a hydrologically open system. At overflow, lake level reached ~460 masl, which is 100 m higher than today. During this time period the lake overflowed into the Nile River via the Turkana-Nile River (Garcin et al., 2012)(Figs. 1 and 4). Changes in TOC over this interval may represent decadal-scale drops in lake level, dilution by allochthonous material, or both (Fig. 2).

After 5 ka, the pH of deep water increased as indicated by an abrupt increase in TIC. From 5 ka to ~4 ka, inorganic carbon increased and organic carbon decreased over a few hundred years, accompanied by an increase in sediment bioturbation, indicating a regression to lake levels comparable to that of the modern lake. It was during this interval of time that the lake became hydrologically closed and no longer contributed outflow to the White Nile drainage.

The seismic reflection data display a significant angular unconformity dated at ~2.3 ka by correlation to the cores (Fig. 7). In deep water (>55 m), sediment layers are conformable and no evidence of lowstand conditions is observed. The limited spatial extent of this unconformity suggests there was moderate lowstand (~40 m below modern lake level) during the late Holocene. This lowstand is corroborated by radiocarbon-dated shorelines that indicate a regression beginning at ~5.2 ka (Garcin et al., 2012). Following this lowstand, lake level once again increased to near modern levels as indicated by burial of the lowstand unconformity. TOC and TIC values remain relatively constant to the top of the sediment record (Fig. 2) and no additional truncations are identified in seismic data. Archaeological sites dated to ~1000 yr BP thought to have been located lakeside indicate lake level may have been ~20 m (~380 masl) higher than today (Owen et al., 1982). This suggests moderate a lake level rise in the latest Holocene before it returned to its current level (~360 masl)(Fig. 2).

5.2 Lake Turkana's connection with the Nile River

The spill point of Lake Turkana drainage is ~90 km northwest of the present-day lakeshore, where it connects to the watershed of the White Nile via the relict Turkana-Nile

River (Fig. 1). The Nile River has been the primary water source for inhabitants of the desert of Egypt and Sudan since prehistoric times (Nicoll, 2001; Stanley et al., 2003; Williams et al., 2006; Williams, 2009). Nile River historical flow records have shown significant fluctuations in the past; the influence of flow changes on contemporaneous civilizations is well documented (Stanley et al., 2003; Williams et al., 2006; Williams, 2009). Nicoll (2001) describes a decline in occupancy in the northern Nile region probably related to a changing environment and increase in aridity starting around 6 ka and near abandonment by 4.2 ka based on the frequency of hearths occurring in the archeological record. Lake Turkana's transition from a hydrologically open to a closed basin just after ~5 ka was significant for the sustainability of the base flow of the Nile River. Evidence showing a slow decline in plant and animal diversity in the Nile region (Said, 1993; Stanley et al., 2003) is correlative with a change from deep, possibly stratified water in Lake Turkana to a closed, evaporative lake system (Fig. 2). It is during this time (~6–4 ka) when fine-grained, organic rich sediments (up to 6% TOC) slowly transitioned to slightly coarser grained material with less organic matter and higher percentages of carbonate (1–3% TIC). This transition marks the last contribution of Lake Turkana to the White Nile River.

5.3 Regional lake level comparison

Extreme variations in lake level are characteristic of many lakes in East Africa in the late Quaternary. A complex, interconnected system of lake outflows and rivers from the Western Branch of the East African Rift sustain the base flow White Nile River today (Fig. 1)(Blanchet et al., 2013). In the past, Eastern Branch lakes played a more significant role in providing water for the Nile River System. During a time of regional lake highstands, such

as the AHP (~12–~5 ka), an open hydrological system was established across the northern Kenyan Rift Valley.

Lake Victoria (Figs. 9 and 1) is one of the modern sources for the White Nile, overflowing into Lake Albert via the Victoria Nile and Lake Kyoga. Lake Victoria was desiccated during the LGM and transgressed through the late Pleistocene (Johnson et al., 1996; Stager and Johnson, 2000; Beuning et al., 1997a). Lake level was high during the AHP, but diatom studies show that Lake Victoria levels likely dropped during the period when lake level in Lake Turkana was rising, 12–10 ka, (Stager and Johnson, 2000) and oxygen isotope values from lake-sediment cellulose in Victoria greater than 5‰ indicate closed basin values from 13–10 ka (Beuning et al., 1997a). The compound-specific hydrogen isotope proxy data derived from leaf waxes (δD_{wax}) in sediment cores can be used as a proxy for past precipitation accumulation due to the enrichment of deuterium in raindrops via the "amount effect" (Dansgaard, 1964; Rozanski et al., 1993). A compound-specific δD record generated from a Lake Victoria core suggests that Early Holocene Lake Victoria lake levels increased between 10–9 ka due to increased rainfall in the region (Berke et al., 2012a). Strontium isotope ratios of shell and fish remains from the White Nile were used as tracers for the Victoria contribution to the Nile, and indicate that Victoria supplied water to the Nile by 11.5 ka but this flow was probably subsequently disrupted at times during the Holocene (Talbot et al., 2000) and possibly as early at 15 ka (Williams et al., 2006). Neither of those studies, however, address the mid Holocene Victoria lake record in detail. Values of the δD record are less than -110‰ at this time, or D-enriched, suggesting that the amount of rainfall accumulating at this time was probably higher (Berke et al., 2012a), but then slowly decreased to a closed system by around 7.3 ka (Stager

and Johnson, 2000; Beuning et al., 1997a). The oxygen isotope values of cellulose isolated from lake sediment cores, a proxy for the evaporative properties of lake water, decreased after 5.4 ka to modern values of ~4‰, indicating higher Lake Victoria levels since the mid Holocene (Beuning et al., 1997a). Importantly, the balance of evidence suggests that Lake Victoria was an intermittent contributor to the White Nile during much of the AHP, a time when Lake Turkana's level was high and contributing significant volumes of water to the Nile.

Lake Albert (Fig. 4) has two main inputs, the Semliki River draining Lake Edward and the Victoria Nile. Lake Albert discharges to the north, providing 83% of the base flow for the White Nile River (Hurst, 1957). Late Quaternary palynological records from Lake Albert (Fig. 9) suggest dry periods from 18 to 12.5 ka, 11.4 to 10.9 ka and 10.4 to 9.9 ka, but no data exists for much of the early Holocene from Lake Albert (Beuning et al., 1997b). The loss of Lake Albert discharge to the Nile system was detrimental to perennial flow, suggesting that another source was required to sustain the Nile River through the mid-Holocene. Lake Turkana overflowed during the time period that spans all of the dry periods in Lake Albert, and was probably the alternative source of base flow of the White Nile.

Lake Tana is located in the Ethiopian Highlands on the northern side of the drainage divide at an elevation of 1790 m, and is the source of the Blue Nile. It has a complex paleohydrology (Lamb et al., 2007; Marshall et al., 2011) with a history of fluctuations comparable to Lake Turkana (Fig. 9). Since Lake Tana and Lake Turkana share drainages of geographic proximity, and their catchment precipitation is strongly dependent on the passing of the ITCZ, it is unsurprising that they exhibit similar lake level histories. Lake Tana experienced dry intervals from ~18.7 ka to ~15 ka, just before 12 ka and near 8.5 ka

(Lamb et al., 2007). Blanchet et al. (2013) suggest the Blue Nile was less of a contributor to the Nile River after 8.5 ka and that the White Nile supported the main Nile River flow until ~4 ka. No evidence at 4.2 ka for a lowstand event is observed in Lake Tana records, suggesting that a source other than the Blue Nile was responsible for the failure of White Nile flow at the end of the AHP. The new Lake Turkana records suggest that reduced input from Turkana and its upstream tributaries in the mid Holocene were responsible for the failure of the Nile River, which was coincident with societal collapse in Ancient Egypt. Elimination of the annual flood season in the Nile Valley led to migrations out of nascent riparian communities in effort to find alternate water sources (Stanley et al., 2003).

The Omo River discharge off the southern Ethiopian Highlands was likely only one major input to Lake Turkana during the African Humid Period. The Suguta Valley (Figs. 1 and 9), located just to the south of Lake Turkana, is presently the main terminal basin for drainages discharging off the northernmost part of the Kenyan highlands. Today these drainages enter the Suguta Valley and form an ephemeral playa lake (Garcin et al., 2009). When Paleo-Lake Suguta was last at its highstand in the early Holocene, it spilled over into the Lake Turkana watershed and provided an additional hydrological input from the Kenyan Highlands (Garcin et al., 2012; Junginger et al., 2014). The last highstand of Paleo-Lake Suguta was 5–6.5 ka (Junginger et al., 2014), and evidence suggests that Lakes Bogoria and Baringo (Fig. 1) also spilled over into Suguta Valley around 10.5 ka (Young and Renaut, 1979; Renaut and Owen, 1980; Garcin, 2009). The duration of the Baringo-Bogoria highstand event is not known, but this highstand system would have produced an open hydrologic system throughout the northern Kenyan Rift Valley that provided additional input for the Turkana-Nile River.

Additional ancient tributary inputs of the Nile River that cannot be overlooked include ancient fluvial and lacustrine environments in the Eastern Sahara. Pachur and Kröpelin (1987) described the Wadi Howar (17-18°N, 27-31°E) as a large flooded valley with small lakes and streams that flowed eastward out of western Sudan into the White Nile at least intermittently between 9.5 and 4.5 ka. Sediments from the catchment include both lacustrine and fluvial deposits with channels incised into lacustrine clays, suggesting significant water level fluctuation over the first half of the Holocene (Pachur and Kröpelin, 1987). We postulate that this tributary along with Lake Turkana and its upstream inputs into the Turkana-Nile provided additional flow to the White Nile during the AHP. Both ultimately waned at or shortly before the downfall of the Old Kingdom of Egypt at 4.2 ka.

5.4 Climatic implications

It is widely documented that much of northern and eastern Africa was more humid from approximately 12 to 6 ka (Ritchie et al., 1985; deMenocal et al., 2000; Castañeda et al., 2009; Garcin et al., 2012; Junginger and Trauth, 2013) due to changes in insolation-driven climate processes, and the new lithological and geochemical data from Lake Turkana are broadly consistent with those observations. Turkana's ancient upstream inputs, Lake Bogoria, Lake Baringo, and Paleolake Suguta also overflowed during different intervals of the AHP (Young and Renaut, 1979; Garcin et al., 2009) From these records of the Eastern Branch rift valley lakes, it is clear that the durations of lake highstands increase toward the north. Lake Bogoria and Baringo were last at highstand around 10.5 ka (Young and Renaut, 1979) and Lake Suguta was open with Lake Turkana until at least 8.2 ka (Garcin et al., 2009) and probably until 5-6.5 ka (Junginger et al., 2014). Lake Turkana was open through

the mid Holocene. Even farther to the north, Lake Abhe (11.18°N, 41.80°E; Fig. 9) remained high until around 4 ka (Gasse et al., 1977).

The large-scale climate implications derived from these records are complex due to the nature of African climate. Today Lake Turkana experiences two monsoonal rainy seasons from the twice-a-year passing of the ITCZ, but with minimal annual cumulative rainfall over the lake surface (<200 mm/yr) and high rates of evaporation (>1500 mm/yr)(Yuretich and Cerling, 1983). The ITCZ tends to follow the areas of peak insolation, thus slightly changing the pathway of high rainfall migration over long timescales. Greater annual inter-hemispheric variation in solar insolation occurred during the AHP that increased precipitation at northern tropical latitudes in Africa (Verschuren et al., 2009). During the AHP, the ITCZ annual migration path was shifted northward, residing north of the equator for more of the year, providing more rainfall for the northern Kenya Rift region. Whereas the specific location of high rainfall over the watershed is uncertain, it is evident that the annual hydrologic input to the lake was greater during the AHP, resulting in overfilling of Lake Turkana.

An additional supplier for moisture to East Africa is the air mass associated with the Congo Basin, which derives its moisture from the Atlantic Ocean, and the boundary between easterly-derived Indian Ocean air and westerly-derived Atlantic Ocean air is known as the Congo Air Boundary (CAB)(Nicholson) Today it is rare when moisture from the CAB travels as far east as the Lake Turkana region (Junginger and Trauth, 2013). Additionally, the easternmost parts of East Africa are at least partially isolated from Congo Basin moisture, due to the high topographic relief of the Rift Valley separating moisture zones across East Africa (Tierney et al., 2011b; Berke et al., 2012a). Lake Turkana lies in a

regional depression without the orographic constraint of a large footwall uplift near the confluence of the ITCZ and the easterly shifted CAB. Enhanced pressure gradients over the western Indian Ocean forced the CAB eastward during the AHP, allowing for more annual rainfall to accumulate in the Turkana and Suguta regions (Junginger and Trauth, 2013). The unique positioning along this boundary provided the Turkana area with two different moisture sources during the AHP.

Due to its proximity to the coast, the Eastern Branch of the rift valley is more sensitive to the behavior of the Indian Ocean monsoons, Indian Ocean SST variability, and advection of moisture from the ocean onto the land surface. The reduction in lake surface elevations northward along the Eastern Branch of the rift valley suggests a coupled reduction in advection of Indian-ocean moisture along the coast through the mid Holocene. Lake Challa, a crater lake on the southeastern flank of Mt. Kilimanjaro, is reliant upon Indian Ocean for moisture. Hydrogen isotope (δD_{wax}) records from Lake Challa show a decrease in moisture availability as the AHP progressed, supporting a disturbance in Indian Ocean monsoon dynamics during the African Humid Period (Tierney et al., 2011b). Lake Abhe, in the horn of Africa, shows high lake levels longer than most other records (Gasse et al., 1977), also supporting a northward shift of increased rainfall. A recent study by Tierney et al., (2013) suggests that Indian Ocean SSTs have a strong control on rainfall amount along the eastern coast of Africa.

Increased insolation during the AHP and associated land surface temperature increase would have led to greater advection of moisture onto the continent from both the Atlantic and Indian Oceans, and extended the monsoonal rainy seasons. With an increase in annual convergence in the northern tropics, the Turkana region received more annual

cumulative rainfall over not just the Ethiopian highlands, but likely over the lake surface. In addition to the enhanced ITCZ and possibly additional CAB influence, increased vegetation coverage during more humid intervals increases moisture recycling and can lead to higher cumulative rainfall in a region (deMenocal et al., 2000). Climate feedbacks such as increased cloud cover coupled with vegetation feedbacks would also have reduced the opportunity for evaporation (Kutzbach and Street-Perrott, 1985; Lenters et al., 2005). This is evident in the lake record from Turkana. High values of organic carbon and deepwater facies suggesting water column stratification, requiring a deeper, more stable lake.

The lake level record from Lake Turkana indicates significant fluctuations in rainfall since the LGM. Widespread, laterally continuous seismic sequences and organic-rich sediment (Fig. 4) intervals from this study indicate that during the AHP, Lake Turkana was a deep lake that was likely stratified. The increased rainfall that facilitated a deep lake and vegetated landscape was probably affected by the intensification of Indian Ocean Monsoons and is also consistent with an incursion of Atlantic-derived moisture from the eastward movement of the CAB. Through the mid Holocene, the locus of precipitation progressed northward, and was likely due to a shift in warm SSTs to the northern Indian Ocean. This is manifested in lower lake levels in East African Lakes Challa and Turkana, but for highstands in more northerly lakes such as Abhe (Tierney et al., 2011b, 2013; Gasse et al., 1977). In Lake Turkana this is evident from seismic character that is less laterally extensive, lower frequency subsequences that onlap further basinward than AHP sequences (Fig. 4).

6 Conclusions

- The water level in Lake Turkana fluctuated by approximately 200 m since the Last Glacial Maximum. Evidence from sediment and facies type, geochemical analyses, geophysical measurements, and paleoecological indicators indicate that lake level has fluctuated significantly over the past 20 ka in the Turkana Basin, from extreme lowstands and likely desiccation during the LGM to highstand conditions during the AHP.
- There is evidence at 18.5 ka and 17 ka for lake levels more than 100 m below current lake level, and evidence at ~14 ka and 2.3 ka for lake levels 10's of meters lower than today.
- Stable, high lake levels and an open system with the Nile River occurred abruptly beginning at ~12.5 ka and lasting until ~5 ka.
- During the AHP, Lake Turkana, along with upstream watersheds, spilled over into the watershed of the Nile River, providing a significant water source that sustained White Nile flow.
- The dramatic changes in Turkana lake levels presented here are consistent with shifts in the migration path of the ITCZ and intensification of African Monsoons during the AHP. Data presented here cannot characterize source of precipitation in the Turkana catchment, but the timing and amount of rainfall is consistent with influence of Congo-derived moisture (CAB migration) during the AHP.
- Lake level fluctuations approximate trends in mean solar insolation, however the onset of lake level extremes are much more abrupt than rates of insolation change.
- Sediment and seismic records presented here suggest that the hydrological closure of Lake Turkana and disconnection to the White Nile watershed at ~5 ka is

contemporaneous with documented Nile low flow and the decrease in diversity of plants and animals from Predynastic Egypt (~6 ka) through the time of the fall of the Old Kingdom (~4200 ka).

7 Acknowledgements

We thank the government of Kenya for research permissions. Financial support was provided by the sponsors of the Syracuse University Lacustrine Rift Basins Research Program. We thank the National Oil Corporation of Kenya for assistance during field operations. The authors thank the people of Loiyangalani and the Turkana Rift Valley, for their cooperation, assistance, and hospitality during multiple field seasons at Lake Turkana. We would also like to acknowledge the collaborators and research staff at Syracuse University as well as Dr. James Russell at Brown University, Dr. Erik Brown and Aaron Lingwall at the Large Lakes Observatory at the University of Minnesota-Duluth, and the Lacustrine Core Repository (LacCore) at the University of Minnesota-Twin Cities where sample processing was carried out. Support for radiocarbon dating was provided by the U.S. National Science Foundation. Dr. Maarten Blaauw provided considerable assistance in generating the age model. Seismic data analysis was completed using software provided on a grant from Landmark Graphics Corporation. Reviews from Editor Finn Surlyk and two anonymous reviewers helped greatly improve the original version of this manuscript.

8 References

Abell, P.I., 1982. Paleoclimates at Lake Turkana, Kenya, from oxygen isotope ratios of gastropod shells. Nature, 297, 321–323.

Abell, P.I., Awramik, S.M., Osborne, R.H., and Tomellini, S., 1982. Plio-Pleistocene Lacustrine Stromatolites from Lake Turkana, Kenya: morphology, stratigraphy and stable isotopes. Sediment. Geol. 32, 1-26.

Berke, M.A., Johnson, T.C., Werne, J.P., Grice, K., Schouten, S., Sinninghe, J.S., 2012a. Molecular records of climate variability and vegetation response since the Late Pleistocene in the Lake Victoria basin, East Africa. Quat. Sci. Rev. 55, 59–74.

Berke, M. a., Johnson, T.C., Werne, J.P., Schouten, S., Sinninghe Damsté, J.S., 2012b. A mid-Holocene thermal maximum at the end of the African Humid Period. Earth Planet. Sci. Lett. 351-352, 95–104.

Beuning, K.R.M., Kelts, K., Ito, E., Johnson, T.C., 1997a. Paleohydrology of Lake Victoria, East Africa, inferred from 18O/16O ratios in sediment cellulose. Geology, 25, 1083–1086.

Beuning, K.R.M., Talbot, M.R., Kelts, K., 1997b. A revised 30,000-year paleoclimatic and paleohydrologic history of Lake Albert, East Africa. Palaeogeogr. Palaeoclimatol. Palaeoecol. 136, 259–279.

Blaauw, M., Christen, J.A., 2011. Flexible Paleoclimate Age-Depth Models Using an Autoregressive Gamma Process. Bayesian Anal. 6, 457–474.

Blanchet, L., Tjallingii, R., Frank, M., Lorenzen, J., Reitz, A., Brown, K., Feseker, T., Br, W., 2013. High- and low-latitude forcing of the Nile River regime during the Holocene

inferred from laminated sediments of the Nile deep-sea fan. Earth Planet. Sci. Lett. 364, 98–110.

Brown, F.H. and Carmichael, I.S.E., 1971. Quaternary volcanoes of the Lake Rudolf region; II, The lavas of North Island, South Island and the Barrier. Lithos. 4, 305–323.

Butzer, K.W., Isaac, G.L., Richardson, J.L., Washbourn-Kamau, C., 1972. Radiocarbon Dating of East African Lake Levels. Science, 175, 1069–1076.

Butzer, K.W., 1976. Early hydraulic civilisation in Egypt. University of Chicago Press, Chicago.

Camberlin, P., Janicot, S., Poccard, I., 2001. Seasonality and atmospheric dynamics of the teleconnection between African rainfall and tropical sea-surface temperature: Atlantic vs. ENSO. Int. J. Climatol. 21, 973–1005.

Castañeda, I.S., Mulitza, S., Schefuß, E., Lopes dos Santos, R.A., Sinninghe-Damste, J.S., Schouten, S., 2009. Wet phases in the Sahara/Sahel region and human migration patterns in North Africa. Proc. Natl. Acad. Sci. 106, 20159–20163.

Champion, A.M., 1935. Teleki's Volcano and the Lava Fields at the Southern End of Lake Rudolf. Geogr. J. 85, 323–336.

Curtis, P.C., 1991. Competing magmatic processes at a continental rift: Petrology and geochemistry of Quaternary volcanoes in the Turkana Rift Zone, East Africa. UNC Diss.

Dansgaard, W., 1964. Stable isotopes in precipitation. Tellus XVI, 4, 436 – 468.

deMenocal, P., Ortiz, J., Guilderson, T., Adkins, J., Sarnthein, M., Baker, L., Yarusinsky, M., 2000. Abrupt onset and termination of the African Humid Period : rapid climate responses to gradual insolation forcing. Quat. Sci. Rev. 19, 347–361.

Dunkelman, T.J., Karson, J.A., Rosendahl, B.R., 1988. Structural style of the Turkana Rift, Kenya. Geology, 16, 258–261.

Dunkley, P.N, Smiith, M., Allen, D.J., and Darling, W.G., 1993. The geothermal activity and geology of the Northern sector of the Kenay Rift Valley. British Geological Survey Research Report SC/93/1, NERC, Nottingham.

Furman, T., 2004. East African Rift System (EARS) Plume Structure: Insights from Quaternary Mafic Lavas of Turkana, Kenya. J. Petrol. 45, 1069–1088.

Garcin, Y., Junginger, A., Melnick, D., Olago, D.O., Strecker, M.R., Trauth, M.H., 2009. Late Pleistocene–Holocene rise and collapse of Lake Suguta, northern Kenya Rift. Quat. Sci. Rev. 28, 911–925.

Garcin, Y., Melnick, D., Strecker, M.R., Olago, D., Tiercelin, J.-J., 2012. East African mid-Holocene wet–dry transition recorded in palaeo-shorelines of Lake Turkana, northern Kenya Rift. Earth Planet. Sci. Lett. 322–334.

Gasse, F., 1977. Evolution of Lake Abhe (Ethiopia TFAI), from 70,000 bp: Nature, 265, 42–45.

Gasse, F., 2000. Hydrological changes in the African tropics since the Last Glacial Maximum. Quat. Sci. Rev. 19, 189–211.

Halfman, J.D., Johnson, T.C., 1988. High-resolution record of cyclic climatic change during the past 4 ka from Lake Turkana, Kenya. Geology, 16, 496–500.

Halfman, J.D., Johnson, T.C., Showers, W.J., Lister, G.S., 1989. Authigenic low-Mg calcite in Lake Turkana, Kenya. J. African Earth Sci. (and Middle East), 8, 533–540.

Halfman, J.D., Jacobson, D.F., Cannella, C.M., Haberyan, K.A., Finney, B.P., 1992. Fossil diatoms and the mid to late Holocene paleolimnology of Lake Turkana, Kenya: a reconnaissance study. J. Paleolimnol. 7, 23–35.

Halfman, J.D., Johnson, T.C., Finney, B.P., 1994. New AMS dates, stratigraphic correlations and decadal climatic cycles for the past 4 ka at Lake Turkana, Kenya. Palaeogeogr. Palaeoclimatol. Palaeoecol. 111, 83–98.

Hargrave, J. E., Hicks, M. K., and Scholz, C. A., 2014, Depositional environments of lacustrine carbonates of the south basin of Lake Turkana, Kenya. J. Sed. Res. in press.

Hopson, B.J., ed., 1982. A report on the findings of the Lake Turkana Project 1972-1975. Government of Kenya and the Ministry of Overseas Development, London.

Hurst, H.E., 1957. The Nile: A general account of the river and the utilization of its waters, second ed. Constable, London.

Johnson, T.C., Halfman, J.D., Rosendahl, B.R., Lister, G.S., 1987. Climatic and tectonic effects on sedimentation in a rift-valley lake : Evidence from high-resolution seismic profiles, Lake Turkana, Kenya. GSA Bull. 98, 439–447.

Junginger, A., Trauth, M.H., 2013. Hydrological constraints of paleo-Lake Suguta in the Northern Kenya Rift during the African Humid Period (15 – 5 ka BP). Glob. Planet. Change, 111, 174–188.

Junginger, A., Roller, S., Olaka, L. a., Trauth, M.H., 2014. The effects of solar irradiation changes on the migration of the Congo Air Boundary and water levels of paleo-Lake Suguta, Northern Kenya Rift, during the African Humid Period (15–5ka BP). Palaeogeogr. Palaeoclimatol. Palaeoecol. 396, 1–16.

Karson, J.A. and Curtis, P.C., 1994. Quaternary volcanic centres of the Turkana Rift, Kenya. J. of African Earth Sci. 18, 15–35.

Kutzbach, J.E., Street-Perrott, F.A., 1985. Milankovitch forcing of fluctuations in the level of tropical lakes from 18 to 0 kyr BP. Nature 317, 130–134.

Lake Turkana Wind Power, 2012. Lake Turkana Wind Power Project profile website: http://ltwp.co.ke/the-project/project-profile, accessed August 2013.

Lamb, H.F., Bates, C.R., Coombes, P. V., Marshall, M.H., Umer, M., Davies, S.J., Dejen, E., 2007. Late Pleistocene desiccation of Lake Tana, source of the Blue Nile. Quat. Sci. Rev. 26, 287–299.

Lenters, J.D., Kratz, T.K., Bowser, C.J., 2005. Effects of climate variability on lake evaporation: Results from a long-term energy budget study of Sparkling Lake, northern Wisconsin (USA). J. Hydrol. 308, 168–195.

Lyons, R.P., Scholz, C.A., Buoniconti, M.R., Martin, M.R., 2011. Late Quaternary stratigraphic analysis of the Lake Malawi Rift, East Africa: An integration of drill-core and seismic-reflection data. Palaeogeogr. Palaeoclimatol. Palaeoecol. 303, 20–37.

Marshall, M.H., Lamb, H.F., Huws, D., Davies, S.J., Bates, R., Bloemendal, J., Boyle, J., Leng, M.J., Umer, M., Bryant, C., 2011. Late Pleistocene and Holocene drought events at Lake Tana, the source of the Blue Nile. Glob. Planet. Change, 78, 147–161.

Nicoll, K., 2001. Radiocarbon chronologies for prehistoric human occupation and hydroclimatic change in Egypt and Northern Sudan. Geoarchaeology, 16, 47–64.

Ochieng, J. O., Kagasi, J., compilers, 1988. Loiyangalani Degree Square 19. Kenyan Mines and Geological Department and the British Geological Survey, scale 1:250 000, 1 sheet.

Owen R.B., Barthelme, J.W., Renaut, R.W., Vincens, A., 1982. Palaeolimnology and archaeology of Holocene deposits north-east of Lake Turkana, Kenya. Nature, 298, 523–529.

Pachur, H.J., Kröpelin, S., 1987. Wadi howar: paleoclimatic evidence from an extinct river system in the southeastern Sahara. Science, 237, 298–300.

Renaut, R.W. and Owen, R.B., 1980. Late Quaternary fluvio-lacustrine sedimentation and lake levels in the Baringo basin, northern Kenya, Rift Valley. Recherches Geologiques en Afrique. 5, 130-133.

Ricketts, D., Johnson, C., 1996. Climate change in the Turkana basin as deduced from a 4000 year long d18O record. Earth Planet. Sci. Lett. 142, 7–17.

Ritchie, J.C., Eyles, C.H., Haynes, C. V., 1985. Sediment and pollen evidence for an early to mid-Holocene humid period in the eastern Sahara. Nature, 314, 352–355.

Rozanski, K., Araguás-Araguás, L., Gonfiantini, R., 1993. Isotopic Patterns in Modern Global Precipitation, in: Swart, P.K., Lohmann, K.C., McKenzie, J., Savin, S. (Eds.), Geophysical Monograph Series. AGU, Washington, D. C., pp. 79–93.

Said, R., 1993. The River Nile. Pergamon Press, Oxford.

Stager, J. C., Johnson, T. C., 2000. A 12,400 14C yr offshore diatom record from east central Lake Victoria, East Africa. J. Paleolimnol. 23, 373–383.

Stanley, J-D., Krom, M.D., Cliff, R. a., Woodward, J.C., 2003. Short contribution: Nile flow failure at the end of the Old Kingdom, Egypt: Strontium isotopic and petrologic evidence. Geoarchaeology, 18, 395–402.

Talbot, M.R., Williams, M.A.J., Adamson, D.A., 2000. Strontium isotope evidence for late Pleistocene reestablishment of an integrated Nile drainage network. Geology, 28, 343–346.

Tierney, J.E., Russell, J.M., 2009. Distributions of branched GDGTs in a tropical lake system: Implications for lacustrine application of the MBT/CBT paleoproxy. Org. Geochem. 40, 1032–1036.

Tierney, J.E., Lewis, S.C., Cook, B.I., LeGrande, A.N., Schmidt, G. A., 2011a. Model, proxy and isotopic perspectives on the East African Humid Period. Earth Planet. Sci. Lett. 307, 103–112.

Tierney, J.E., Russell, J.M., Sinninghe Damsté, J.S., Huang, Y., Verschuren, D., 2011b. Late Quaternary behavior of the East African monsoon and the importance of the Congo Air Boundary. Quat. Sci. Rev. 30, 798–807.

Tierney, J.E., Smerdon, J.E., Anchukaitis, K.J., Seager, R., 2013. Multidecadal variability in East African hydroclimate controlled by the Indian Ocean. Nature, 493, 389–92.

Trauth, M.H., Deino, A., Strecker, M.R., 2001. Response of the East African climate to orbital forcing during the last interglacial (130–117 ka) and the early last glacial (117–60 ka). Geology, 29, 499–502.

Verschuren, D., Sinninghe Damsté, J.S., Moernaut, J., Kristen, I., Blaauw, M., Fagot, M., Haug, G.H., 2009. Half-precessional dynamics of monsoon rainfall near the East African Equator. Nature, 462, 637–41.

Williams, M.A.J., Talbot, M., Aharon, P., Abdl Salaam, Y., Williams, F., Brendeland, K.I., 2006. Abrupt return of the summer monsoon 15,000 years ago: new supporting evidence from the lower White Nile valley and Lake Albert. Quat. Sci. Rev. 25, 2651–2665.

Williams, M.A.J., 2009. Late Pleistocene and Holocene environments in the Nile basin. Glob. Planet. Change, 69, 1–15.

Young, J.A.T. and Renaut, R., 1979. Radiocarbon date from Lake Bogoria, Kenya Rift Valley. Nature, 278, 243-244.

Yuretich, R.F., 1979. Modern sediments and sedimentary processes in Lake Rudolf (Lake Turkana) eastern Rift Valley, Kenya. Sedimentology, 26, 313–331.

Yuretich, R.F., Cerling, T.E., 1983. Hydrogeochemistry of Lake Turkana, Kenya : Mass balance and mineral reactions in an alkaline lake. Geochim. Cosmochim. Acta, 47, 1099–1109.

Yuretich, R.F., 1986. Controls on the composition of modern sediments, Lake Turkana, Kenya. GSA Spec. Publ. 25, 141–152.

9 Figures

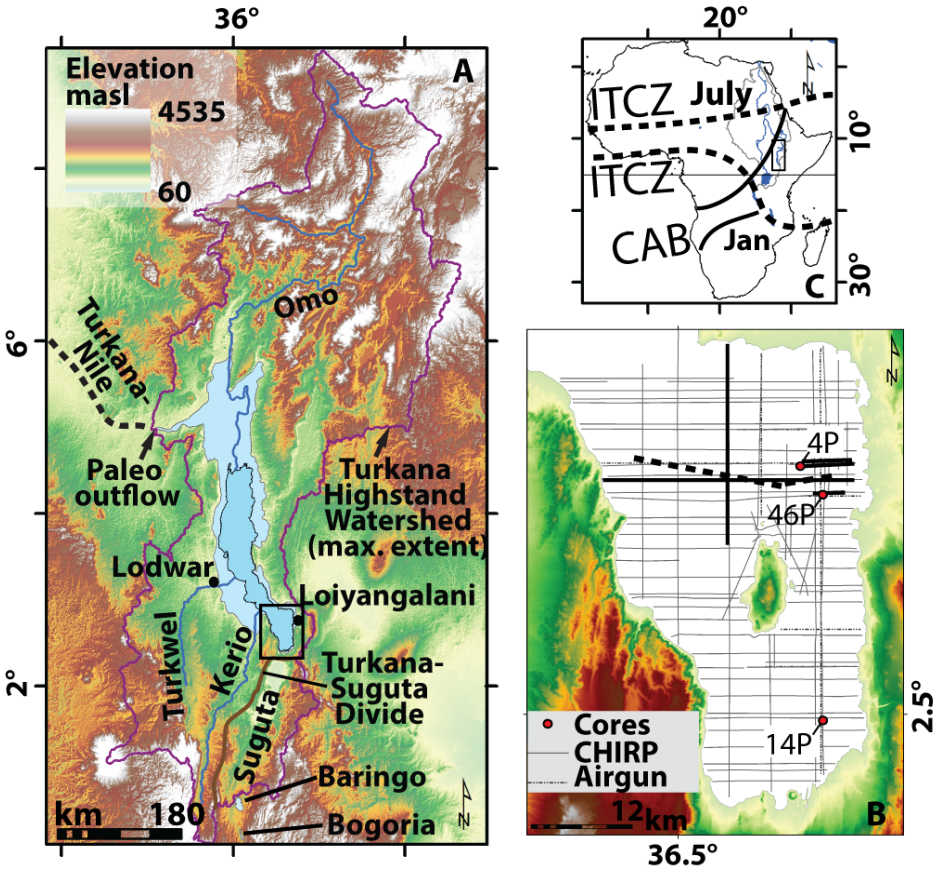

Fig. 1. (**A)** Topography of Lake Turkana and its watershed with black box indicating study area. Lake Turkana Highstand Watershed delineated (fuchsia). Blue polygon with black outline defines current Lake Turkana shoreline. Palest blue polygon indicates highstand shoreline of Lake Turkana. Brown line indicates current drainage divide between Suguta Valley and Lake Turkana. Black dashed line delineates paleo-river connecting Lake Turkana to the White Nile. Black arrow indicates location of outflow location of Lake Turkana during highstand. Other geographic locations added for reference. (**B)** Data map of South Basin of Lake Turkana. Gray solid lines are CHIRP seismic tracklines, featured profiles traced in black. Thin, dot-dashed black lines indicate Airgun seismic tracklines. Bold dashed line is MCS trackline. Red dots are piston core locations. (**C)** Black box outlines location of Lake Turkana on the African continent

and bold dashed lines denote northern- and southernmost extent of the annual migration of the ITCZ and thin, solid lines denote the location of the CAB at its extremes. Nile River watershed is (including highstand Lake Turkana) in grey, and blue lines are major rivers.

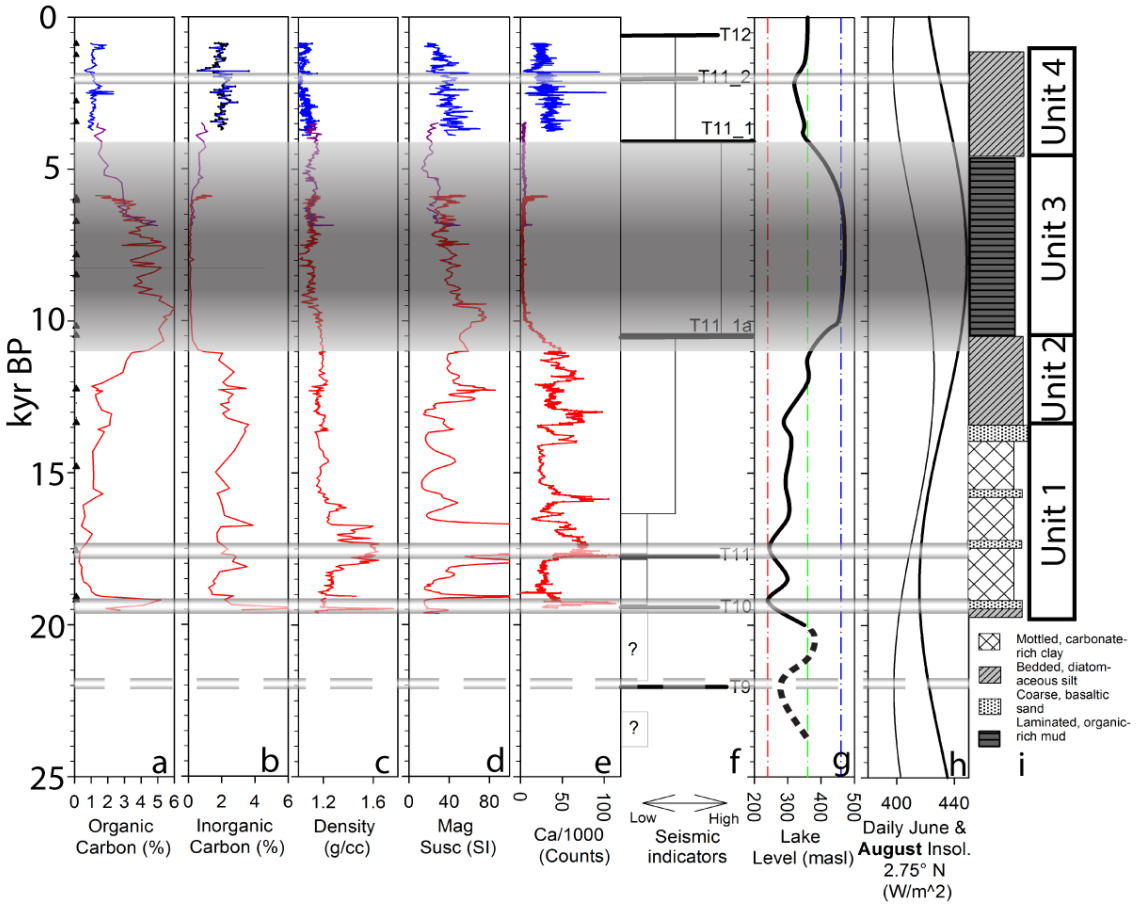

Fig. 2. Summary of data used for interpretation of lake level through time. The 3 different cores from which the data are derived are plotted in blue (4P), purple, (14P), and red (46P). Vertical axis is time in Cal. Yr BP. (**a**) Organic carbon is plotted in weight percent, and was sampled in each core at an 8-cm interval. Black triangles are sample locations for radiocarbon dating. (**b**) Inorganic carbon is plotted in weight percent, and was sampled in core at an 8-cm interval. (**c**) Gamma Ray Attenuated Porosity Evaluation measures saturated bulk density in g/c^3. (**d**) Magnetic susceptibility and (**e**) calcium are both reported as counts per second, whereas calcium is divided by 1000 for simplification. (**f**) Bold black lines with labels denote significant horizons from high-resolution CHIRP seismic reflection data. Box line thicknesses indicate inferred depth of lake based on seismic reflection data. (**g**) Quantitative lake level curve in black. Dot-dashed

lines indicate lake levels of significance: red, desiccated lake; green, modern lake level; blue, highstand lake level. (**h**) Mean annual insolation curves for June and August (bold) for 2.75°N. (**i**) Sediment column and sedimentary unit boundaries as described in text.

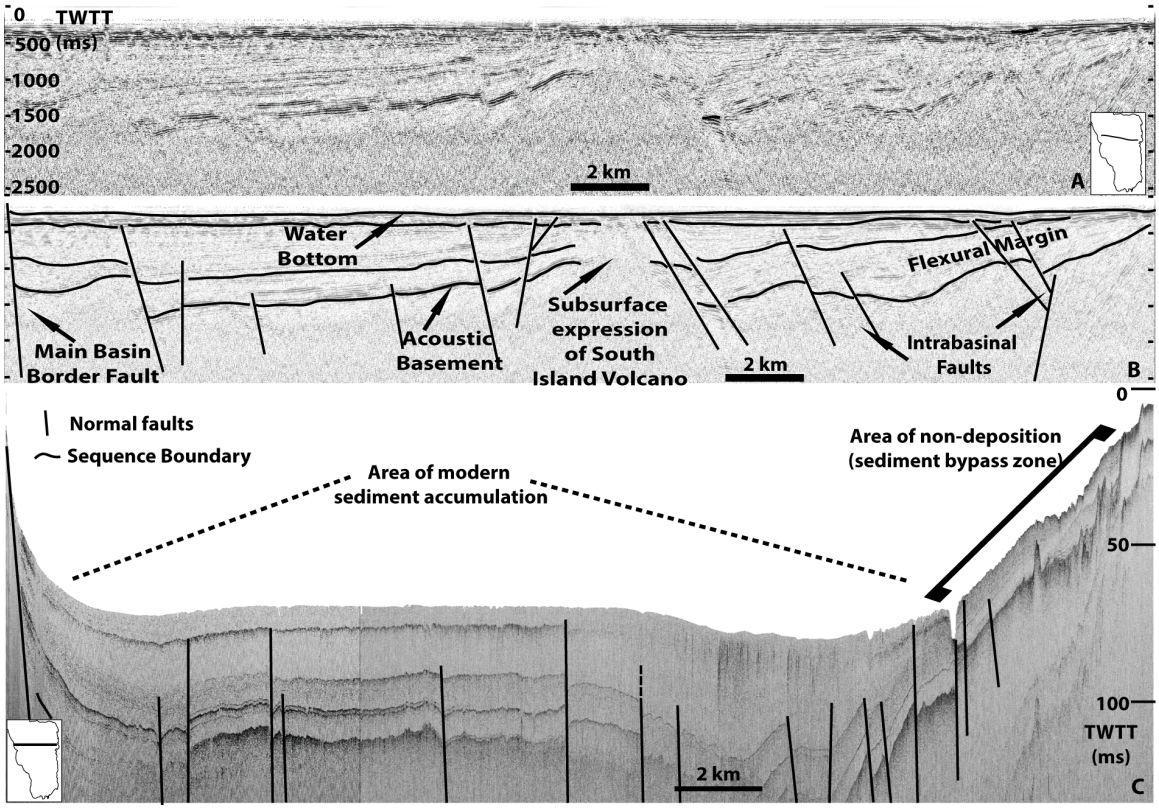

Fig. 3. Upper panels: Legacy multi-channel seismic reflection data across the south basin (Project PROBE profile 84-342). Vertical scale is two-way travel time in milliseconds. Uninterpreted section in uppermost panel; interpreted section in the center panel with major horizons (black horizontal lines) and major faults (black vertical lines). Lower panel is the nearly coincident high-resolution CHIRP seismic line with faults indicated by black lines.

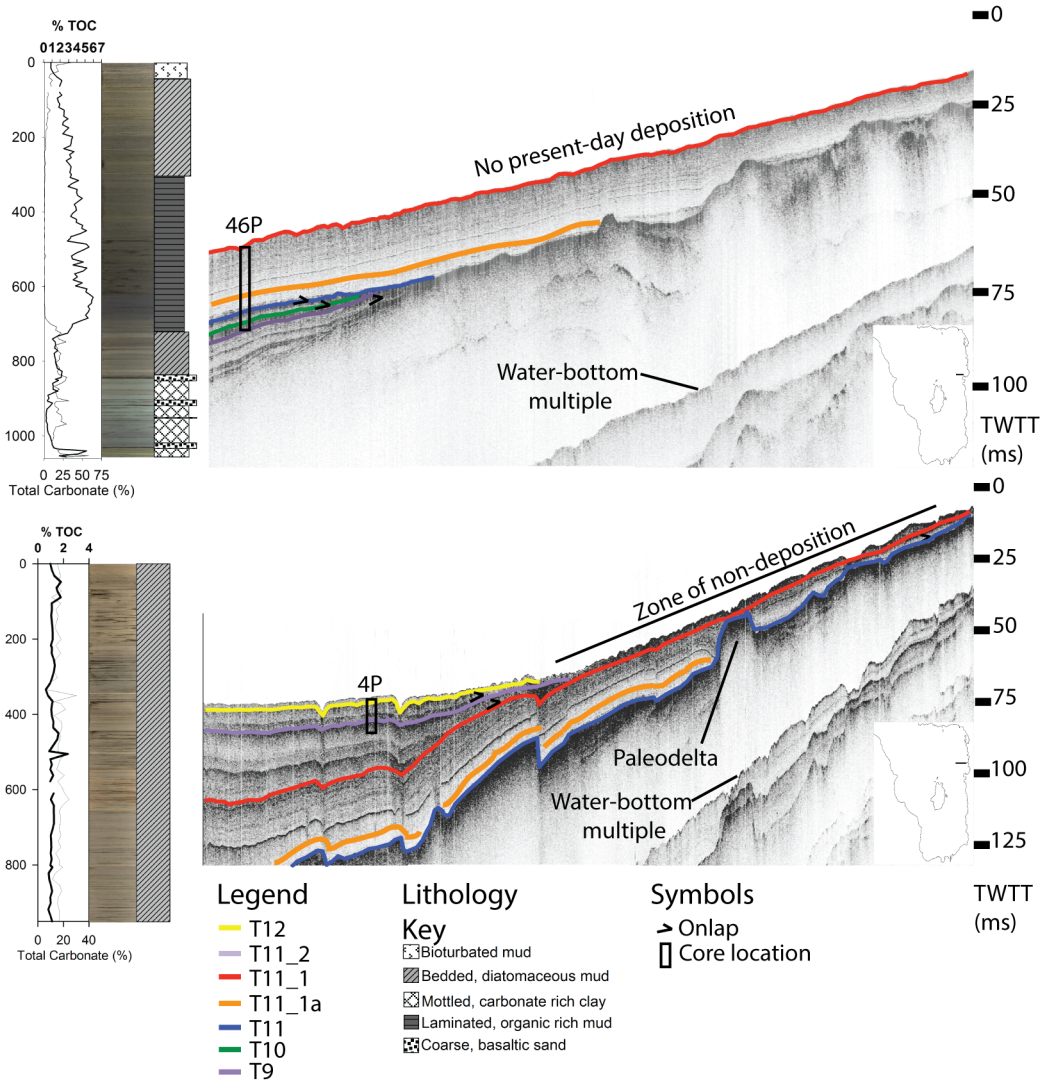

Fig. 4. CHIRP seismic lines where key sediment cores were collected. Upper panel displays 46P projected on seismic data. Small black arrows indicate onlapping surfaces discussed in text. Corresponding high-resolution core image and simplified stratigraphic section are at left. Downcore geochemical data are total organic carbon (bold black line) and calculated total carbonate (thin black line), each sampled at 8-cm interval. Lower panel provides the same information for core 4P. The letter "T" followed by a number, which increases with stratigraphic level, denote sequence boundaries names. Named horizons with an underscore and followed by

an additional number denote subsequence boundaries and marker horizons. Named horizons are also described in Table 2.

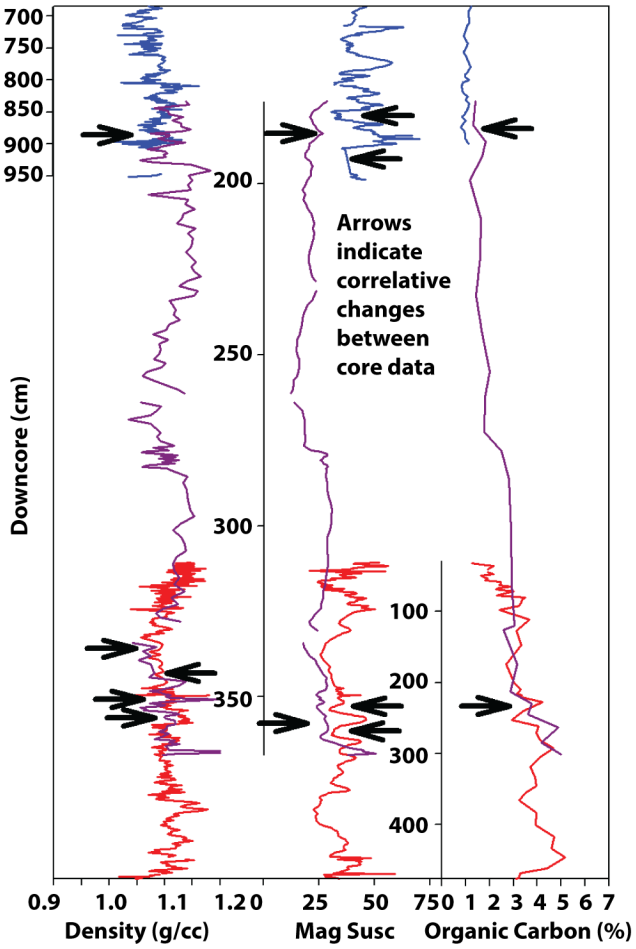

Fig. 5. Down core measures of saturated bulk density, magnetic susceptibility, and organic carbon, in depth, in all three cores illustrating stratigraphic overlap. Overlapping parts of 4P (blue), 14P (purple), and 46P (red). Note that 14P data bridge 1.2-kyr gap between the bottom of 4P and the top of 46P. Black arrows indicate key correlative changes in geophysical or geochemical parameters between cores. Vertical axis is depth in centimeters plotted downcore. Note that vertical axes are set at different scales for graphical clarity.

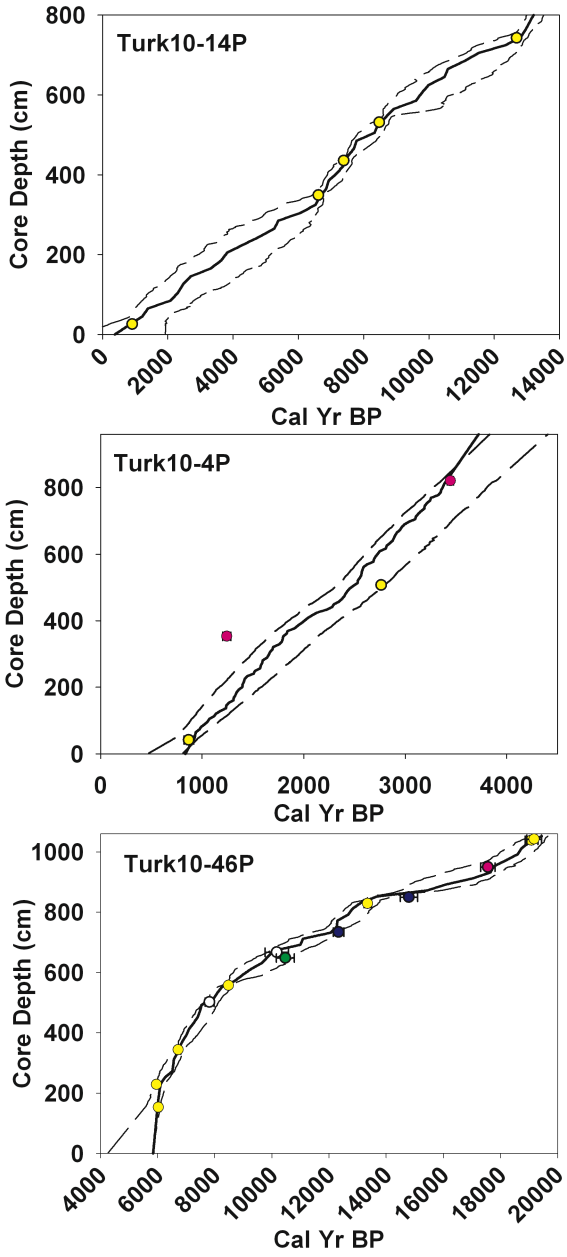

Fig. 6. Radiocarbon dates from three separate piston cores modeled in Bacon (Blaauw and Christen, 2011). Dots indicate average age of core material dated; the color of the dot indicates sample material. Yellow circles are bulk organic carbon, pink circles are bulk inorganic carbon, white circles are macrophytes, green circles are charcoal, dark blue circles are shell material. Error or radiocarbon ages are plotted as brackets on circles. Most errors are within the size of the

circle. Solid lines are best-fit outputs. Dashed lines indicate extremes of possible MCMC model outcomes. Errors on younger dates are smaller than the plotted circles.

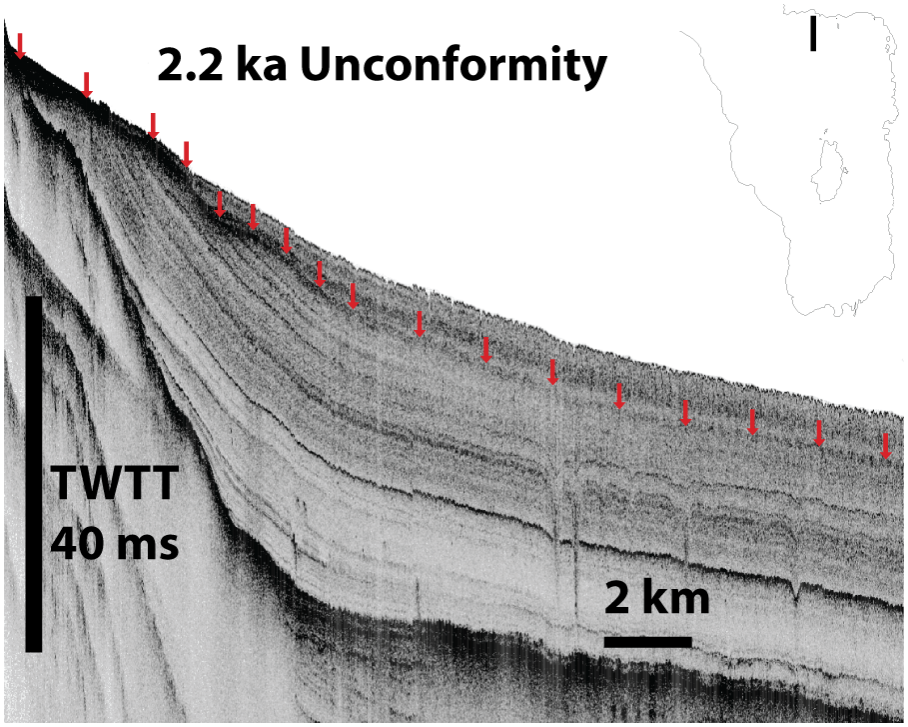

Fig. 7. Late Holocene (2.2 ka) unconformity (red arrows) in high-resolution seismic data, and its correlative conformable surface at toward the basin center.

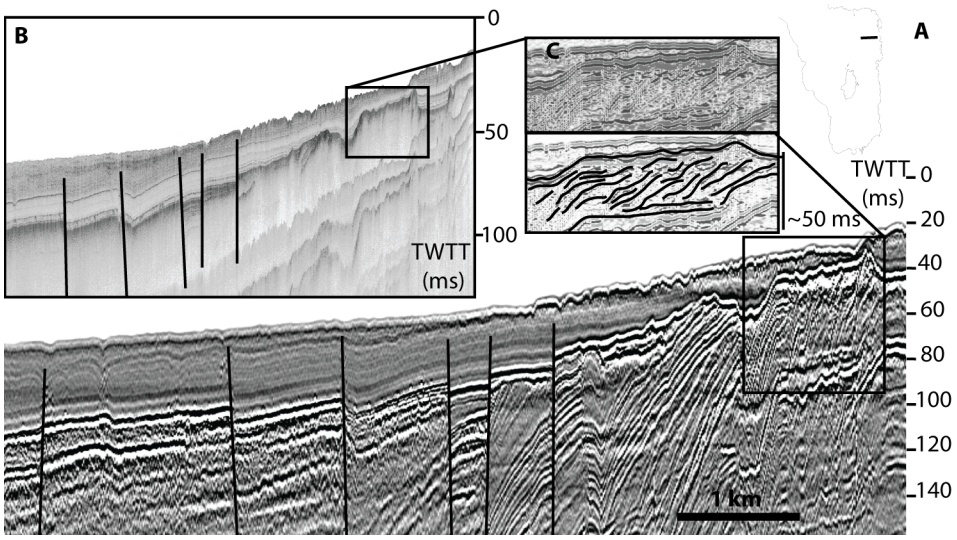

Fig. 8. (**A)** Airgun seismic line approximately perpendicular and adjacent to the eastern shoreline displaying progradational internal reflections, interpreted as a paleodelta. Vertical scale is two-way travel time in milliseconds. Location map of trackline is in upper right. (**B)** CHIRP seismic line coincident with Airgun seismic reflection profile. Vertical scale is two-way travel time in milliseconds. Black box outlines the interpreted buried paleodelta. Black vertical lines are faults. (**C)** Enlarged view of buried paleodelta. Upper panel is raw profile and lower panel is dimmed profile with interpreted dipping internal reflections.

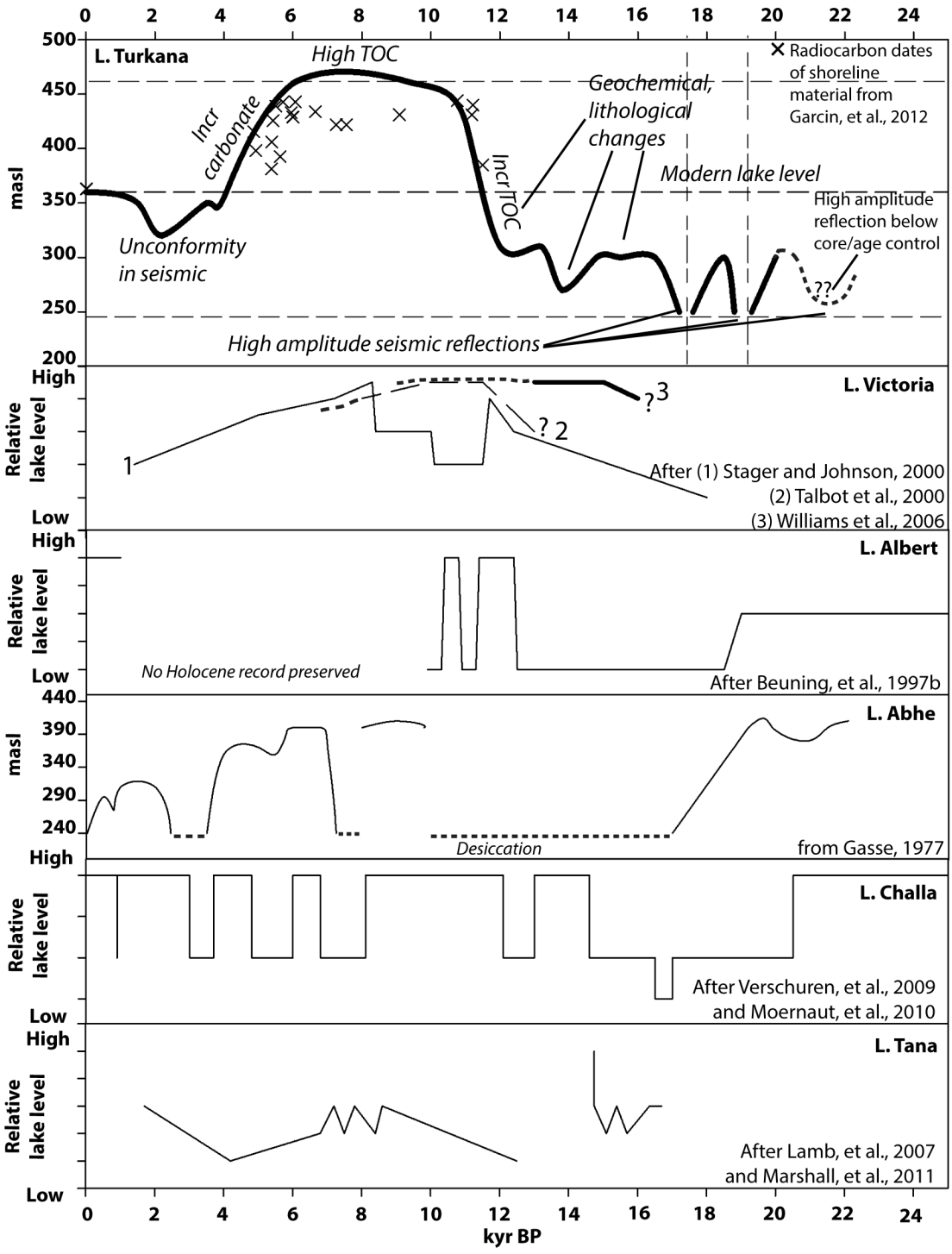

Fig. 9. Uppermost panel is interpreted lake level (black line) of Lake Turkana derived from datasets presented in this study plus shoreline radiocarbon dates from Garcin et al., 2012 (black X). Dashed horizontal lines indicate modern lake level at 360 masl and highstand lake level at

440 masl; lake desiccation is indicated at 250 masl. Panels for Lakes Victoria, Albert, Challa and Tana are relative lake levels as indicated in publications cited in figure (Beuning et al., 1997b; Stager and Johnson, 2000; Talbot et al., 2000; Williams et al., 2006; Lamb et al., 2007; Verschuren et al., 2009; Moernaut et al., 2010; Marshall et al., 2011). Lake Abhe's lake level record in meters above seal level is reconstructed from Gasse et al., 1977.

Table 1

Radiocarbon ages of sediment cores from Lake Turkana

Sample ID	Dated material[1]	^{14}C age (yr BP)	Cal. age (cal. yr BP)	Lab #
Turk10-46P-6.5	M	1,549 ± 35	1,445 ± 80	AA94270
Turk10-46P-152.5	OM	5,245 ± 39	6,031 ± 77	AA98964
Turk10-46P-228	OM	5,225 ± 45	5,960 ± 42	AA95191
Turk10-46P-343	OM	5,913 ± 45	6,723 ± 84	AA95194
Turk10-46P-501.5	M	6,992 ± 89	7,819 ± 156	AA94271
Turk10-46P-556.5	OM	7,684 ± 56	8,484 ± 52	AA98965
Turk10-46P-647.5	M	9,230 ± 240	10,470 ± 316	AA94262
Turk10-46P-666.5	M	9,080 ± 140	10,170 ± 411	AA94273
Turk10-46P-733.5	GS	10,330 ± 50	12,234 ± 184	Beta335253
Turk10-46P-828	OM	11,434 ± 53	13,350 ± 127	AA98966
Turk10-46P-849	OS	12,490 ± 60	14,800 ± 302	Beta335254
Turk10-46P-949	CM	14,790 ± 70	17,560 ± 252	Beta335255
Turk10-46P-1038	OM	15,909 ± 89	19,090 ± 222	AA98967
Turk10-46P-1042	OM	16,111 ± 89	19,180 ± 256	AA95193
Turk10-4P-41	OM	958 ± 33	869 ± 48	AA98957
Turk10-4P-353	CM	1,310 ± 30	1,243 ± 40	Beta335251
Turk10-4P-506.5	OM	2,636 ± 35	2,765 ± 15	AA98963
Turk10-4P-820	CM	3,230 ± 30	3,445 ± 31	Beta335252
Turk10-14P-25	OM	1,017 ± 41	918 ± 49	AA98956
Turk10-14P-348.5	OM	5,816 ± 40	6,619 ± 51	AA98958
Turk10-14P-435	OM	6,493 ± 43	7,396 ± 47	AA98959
Turk10-14P-531	OM	7,686 ± 46	8,482 ± 48	AA98960
Turk10-14P-742	OM	10,704 ± 49	12,693 ± 48	AA98961
Turk10-14P-806	OM	11,269 ± 65	13,170 ± 103	AA98962

[1] *M = Macrophyte; OM = Organic Mud; OS = Ostracode Shells; CM = Carbonate mud; GS = Gastropod Shells*

Table 2

Horizons discussed in text and figures

Horizon Name	**Age** *(ka)*	**Significance**
T9	20+ ?	Lowest correlatable horizon in CHIRP seismic
T10	18.5	Desiccation surface
T11	17	Desiccation surface
T_11_1a	10.2	Marker horizon; transition into AHP section
T11_1	4.7	Marker horizon; transition out of AHP section
T11_2	2.2	Unconformity marking late Holocene lowstand
T12	~0.7	Uppermost correlatable horizon below SWI

Late Quaternary atmospheric circulation over the Turkana Rift, East Africa

Amy Morrissey[1*], Christopher A. Scholz[1], James M. Russell[2]

[1]Dept. of Earth Sciences, Syracuse University, Syracuse, NY 13244, USA

[2]Dept. of Geological Sciences, Brown University, Box 1846, Providence, RI 02912, USA

*corresponding author: Amy Morrissey, Dept. of Earth Sciences, Syracuse University, 204 Heroy Geology Laboratory, Syracuse, New York, 13244, USA, +1-315-443-4334, E-mail address: amorriss@syr.edu

Abstract

The late Quaternary water level history of Lake Turkana, Kenya, has long-been used as a gauge of the paleohydrology of northern equatorial Africa. However, the atmospheric circulation changes that cause hydrologic variations in this region remain poorly understood. At present, precipitation at Lake Turkana (2° N) is delivered by the twice-annual passage of the Intertropical Convergence Zone, and back-trajectory analysis indicates that virtually all the moisture is sourced from the Indian Ocean. We present a ~20-kyr compound-specific (C_{28} *n*-alkanoic acids) hydrogen isotope (δD_{wax}) record derived from three new, ~10 m sediment cores from Lake Turkana, coupled with an evaluation of the controls on the δD of precipitation (δD_{precip}), to evaluate changes in precipitation amount and changes in the relative contributions of other moisture sources to this region during the African Humid Period (AHP). We observe abrupt D-depletion associated with the AHP beginning at 13.7 ka and continuing until the ~4ka. Using present-day

relationships between the δD the hydrogen isotope composition and amount of modern precipitation from central Kenya, we estimate the amplitude of possible amount effects for the AHP using quantitative precipitation estimates from a lake basin fill model. Amount effect values of approximately -18‰, -23‰, -25‰, -36‰ were calculated for changes relative to modern in precipitation amounts of 0%, 26%, 40%, and 100%, respectively. After accounting for these effects, precipitation during the AHP is D-depleted relative to a 100% increase in precipitation amount. We suggest this excess in D-depletion is driven by an influx of moisture derived from the Congo Basin, and estimate that at least 45% of the moisture supplied to this part of East Africa during the AHP was Congo-derived. Results from Lake Turkana are consistent with other regional δD_{wax} records from Lake Tana in Ethiopia (12° N) southward to Lake Malawi (9°-14° S), that indicate an eastward migration of the Congo Air Boundary during the AHP, although the timing and magnitude of D-depletion among the δD_{wax} records however suggest Congo Basin influence was not uniform across space and time. These results confirm an important role for both meridional and zonal reorganizations of the atmospheric circulation over East Africa during the African Humid Period.

1 Introduction

Extreme fluctuations in precipitation during the late Quaternary in East Africa are evident from lake levels and other proxy records (Johnson et al., 1996; deMenocal, 2000; Lamb et al., 2007; Verschuren et al., 2009; Stager et al., 2011; Garcin et al., 2009, 2012a; Tierney et al., 2011; Junginger et al., 2013; Costa et al., 2014; Morrissey and Scholz, 2014). Geographical coverage of paleo-precipitation data sets is limited however, and available records are mostly from lake basins located in relatively humid regions or from marine sediments that accumulate leaf waxes from vast and often poorly constrained areas. In contrast, Lake Turkana is a large, low elevation lake (360 m asl) in an arid environment, making it extremely sensitive to precipitation changes. This study presents a new 20-kyr record of the hydrogen isotopic composition of terrestrial leaf waxes (*n*-alkanoic acids, hereafter δD_{wax}), refining our understanding of the Late Quaternary atmospheric circulation and past climates of East Africa.

Coupled changes in the latitudinal migration of the Intertropical Convergence Zone (ITCZ) and the strength of the African Monsoons are commonly invoked as leading causes of variation in rainfall across tropical East Africa on many timescales, particularly in Northern and Southern Africa where the monsoon limit defines sharp changes in climate regimes (i.e., Castañeda et al., 2009; Nicholson, 2009; Schefuss et al., 2011; Foerster et al., 2012; Junginger et al., 2013). Yet in the present, both meridional changes in the position of the ITCZ as well as zonal changes in the position of the Congo Air Boundary (CAB), a convergence zone between westerly and easterly flows from the Atlantic and Indian Ocean, are important controls on past East African precipitation. In equatorial East Africa, east-

west migration of the CAB since the Last Glacial Maximum (~19 ka; LGM) is thought to play an important role in the variation in equatorial east Africa precipitation, and is thought to have influenced past rainfall changes on many timescales, especially during the African Humid Period (AHP), when many African lakes were at higher levels than today (Liu et al., 2003; Tierney et al., 2008, 2011; Junginger and Trauth, 2013; Junginger et al., 2014; Costa et al., 2014). Recent studies utilizing the hydrogen isotopic (δD) composition of leaf waxes from terrestrial plants have begun to elucidate changes in the position and intensity of convection within the ITCZ and CAB, and suggest that changes in both precipitation amount and moisture sources are key to interpreting the mechanisms driving African precipitation change over the last ~30 ka (Tierney et al., 2008, 2011, 2013; Schefuss et al., 2011; Berke et al., 2012; Costa et al., 2014). Records of the isotopic composition of East African precipitation can be used to reconstruct these processes, yet the controls on isotopic composition of precipitation over East Africa are complex. The hydrogen isotopic composition of precipitation (δD_{precip}) can be modified by an "amount effect" (Dansgaard, 1964), in which high rates of precipitation give rise to D-depletion relative to lower rates of precipitation. Changes in precipitation sources, degree of recycling, and transport also play key roles in controlling δD_{precip}. The hydrogen isotopic composition of terrestrial leaf waxes primarily records changes in the isotopic composition of precipitation, and hence provides information on moisture sources and their variability (Sessions et al., 1999, 2001; Huang et al., 2002, 2004; Sachse et al., 2012; Garcin et al., 2012b). However because evaporation and plant metabolic processes modify the isotopic composition of precipitation, a δD_{wax} value is not a direct record of the isotope composition of rainfall (Sessions et al., 1999; Huang et al., 2002, 2004; Sachse et al., 2004). Vegetation type and a metabolic difference between C_3 and

C_4 plants also have an effect on the fractionation of hydrogen isotope compositions of organic compounds (Huang et al., 2002, 2004; Chikaraishi et al., 2004). $\delta^{13}C_{wax}$ is useful for constraining past changes in regional vegetation in East Africa, and allows us to constrain changes in the D/H apparent fractionation between plant types allows us to correct for vegetation effects on the δD_{wax} record (Sachse et al., 2012).

Here we present new isotopic reconstructions of vegetation and atmospheric processes based upon $\delta^{13}C_{wax}$ and δD_{wax} from Lake Turkana, Kenya. We present the first late-Pleistocene to Holocene vegetation record from Lake Turkana based upon $\delta^{13}C_{wax}$, and use these data to correct for vegetation effects on δD_{wax}. We then evaluate past changes in rainfall amount and the moisture sources from Turkana catchment rainfall, as well as other possible influences, on the δD_{wax} record. Modern precipitation data from East Africa are used to estimate an amount effect for the Turkana region, providing important constraint on past precipitation variability and moisture source contributed to the AHP. This record provides an important perspective in the understanding of AHP climate dynamics and zonal moisture in East Africa not yet derived from other data sets.

2 Study site

Lake Turkana (2-5° N, 36-36.5° E, 360 m asl; Fig. 1) is the largest lake in the Eastern Branch of the East African Rift System. The lake is 250 km long and ~30 km wide with a mean depth of 35 m. The lake is well-mixed due to strong diurnal winds from the southeast, driven by cooling of high topography adjacent to the lake (Hopson, 1982) as well as a persistent unidirectional wind from the northeast, with an average wind speed of 11 ms^{-1} (Burlando et al., 2010). The climate in the Turkana region is extremely arid with less than

200 mm yr^{-1} of precipitation and over 2300 mm yr^{-1} of evaporation at lake level at the bottom of the rift valley (Ferguson and Harbott, 1982; Nicholson et al., 1998). Rainfall over the lake occurs during the twice annual passage of the ITCZ in ~April and ~November. The Omo River enters Lake Turkana at the northernmost shore from the Ethiopian Highlands and provides 80-90% of the hydrological input to the lake (Yuretich, 1979). The Omo River also provides a large amount of the sediment load, especially for the north and central basins (Yuretich, 1979). Lake Turkana is a hydrologically closed basin, with a drainage basin area of ~148,000 km^2 but, at its highstand, Lake Turkana overflows into the White Nile River drainage (Hopson, 1982; Garcin et al., 2009).

The South Basin, where the cores for this study were recovered, reaches 120 m in depth and receives minimal input from the Omo sediment plume (Yuretich, 1979, Cerling, 1986). Organic matter extracted from cores in the South Basin is a mixture of material from aquatic and terrestrial sources, with weight percentages of total organic carbon ranging from ~0.5% to ~7% (Morrissey and Scholz, 2014). The Kerio and Turkwel Rivers drain the areas to the west and south of the lake, and ephemeral rainy-season streams provide the remaining hydrological input.

Vegetation surrounding the modern lake is mostly subdesert steppe and includes *Acacia*, *Commiphora, Chenopodiaceae/Amaranthaceae* and *Gramineae* (Hemming, 1972; Vincens, 1982; Mohammed et al., 1995). These plants all use either the C_3 or C_4 photosynthetic pathway; none of the plant groups identified in the region from previous work use Crassulacean Acid Metabolism. No pollen or vegetation information for the AHP is available from Lake Turkana.

3 Materials and Methods

3.1 Core Acquisition and Chronology

Three Kullenberg piston cores, Turk10-4P, Turk10-14P, and Turk10-46P, were collected from the South Basin of Lake Turkana in water depths of 52, 56, and 58 m, and are 9.7, 8.5, and 10.6 m in length, respectively (Fig. 1; Morrissey and Scholz, 2014). Twenty-four AMS ^{14}C samples of bulk organic matter, bulk carbonate, plant material, or shells provided chronologic control, and a Bayesian age-depth program, "Bacon" (Blaauw and Christen, 2011) was used to generate an age model for the composite core record. The three cores were stratigraphically correlated using magnetic susceptibility, gamma ray density and organic carbon content to generate a composite record that spans from ~20 ka to ~0.4 ka (Morrissey and Scholz, 2014).

3.2 Extraction and Isotope Measurements

We measured the hydrogen isotope composition of the dominant terrestrial homologue (C_{28}) of the long-chain *n*-alkanoic acids, leaf waxes, in 60 sediment samples from these cores. Samples were prepared for isotopic analysis as described in Konecky et al. (2011). Lipids were extracted from sediment samples using a Dionex 350 accelerated solvent extractor. Fatty acids were separated from other lipids using aminopropyl columns, and the fatty acids were methylated using acidified methanol of a known isotopic composition. The resulting fatty acid methyl esters were purified using a Si-gel column prior to isotopic analysis. Samples were analyzed using a gas chromatograph interfaced to a Delta XL isotope ratio mass spectrometer at Brown University. While analyses focused on C_{28} *n*-acid, the C_{26} homologue was also measured in a subset of samples (Fig. 2). All samples

were measured in duplicate or triplicate, depending upon the amount of sample material available; all δD_{wax} measurements are reported relative to VSMOW and have been corrected for the added methyl group. Measurements made in duplicate have an average difference of 2.2‰; measurements made in triplicate have an average error of 2.2‰ and a maximum error of 4.4‰. The average sampling interval is ~320 yr, however, in samples that date between ~17 and ~13.7 ka, leaf wax concentrations were below reliable detection limits and are not reported. All δD_{wax} values were corrected for the ice volume effects on the isotopic composition of seawater by using the shifts in LR04 benthic oxygen isotope stack (Lisiecki and Raymo, 2005) scaled to hydrogen isotopes, using the D-O relationship of meteoric water assuming a 1‰ enrichment of $\delta^{18}O$ at the LGM (Schrag et al., 1996).

We also measured the carbon isotopic composition ($\delta^{13}C_{wax}$) of the C_{28} homologue, as well as the C_{26} and C_{30} homologues, on a subset of samples (Fig. 2). $\delta^{13}C_{wax}$ was measured in duplicate on a Thermo Finnegan Delta XL gas chromatograph-isotope ratio mass spectrometer at Brown University. All $\delta^{13}C_{wax}$ values are reported relative to VPDB and were corrected for the addition of the added methyl group. C_{28} *n*-acid measurements had an average $\delta^{13}C_{wax}$ difference of 0.05‰ and maximum of 0.48‰. The average $\delta^{13}C_{wax}$ sampling interval is ~800 yr over the whole core.

3.3 Backwards Trajectory Models

The NOAA Hybrid Single Particle Lagrangian Integrated Trajectory (HYSPLIT) 4 Model (Draxler and Hess, 1998) was used to determine pathways of moisture transport for precipitation reaching Lake Turkana (Fig. 3). HYSPLIT backwards-models of air mass

trajectories were generated for Lake Turkana for every month for five years (2004–2008) using the NCEP Global Reanalysis dataset (Fig. 3). Models were run in reverse from the location of the South Basin of Lake Turkana (2.6° N, 36.6° E) for 174 hours with a new trajectory started every 6 hours. Monthly rainfall data from 1960-2013 from Lodwar and Nairobi, Kenya were acquired from the NOAA National Climatic Data Center to determine seasonal variations in modern rainfall, and precipitation and hydrogen isotope data from Muguga and Kericho, Kenya for 1967 and 1968 were acquired from the GNIP database (Fig. 1). The same HYSPLIT models were run for the location of Muguga from 2008 to 2011 to determine moisture sources for comparison to instrumental precipitation datasets.

4 Results

4.1 Leaf Wax Isotope results

δD_{wax} values from Lake Turkana sediment average -111‰, and vary from -144‰ during the peak of the African Humid Period (AHP) to -69‰ during the LGM (Fig. 2). Waxes deposited between the LGM and ~17 ka are relatively D-enriched and vary from -69‰ to -104‰. Between ~17 and 13.7 ka, δD_{wax} could not be measured from samples from these cores due to low compound concentrations. This time period corresponds to a period of severely low lake level at Lake Turkana, when total organic carbon values preserved in sediment cores were ~≤1% (Morrissey and Scholz, 2014). At 13.7 ka, values near -93‰ are similar to the LGM, and δD_{wax} then abruptly shifts to more D-depleted values reaching -116‰ over an interval of ~600 years. From 13.7 ka to ~6.1 ka, δD_{wax} remains depleted, with an average of -125‰. δD_{wax} exhibits several ~10‰ fluctuations during the AHP, as well as a ~30‰ D-enrichment at 8.1 ka. Between 7 and 6 ka, δD_{wax}

gradually become more enriched, then varies between -89‰ and -120‰ with an average of -110‰ until ~1.5 ka. After 1.5 ka, δD_{wax} becomes progressively more enriched towards the top of the record. Values after 1.4 ka are the most enriched since the LGM.

$\delta^{13}C_{wax}$ varies from -33‰ to -20‰ with an average of -28‰ (Fig. 2). Between 19.5 ka and 13.5 ka, $\delta^{13}C_{wax}$ varies between -22‰ and -27‰. Values are more depleted (-30‰ to -33‰) from 11.4 until 3.6 ka with the exception of an enriched sample (-24‰) at 9.2 ka. After 3.6 ka, $\delta^{13}C_{wax}$ becomes more enriched reaching values of up to -20‰ at 0.4 ka. The $\delta^{13}C_{wax}$ of C_{26} and C_{28} *n*-acid (r^2 = 0.27, p = <0.0001) but the number of samples is low (n = 19). $\delta^{13}C_{wax}$ is inversely correlated with δD_{wax} with an r^2 of 0.59 (Fig. S1).

4.2 Backwards trajectory analysis

Results from HYSPLIT analysis at both Lake Turkana and Muguga indicate that nearly all of the air masses that influence these sites are derived from the Indian Ocean; however, the region of the Indian Ocean from which the air masses are derived differs throughout the year. The two main directions which air masses travel correspond to the two annual African Monsoons experienced by much of the East African tropics. During the April and May rainy season (Fig. 3), air masses are derived from the SE, and enter East Africa near the coast of Mombasa and Dar es Salaam (Fig. 1). During the second rainy season in November and December (Fig. 3), air masses flow from the NE, off the coast of Somalia.

5 Discussion

Our data document very large variations in vegetation, rainfall, and atmospheric circulation over Lake Turkana during the late Pleistocene and Holocene. Below we discuss these data in the context of other regional records of past climate.

5.1 Changing Vegetation and its Impacts on δD_{wax}

Moisture availability, temperature, and atmospheric CO_2 concentrations are important determinants of the relative abundances of C_3 and C_4 plants in Africa. Of these, precipitation is thought to be the dominant control, due to the strong effects of precipitation on the relative abundances of trees, which are mostly C_3 plants, versus grasses (mostly C_4) in semi-arid to arid savannahs and steppe (Mohammed et al., 1995). The landscape surrounding Lake Turkana today sustains sparse plant life near the water's edge (Hemming, 1972; Hopson, 1982; Vincens, 1982; Mohammed et al., 1995) and a mix of grasses, chenopods, etc. in the catchment. Our $\delta^{13}C_{wax}$ data document substantial changes to this community through time.

Depleted $\delta^{13}C_{wax}$ values near ~30‰ (Fig. 2) indicate C_3 plants were especially prevalent on the landscape during the AHP. This stands in contrast to the present, where C4 plants dominate and $\delta^{13}C_{wax}$ values average ~20‰. The range of values of $\delta^{13}C_{wax}$ from Lake Turkana is greater than that reported from other locations within East Africa: the overall range in $\delta^{13}C_{wax}$ values is ~13‰ in Turkana, whereas it is ~2‰ in Lake Malawi ~6.5‰, at Lake Tana and ~11.5‰ at Lake Tanganyika (Tierney et al., 2010; Konecky et al., 2011; Costa et al., 2014). Indeed, the maximum difference observed at Turkana is comparable to the maximum difference in $\delta^{13}C_{wax}$ compositions between C_3 and C_4 plants of ~14.9‰ (Smith and Freeman, 2006; Chikaraishi and Naraoka, 2007). The range in values

in the Turkana record indicate a significant shift in vegetation regimes between ~13 to 3.8 ka and suggest a more hospitable environment may have persisted in the Turkana region during the AHP. The $\delta^{13}C_{wax}$ record collected as part of this study is the only early and mid Holocene vegetation proxy derived from the Turkana region to date and indicates large changes in the vegetation of this hyperarid basin during the wet conditions of the African Humid Period.

The δD_{wax} and $\delta^{13}C_{wax}$ records derived from the sediment cores are highly correlated ($r^2 = 0.60$) (Fig. 2). While this effect is likely due to the fact that δD_{wax} records hydrologic changes that affect plant distribution, it likely also suggests that changes in vegetation affected the hydrogen isotope record. Differing biosynthetic processes between C_4 and C_3 plant types can produce D-enrichment of up to 20‰ in environments with 100% C_4 plants compared to environments with 100% C_3 plants (Sachse et al., 2012). Changes in the relative abundance of C_4 versus C_3 plants can be estimated from $\delta^{13}C_{wax}$ values (Schefuss et al., 2011; Costa et al., 2014), which vary from approximately -22‰ to -37‰ for C_4 and C_3 plants, respectively (Chikaraishi et al., 2004). Variations in $\delta^{13}C_{wax}$ can thus be used to evaluate the influence of these plant types on the δD_{wax} record.

The δD_{wax} samples with contemporaneous $\delta^{13}C_{wax}$ values were corrected for vegetation type, assuming a maximum 20‰ difference in δD_{wax} between C_4 and C_3 plants using the same water source (Fig. 4) (Castañeda, et al., 2009). Given this 20‰ difference, δD_{wax} from Lake Turkana could potentially vary by up to 17‰, solely due to differences in types of vegetation through time. In particular, the replacement of C_4 by C_3 vegetation amplifies the δD depletion observed during the African Humid Period relative to the LGM and late Holocene at Lake Turkana (Fig. 4). After correction, the full range of vegetation-

corrected δD_{wax} from Lake Turkana is approximately 70‰, which must reflect changes in the δD of precipitation itself, likely due either to changes in the amount of precipitation or in precipitation sources.

5.2 Isotope Climatology

Numerous processes control the isotopic composition of precipitation including rainout and rainfall amounts, moisture source, moisture transport, and evapotranspiration from the landscape and vegetation. While many of these processes cannot be constrained in paleodata, recent work has highlighted the importance of changing moisture sources during past climate changes in East Africa. At present, moisture within air masses from the Congo Basin and the Indian Ocean has different isotopic compositions, which creates spatial variability in the isotopic composition of precipitation across Africa (Rozanski et al., 1993). Due to its proximity to the equator, Lake Turkana in northern Kenya receives rainfall at two different times of the year associated with the twice-annual passage of the ITCZ through the region. HYSPLIT air mass backwards trajectory models show that modern Lake Turkana receives moisture exclusively from the Indian Ocean (Fig. 3). Climate stations near Lake Turkana also receive the majority of their moisture from the Indian Ocean (Figure S3), and hydrogen isotope values of this precipitation have a relatively D-depleted average composition of -13.7‰ in Muguga in central Kenya (Fig. 1) (Rozanski et al., 1993).

The unimodal source stands in contrast to many other sites of previous δD_{wax} reconstructions from the region that receive moisture from both the Indian Ocean and Congo Basin sources at different times of the year. For instance, Lake Tana in Ethiopia

receives moisture from multiple sources, but during the AHP it received a greater contribution from Atlantic-derived sources (Costa et al., 2014); a study of Lake Challa in central Kenya also suggests an increased influence of an easterly CAB during the AHP (Tierney et al., 2011). A change in source is one possible hypothesis for the AHP D-depletion present in the Turkana record.

A strong inverse relationship between the amount and isotope composition of rainfall has been observed at tropical latitudes (Dansgaard, 1964; Rozanski, et al., 1993). The "amount effect" operates mainly at the level of individual rainfall events, and it is difficult to extrapolate to paleo- or even monthly precipitation records due to the interactions between moisture transport, rainout, and local rainfall amounts. However, the hydrogen isotope compositions of monthly precipitation for 1967 and 1968 from Muguga and Kericho, Kenya, south of Lake Turkana, are inversely correlated ($r^2 = 0.1788$, $p = 0.02$, $n = 30$) (S2) to monthly precipitation amounts. Muguga, like Lake Turkana, receives all of its precipitation from Indian Ocean-derived moisture sources. The sources of moisture and seasonality are the same for Lake Turkana and Muguga (Fig. 5); this suggests that an amount effect likely exists at Lake Turkana, as is common of many regions in the tropics (Dansgaard, 1964; Rozanski et al., 1993) (Fig. 5). To approximate the possible impacts of an amount effect on the δD_{wax} record from Lake Turkana, a cumulative total of monthly δD values was derived from weighted monthly precipitation at Muguga (S Table 1). The month with the least amount of rain (July) was then subtracted from this amount to yield the amplitude of D-depletion in precipitation produced by rainfall amounts on a monthly basis. The computed amplitude for modern rainfall amount effect is ~18‰ per month (S Table 1).

Multiple lake level reconstructions derived for Lake Turkana indicate that lake level was much higher during the AHP (Halfman and Johnson, 1988; Garcin et al., 2009, 2012a; Morrissey and Scholz, 2014). While the amount of precipitation increase that caused basin filling during this time period is not precisely known, a recent modeling study of paleo Lake Suguta, located in the valley immediately south of Lake Turkana that shares a similar AHP lake level history, indicates a minimum 26% increase in precipitation is required to fill Lake Suguta, and a maximum increase of 40% may have occurred during the peak of the AHP (Junginger and Trauth, 2013). These calculated percentages were used to estimate possible isotope depletion resulting from an increase in precipitation amount at the Turkana area during the AHP (Fig. 4). Increases in precipitation of 26% and 40% (relative to ~200 mm modern accumulation) at Lake Turkana correspond to an additional ~52 mm and ~80 mm of rainfall, respectively, and δD depletion of -23‰ and -25‰. These were each applied to the vegetation-corrected dataset. An extreme case of a 100% precipitation increase (-36‰) was modeled for comparison. Calculations with both the 26% and 40% increases in precipitation yield reasonable results (Fig. 4) as neither yields AHP isotope values more enriched than modern values. Yet even after this calculation, the AHP appears D-depleted and this residual depletion is likely due to change in moisture source.

5.4 Changes in Moisture source to Lake Turkana

The vegetation-corrected δD_{wax} values vary by more than 70‰ between the relatively enriched values around the LGM and depleted values during the AHP, and the amplitude of change in δD_{wax} is greater than the most liberal realistic estimations of an amount effect. While the amount effect is very difficult to constrain on modern, let alone

paleo times-scales, this suggests that there must be another cause for D-depletion during the AHP. We suggest that the eastward movement of the Congo Air Boundary may explain the severely depleted δD_{wax} values at Lake Turkana during the AHP, due to transport of Atlantic moisture via the Congo Basin.

Sources of moisture over East Africa include the Indian Ocean, the Atlantic Ocean by way of West Africa, or Mediterranean, Red Sea and Gulf of Aden sources (Camberlin et al., 2001; Castañeda et al., 2009; Gimeno et al., 2010; Tierney et al., 2011, 2013; Costa et al., 2014). These different sources may provide precipitation to different areas at various times of the year, and account for differing percentages of annual cumulative rainfall (Levin et al., 2009; Costa et al., 2014). Regions closest to the eastern coast of the continent rely on monsoonal rains derived from the Indian Ocean, and HYSPLIT modeling indicates Lake Turkana's moisture is derived from the Indian Ocean-derived monsoons. However, sites further to the west receive significant contributions of moisture from the Atlantic Ocean. These air masses traverse the heavily vegetated Congo Basin and West African lowland rainforests, where high rates of transpiration result in minimal isotopic distillation and relatively enriched water vapor. However, this moisture becomes D-depleted as it moves out of the Congo Basin over drier land to the East African Rift, resulting in a D-depleted isotopic composition distinguishable from other East African moisture sources (Konecky et al., 2011; Tierney et al., 2011; Costa et al., 2014).

Based upon our estimates of the amount effect, changes in moisture source may have had an effect of up to -18‰ on the δD_{wax} record in Turkana. Other studies suggest that a change in moisture source caused changes in δD_{wax} isotope compositions over time at locations in East Africa (e.g. Costa et al., 2014). Significant depletion at Lake Tana in the

Ethiopian Highlands during the AHP is attributed to eastward movement of the CAB for several thousand years, allowing more Congo-derived moisture to contribute to the rainfall in the Tana region (Costa et al., 2014). The study from Lake Tana used modern rainfall amounts from different regional sources to calculate a -4‰ change with a 30% increase in Congo-derived moisture (Costa et al., 2014). To use this value to explain the residual depletion amount of -6‰ to -18‰ for the Lake Turkana record, (Fig. 4) the percentage of moisture from a Congo source would have to account for a higher percentage of precipitation than at Lake Tana. It is, however, difficult to explain an -18‰ or higher D-depletion at Turkana using the relationship developed at Lake Tana, as it requires greater than 100%Congo-derived moisture increase. Further modification of the moisture source as it moves eastward may explain the elevated D-depletion, such as additional rainout (relative to modern). Lake Turkana is also farther east than Lake Tana, suggesting larger fractionation of the moisture source is possible as it moves across land. Additionally, the area surrounding Lake Turkana is much drier, which enhances distillation, leading to enhanced D-depletion.

Today Atlantic-derived air masses do not provide significant moisture to precipitation in the vicinity of Lake Turkana. Most rainfall associated with Atlantic moisture falls over and around the Congo Basin (Fig. 1) (Schefuss et al., 2005; Tierney et al., 2008), in the western rift valley, or on high elevations to the north, such as the Ethiopian Highlands (Levin et al., 2009; Costa et al., 2014). Past studies of other lakes in the East African Rift System (EARS) suggest that depleted δD_{wax} during the AHP was mainly due to increased precipitation (Berke et al., 2012). Berke et al. (2012) argue that more significant depletion at Lake Victoria during the AHP was due to increased precipitation rather than

input from a more depleted precipitation source, because the high mountains to the west of Lake Victoria would have prevented eastward migration of the Congo air masses. However, in the present high seasonal precipitation rates have been documented in association with strong westerlies produce localized convergence in modern climatological studies at Lake Victoria (Nicholson, 1998), and other studies suggest that the CAB migrated far enough eastward during the AHP to influence not only Lake Victoria, but also lakes and regions in the Eastern Branch of the EARS as far away as Mt. Kilimanjaro (Tierney et al., 2011; Junginger et al., 2014; Costa et al., 2014). The δD_{wax} record from Lake Turkana supports the inference for significant influence from Congo-derived moisture during the AHP as has been suggested by studies in the past (Ricketts and Johnson, 1996; Morrissey and Scholz, 2014), and further suggests that this moisture source may have been large, in not dominant, in the Turkana basin. The additional precipitation source allowed Lake Turkana to overflow for several thousand years during the early Holocene and provided an input to the White Nile River (Morrissey and Scholz, 2014).

5.5 Insolation variability and long-term climate changes

High precipitation in Northern and Eastern Africa during the AHP occurred during periods of increased northern hemisphere summer insolation (Fig. 6) (deMenocal et al., 2000; Tierney et al., 2008, 2011; Berke et al., 2012; Costa et al., 2014). The long-term precipitation changes as indicated by δD_{wax} from Lake Turkana also follow boreal summer insolation changes; however, there are some important differences in the onset and termination of increased moisture observed in this data set relative to other regional records. Relatively depleted δD_{wax} values of ~-140‰ occur from Turkana between 11 and

8.2 ka, while peak insolation in low latitudes of the Northern Hemisphere occurred at 11.1 ka. The most depleted values occur at 8.4 ka, nearly three millennia after insolation began to decrease. This may suggest that an unfavorable atmospheric configuration may have deprived the area of precipitation at times of peak insolation or a contribution of nonlinear feedbacks associated with ecological turnover resulted in a lagged response of regional precipitation to insolation forcing.

The offset between peak insolation and peak isotope depletion may also be due to the ambiguity in relative contributions between moisture source and precipitation amount over time. While we suggest that both of these factors affected the δD_{wax} record preserved at Lake Turkana, as highlighted above the relative differences in the effect of one or the other are difficult to separate. The model presented here suggests that at the time of initial depletion, both source and amount also changed, however that may not actually be the case. For instance, the intensification of the monsoons and increase in rainfall amount may have initially caused D-depletion at 13.7 ka, the influence of the CAB migration may not have occurred until later when peak depletion is seen at 8.4 ka instead of during peak insolation. This would imply that different climatological forcings and/or processes cause migration of the ITCZ and of the CAB during the AHP.

5.6 Regional variation during the AHP

The δD_{wax} records collected from East African lakes show a delay in the timing and a decrease in magnitude of change in a south- and eastward direction (Fig. 6) associated with the onset of the AHP. The initial and most dramatic D-depletions associated with the African Humid Period occurs at Lake Tana (12° N) where δD_{wax} shifts from -84‰ to -

163‰ between 13.6 and 11.6 ka (Costa et al., 2014) and at Lake Turkana (2° N) with a shift from -93‰ to -131‰ between 13.7 and 12.7 ka. While slight depletions occur at Lakes Challa and Tanganyika as early as 15 ka, the largest amplitude depletions do not occur until after YD enrichment (Tierney et al., 2008; Tierney et al., 2011). At Lake Challa (3° S), depletion from -81‰ to -116‰ occurs between 12.2 and 11.4 ka (Tierney et al., 2011) and Lake Tanganyika (6° S) follows at 11.8 ka with depletion from -95‰ to -129‰ (Tierney et al., 2008). Lake Malawi (10° S) shows negligible response to AHP forcing (Konecky et al., 2011). Farther to the east, a δD_{wax} record from the Gulf of Aden, thought to record δD_{precip} over Somalia and the Afar, displays an onset of D-depletion that is similar in timing but of much lower magnitude (<-35‰) compared to Lakes Tana and Turkana (Tierney and deMenocal, 2013; Costa et al., 2014).

Similar variability occurs at the termination of the AHP. Values at Lake Tana are abruptly enriched to late Holocene values at ~7.5 ka (Costa et al., 2014), Turkana experiences a more gradual enrichment from 7.5 to 5.8 ka, followed by further enrichment during the late Holocene. Challa's enrichment does not occur until ~5 ka (Tierney et al., 2011), as does late Holocene enrichment at Lake Tanganyika (Tierney et al., 2008). Waxes in the Gulf of Aden remain D-depleted until ~4 ka however, which is more similar to the record from Lake Turkana.

Hydrogen isotopic records that record the African Humid Period across East Africa reveal considerable variability in the amplitude and timing of isotope fluctuations, and therefore in the regional climate changes that caused the AHP. The Turkana δD_{wax} values vary from -93‰ to -137‰ from the onset of the AHP at ~13.7 ka to the peak of the AHP at ~10 ka. At Lake Tana in the Ethiopian Highlands, and in the Gulf of Aden, the transition

from D-enriched to D-depleted values is nearly synchronous with initial D-depletion at Lake Turkana (Fig. 2) at ~13.5 ka. However, these records differ substantially in their amplitudes, with Lakes Tana and Turkana displaying a much larger signal than the Gulf of Aden. This could reflect a stronger contribution of Congo-derived moisture to Tana and Turkana, as the Ethiopian highlands should limit moisture transport from westerly sources to Somalia. Hydrogen isotope values from Lake Tanganyika were already moderately depleted at the time (Tierney et al., 2008), while Lake Challa, which has a comparatively small δD_{wax} signal during the AHP, was already relatively D-depleted at the onset of the AHP and remained D-depleted until ~12 ka, after which it became enriched (values as enriched as -80‰) for a few hundred years (Tierney et al., 2011). The new Turkana data support the theory that the CAB may have migrated seasonally at least as far east as the Kenyan Rift area at the onset of the AHP. D-depleted values that persist during the interval from 13.7 to at least 6 ka require Congo Basin moisture contributions to Lake Turkana and the Kenyan Rift, however the relative contribution of Congo- versus Indian Ocean sources likely fluctuated over the time period as evidenced by fluctuations in δD_{wax} values throughout the time period. Alternatively, precipitation amount was less at times as suggested by fluctuations in the δD_{wax} values.

Through the mid to late Holocene, δD_{wax} values at Lake Turkana slowly become more enriched. The magnitude of change in δD_{wax} from the AHP to present is much less at Turkana when compared to Lake Tana (Costa et al., 2014), and the transition at Turkana is more gradual. This trend at Turkana is similar in the timing of the transition in the δD_{wax} record from the Gulf of Aden (Tierney and deMenocal, 2013), which suggests the Kenyan Rift as well as coastal regions of Kenya and Somalia remained wetter through the mid-

Holocene. Lake Challa and Lake Tanganyika also remain relatively depleted until ~6 ka (Tierney et al., 2011; Tierney et al., 2008). This may suggest a sustained contribution from a southward-shifted, Congo-derived source or gradually diminishing precipitation amounts due to southward ITCZ migration and weakening monsoons through the mid-Holocene than sites to the north. Presently available data cannot quantify these influences, however the spatial variability observed in the records suggests both variability in both the timing and relative contributions of changes in precipitation amount and Congo-derived moisture sources.

Precipitation changes associated with the AHP appear to be temporally and geographically transgressive, based on these records, and the abruptness of precipitation change varies among locations. deMenocal et al. (2000) attribute abrupt responses at the onset and end of the AHP to insolation forcing plus the effects of non-linear feedbacks such as vegetation changes. Others argue that presence or lack of contribution from moisture west of the CAB can enhance abrupt changes seen in δD_{wax} (Tierney et al., 2008; Tierney et al., 2011; Costa et al., 2014). The δD_{wax} record from Lake Turkana suggests that the onset of increased precipitation was abrupt, occurring over just centuries, however the end of the AHP was gradual. The high correlation between the $\delta^{13}C_{wax}$ and δD_{wax} records from Lake Turkana suggests that vegetation feedbacks were likely important in the abrupt response to insolation forcing at the onset of the AHP. However, the persistent correlation between the two isotopes through the gradual end to the AHP suggests that vegetation was sustained after insolation decreased. Since the migration of the ITCZ and monsoonal moisture is more closely coupled to insolation changes than the movement of the CAB, the

sustained vegetation and persistent depletion in δD_{wax} at the end of the of the AHP is likely due to sustained contribution from Congo-derived moisture.

5.7 Northern latitude teleconnections

Between 8.4 and 8.1 ka, there is an enrichment of ~45‰ in the δD_{wax} values at Lake Turkana. This is close in timing to a significant enrichment of ~55‰ at Lake Tana that occurred between 8.5 and 7.8 ka (Costa et al., 2014). This enrichment is short lived at Lake Turkana, with values returning to background depleted values of less than -120‰ by ~7.5 ka. The enrichment may be associated with the 8.2 ka event described at in high latitude ice cores (Alley et al., 1997), and Junginger and Trauth (2013) and Costa et al. (2014) suggest the CAB may have been forced south- and east due to the intensified NE winds. Paleoshorelines below the highstand sill in the South Basin of Lake Turkana are dated to approximately the same time period, which suggest lake level was not at highstand for this interval during the AHP (Garcin et al., 2012a). The δD_{wax} enrichment further confirms a reduction in precipitation in the region during this short-lived lake level lowstand. The short-term signals observed in the Lake Turkana δD_{wax} record suggest a possible teleconnection between high latitude climate phenomenon and tropical climate processes.

6 Conclusions

- δD_{wax} values fluctuated by an amplitude of 74‰ between the relatively D-enriched values around the LGM and D-depleted values during the AHP. This amplitude exceeds that of most other δD_{wax} records from East Africa indicating significant change in precipitation since the LGM.

- The CAB does not migrate far enough eastward to allow Congo basin-derived moisture to Lake Turkana today, and the lake instead relies on moisture from the African Monsoons.
- HYSPLIT backwards modeling of air mass trajectories indicate that modern precipitation at Lake Turkana is derived exclusively from the Indian Ocean.
- Modern seasonal Kenyan precipitation amount correlates with isotopic changes. D-enrichment of precipitation of up to ~25‰ occurs during months of high precipitation, suggesting a significant amount effect could potentially account for amplitude change in the δD_{wax} paleorecord from Lake Turkana.
- Fluctuations in the hydrogen isotope composition of leaf waxes are in part due to changes in vegetation turnover between C_3 and C_4 plants during extreme climate changes in the Turkana region. During the AHP, both carbon and hydrogen isotopes are more depleted, suggesting that C_3 plants likely dominated the landscape during this time.
- During the AHP (~14 ka–6 ka), the CAB migrated at least as far as central Kenya for most of the duration; however enriched δD_{wax} at 8.1 ka interrupt this period of depletion, suggesting a reduction in CAB influence or an extreme alteration of the isotope composition of the CAB air mass. These could be related to high latitude climate teleconnections in the EAR in the late Quaternary or changes in SST gradients in the western Indian Ocean.
- The onset of the AHP signal in the δD_{wax} is rather abrupt, occurring over just a few centuries, and is likely due to insolation-driven increased rainfall and vegetation feedbacks as indicated by highly correlative δD_{wax} and $\delta^{13}C_{wax}$ records. The

termination of the AHP is much more gradual than at other places in East Africa, starting at about 8 ka and reaching late Holocene average values at ~4 ka, and is likely due to sustained contributions from Congo-derived moisture.

- Differences in time of onset, amplitude, duration, and time of termination of AHP moisture among East African δD_{wax} records suggest the AHP was a time transgressive event that had variable influence across the region.

7 Acknowledgements

We thank the government of Kenya for research permissions. Financial support was provided by the sponsors of the Syracuse University Lacustrine Rift Basins Research Program. We thank the National Oil Corporation of Kenya for assistance during field operations. The authors thank the people of Loiyangalani and the Turkana Rift Valley, for their cooperation, assistance, and hospitality during multiple field seasons at Lake Turkana. We would also like to thank Dr. Rafael Tarozo, Dr. Bronwen Konecky, Lily Cohen, and Kassandra Costa for assistance with sample preparations and laboratory procedures at Brown University.

References

Abram, N.J., Gagan, M.K., Liu, Z., Hantoro, W.S., McCulloch, M.T., and Suwargadi, B.W., 2007, Seasonal characteristics of the Indian Ocean Dipole during the Holocene epoch: Nature, v. 445, no. 7125, p. 299–302, doi: 10.1038/nature05477.

Alley, R.B., Mayewski, P.A., Sowers, T., Stuiver, M., Taylor, K.C., and Clark, P.U., 1997, Holocene climatic instability: A prominent, widespread event 8200 yr ago: Geology, v. 25, p. 483–486, doi: 10.1130/0091-7613(1997)025<0483.

Berke, M.A., Johnson, T.C., Werne, J.P., Grice, K., Schouten, S., and Sinninghe, J.S., 2012, Molecular records of climate variability and vegetation response since the Late Pleistocene in the Lake Victoria basin, East Africa: Quaternary Science Reviews, v. 55, p. 59–74.

Blaauw, M., and Christen, J.A., 2011, Flexible Paleoclimate Age-Depth Models Using an Autoregressive Gamma Process: Bayesian Analysis, v. 6, no. 3, p. 457–474, doi: 10.1214/11-BA618.

Broecker, W.S., Kennett, J.P., Flower, B.P., Teller, J.T., Trumbore, S., Bonani, G., Wolfi, W., 1989, Routing of meltwater from the Laurentide Ice Sheet during the Younger Dryas cold episode: Nature, v. 341, p. 318-321.

Burlando, M., Durante, F., and Claveri, L., 2010, The Lake Turkana Wind Farm Project: DEWI Magazin, v. 37, p. 6–15.

Camberlin, P., Janicot, S., and Poccard, I., 2001, Seasonality and atmospheric dynamics of the teleconnection between African rainfall and tropical sea-surface temperature: Atlantic vs. ENSO: International Journal of Climatology, v. 21, no. 8, p. 973–1005, doi: 10.1002/joc.673.

Castañeda, I.S., Mulitza, S., Schefuß, E., Lopes dos Santos, R.A., Sinninghe-Damsté, J.S., and Schouten, S., 2009, Wet phases in the Sahara/Sahel region and human migration patterns in North Africa: Proceedings of the National Academy of Sciences of the United States of America, v. 106, no. 48, p. 20159–20163.

Cerling, T.E., 1986, A mass-balance approach to basin sedimentation: Constraints on the recent history of the Turkana Basin: Palaeogeography, Palaeoclimatology, Palaeoecology, v. 54, p. 63–86.

Chikaraishi, Y., and Naraoka, H., 2003, Compound-specific δD–δ13C analyses of n-alkanes extracted from terrestrial and aquatic plants: Phytochemistry, v. 63, no. 3, p. 361–371, doi: 10.1016/S0031-9422(02)00749-5.

Chikaraishi, Y., Naraoka, H., and Poulson, S.R., 2004, Hydrogen and carbon isotopic fractionations of lipid biosynthesis among terrestrial (C3, C4 and CAM) and aquatic plants.: Phytochemistry, v. 65, no. 10, p. 1369–81, doi: 10.1016/j.phytochem.2004.03.036.

Chikaraishi, Y., and Naraoka, H., 2007, δ13C and δD relationships among three n-alkyl compound classes (n-alkanoic acid, n-alkane and n-alkanol) of terrestrial higher plants: Organic Geochemistry, v. 38, no. 2, p. 198–215, doi: 10.1016/j.orggeochem.2006.10.003.

Costa, K., Russell, J., Konecky, B., and Lamb, H., 2014, Isotopic reconstruction of the African Humid Period and Congo Air Boundary migration at Lake Tana, Ethiopia: Quaternary Science Reviews, v. 83, p. 58–67, doi: 10.1016/j.quascirev.2013.10.031.

Dansgaard, W., 1964, Stable isotopes in precipitation: Tellus XVI, v. 4, p. 436 – 468.

deMenocal, P., Ortiz, J., Guilderson, T., Adkins, J., Sarnthein, M., Baker, L., and Yarusinsky, M., 2000, Abrupt onset and termination of the African Humid Period : rapid climate responses to gradual insolation forcing: Quaternary Science Reviews, v. 19, p. 347–361.

Draxler, R. R., Hess, G. D., 1998, An overview of the HYSPLIT_4 modeling system of trajectories, dispersion, and deposition: Australian Meteorological Magazine, v. 47, p. 295-308.

Foerster, V., Junginger, A., Langkamp, O., Gebru, T., Asrat, A., Umer, M., Lamb, H.F., Wennrich, V., Rethemeyer, J., Nowaczyk, N., Trauth, M.H., and Schaebitz, F., 2012, Climatic change recorded in the sediments of the Chew Bahir basin, southern Ethiopia, during the last 45,000 years: Quaternary International, v. 274, p. 25–37, doi: 10.1016/j.quaint.2012.06.028.

Ferguson, A.J.D. and Harbott, B.J., 1982, Geographical, physical, and chemical aspects of Lake Turkana, in: Hopson, A.J. (Ed.), Lake Turkana: A Report on the Findings of the Lake Turkana Project, 1972-1975. Overseas Development Administration, London, pp. 1–108.

Garcin, Y., Junginger, A., Melnick, D., Olago, D.O., Strecker, M.R., and Trauth, M.H., 2009, Late Pleistocene–Holocene rise and collapse of Lake Suguta, northern Kenya Rift: Quaternary Science Reviews, v. 28, no. 9-10, p. 911–925, doi: 10.1016/j.quascirev.2008.12.006.

Garcin, Y., Melnick, D., Strecker, M.R., Olago, D., and Tiercelin, J.-J., 2012a, East African mid-Holocene wet–dry transition recorded in palaeo-shorelines of Lake Turkana, northern

Kenya Rift: Earth and Planetary Science Letters,, p. 322–334, doi: 10.1016/j.epsl.2012.03.016.

Garcin, Y., Schwab, V.F., Gleizner, G., Kahmen, A., Todou, G., Sene, O., Onana, J-M., Achoundong, G., and Sachse, D., 2012b, Hydrogen isotope ratios of lacustrine sedimentary n-alkanes as proxies of tropical African hydrology: Insights from a calibration transect across Cameroon: Geochimica et Cosmochimica Acta, v. 79, p. 106-126.

Gimeno, L., Drumond, A., Nieto, R., Trigo, R.M., and Stohl, A., 2010, On the origin of continental precipitation: Geophysical Research Letters, v. 37, no. 13, p. L13804, doi: 10.1029/2010GL043712.

Halfman, J.D., and Johnson, T.C., 1988, High-resolution record of cyclic climatic change during the past 4 ka from Lake Turkana, Kenya: Geology, v. 16, p. 496–500, doi: 10.1130/0091-7613(1988)016<0496.

Hemming, C.F., 1972, The South Turkana Expedition: Scientific Papers VIII. The ecology of South Turkana: A Reconnaissance Classification: Geography Journal, v. 138, p. 15 – 40.

Hopson, B.J., ed., 1982, A report on the findings of the Lake Turkana Project 1972-1975: Government of Kenya and the Ministry of Overseas Development, London.

Huang, Y., Shuman, B., Wang, Y., and Iii, T.W., 2002, Hydrogen isotope ratios of palmitic acid in lacustrine sediments record late Quaternary climate variations: Geology, v. 30, p. 1103–1106, doi: 10.1130/0091-7613(2002)030<1103.

Huang, Y., Shuman, B., Wang, Y., and Iii, T.W., 2004, Hydrogen isotope ratios of individual lipids in lake sediments as novel tracers of climatic and environmental change: a surface sediment test: Journal of Paleolimnology, v. 31, p. 363–375.

Huggett, R.., 1998, Soil chronosequences, soil development, and soil evolution: a critical review: Catena, v. 32, no. 3-4, p. 155–172, doi: 10.1016/S0341-8162(98)00053-8.

IAEA/WMO, 2013, Global Network of Isotopes in Precipitation, The GNIP Database, Accessible at: http://www.iaea.org/water.

Junginger, A., and Trauth, M.H., 2013, Hydrological constraints of paleo-Lake Suguta in the Northern Kenya Rift during the African Humid Period (15 – 5 ka BP): v. 111, p. 174–188.

Junginger, A., Roller, S., Olaka, L. A., and Trauth, M.H., 2014, The effects of solar irradiation changes on the migration of the Congo Air Boundary and water levels of paleo-Lake Suguta, Northern Kenya Rift, during the African Humid Period (15–5ka BP): Palaeogeography, Palaeoclimatology, Palaeoecology, v. 396, p. 1–16, doi: 10.1016/j.palaeo.2013.12.007.

Konecky, B.L., Russell, J.M., Johnson, T.C., Brown, E.T., Berke, M.A., Werne, J.P., and Huang, Y., 2011, Atmospheric circulation patterns during late Pleistocene climate changes at Lake Malawi, Africa: Earth and Planetary Science Letters, v. 312, no. 3-4, p. 318–326, doi: 10.1016/j.epsl.2011.10.020.

Lamb, H.F., Bates, C.R., Coombes, P. V., Marshall, M.H., Umer, M., Davies, S.J., and Dejen, E., 2007, Late Pleistocene desiccation of Lake Tana, source of the Blue Nile: Quaternary Science Reviews, v. 26, no. 3-4, p. 287–299, doi: 10.1016/j.quascirev.2006.11.020.

Levin, N.E., Zipser, E.J., and Cerling, T.E., 2009, Isotopic composition of waters from Ethiopia and Kenya: Insights into moisture sources for eastern Africa: Journal of Geophysical Research, v. 114, no. D23, p. D23306, doi: 10.1029/2009JD012166.

Lisiecki, L., and Raymo, M., 2005, A Pliocene-Pleistocene stack of 57 globally distributed benthic $\delta^{18}O$ records: Paleoceanography, v. 20, p. 1-17.

Liu, Z., Otto-Bliesner, B., Kutzbach, J., Li, L., and Shields, C., 2003, Coupled Climate Simulation of the Evolution of Global Monsoons in the Holocene*: Journal of Climate, v. 16, no. 15, p. 2472–2490, doi: 10.1175/1520-0442(2003)016<2472:CCSOTE>2.0.CO;2.

Mohammed, M.U., Bonnefille, R., and Johnson, T.C., 1995, Pollen and isotopic records in Late Holocene sediments from Lake Turkana, Kenya: Palaeoclimatology, Palaeogeography, Palaeoecology, v. 119, p. 371–383.

Morrissey, A. and Scholz, C. A., 2014, Paleohydrology of Lake Turkana and its influence on the Nile River System: Palaeoclimatology, Palaeogeography, Palaeoecology, v. 403, p. 88–100.

Nicholson, S.E., 1998, Historical fluctuations of Lake Victoria and other lakes in the northern Rift Valley of East Africa, in Environmental Change and Response in East African Lakes, ed. Lehman, J.T., Kluwer Academic Publishers, Netherlands.

Nicholson, S.E., 2009, A revised picture of the structure of the “monsoon” and land ITCZ over West Africa: Climate Dynamics, v. 32, no. 7-8, p. 1155–1171, doi: 10.1007/s00382-008-0514-3.

NOAA/NCDC, National Climate Data Center, accessed 9 Feb 2014, http://www.ncdc.noaa.gov/cdo-web/datasets#GHCNDMS.

Ricketts, D. and Johnson, T.C., 1996, Climate change in the Turkana basin as deduced from a 4000 year long d18O record: Earth and Planetary Science Letters, v. 142, p. 7-17.

Rozanski, K., Araguás-Araguás, L., and Gonfiantini, R., 1993, Isotopic Patterns in Modern Global Precipitation, *in* Swart, P.K., Lohmann, K.C., McKenzie, J., and Savin, S. eds., Geophysical Monograph Series, AGU, Washington, D. C., p. 79–93.

Sachse, D., Radke, J., and Gleixner, G., 2004, Hydrogen isotope ratios of recent lacustrine sedimentary n-alkanes record modern climate variability: Geochimica et Cosmochimica Acta, v. 68, no. 23, p. 4877–4889, doi: 10.1016/j.gca.2004.06.004.

Sachse, D., Billault, I., Bowen, G.J., Chikaraishi, Y., Dawson, T.E., Feakins, S.J., Freeman, K.H., Magill, C.R., McInerney, F. A., van der Meer, M.T.J., Polissar, P., Robins, R.J., Sachs, J.P., Schmidt, H.-L., et al., 2012, Molecular Paleohydrology: Interpreting the Hydrogen-Isotopic Composition of Lipid Biomarkers from Photosynthesizing Organisms: Annual Review of Earth and Planetary Sciences, v. 40, no. 1, p. 221–249, doi: 10.1146/annurev-earth-042711-105535.

Saji, N.H., Goswami, B.N., Vinayachandran, P.N., and Yamagata, T., 1999, A dipole mode in the tropical Indian Ocean: Nature, v. 401, no. 6751, p. 360–3, doi: 10.1038/43854.

Schefuss, E., Kuhlmann, H., Mollenhauer, G., Prange, M., and Pätzold, J., 2011, Forcing of wet phases in southeast Africa over the past 17,000 years: Nature, v. 480, no. 7378, p. 509–12, doi: 10.1038/nature10685.

Sessions, A.L., Burgoyne, T.W., Schimmelmann, A., and Hayes, J.M., 1999, Fractionation of hydrogen isotopes in lipid biosynthesis: Organic Geochemistry, v. 30, no. 9, p. 1193–1200, doi: 10.1016/S0146-6380(99)00094-7.

Sessions, A.L., Burgoyne, T.W., and Hayes, J.M., 2001, Determination of the H3 factor in hydrogen isotope ratio monitoring mass spectrometry: Analytical chemistry, v. 73, no. 2, p. 200–7.

Schrag, D.P., Hampt, G., Murray, D.W., 1996, Pore fluid constraints on the temperature and oxygen isotope composition of the glacial ocean: Science, v. 272, p. 1930-1932.

Sinninghe Damsté, J.S., Verschuren, D., Ossebaar, J., Blokker, J., van Houten, R., van der Meer, M.T.J., Plessen, B., and Schouten, S., 2011, A 25,000-year record of climate-induced changes in lowland vegetation of eastern equatorial Africa revealed by the stable carbon-isotopic composition of fossil plant leaf waxes: Earth and Planetary Science Letters, v. 302, no. 1-2, p. 236–246, doi: 10.1016/j.epsl.2010.12.025.

Smith, F. A., and Freeman, K.H., 2006, Influence of physiology and climate on δD of leaf wax n-alkanes from C3 and C4 grasses: Geochimica et Cosmochimica Acta, v. 70, no. 5, p. 1172–1187, doi: 10.1016/j.gca.2005.11.006.

Stager, J.C., Ryves, D.B., Chase, B.M., Pausata, F.S.R., 2011, Catastrophic drought in the Afro-Asian Monsoon region during Heinrich Event 1: Science, v. 331, p. 1299-1302.

Tierney, J.E., Russell, J.M., Huang, Y., Damsté, J.S.S., Hopmans, E.C., and Cohen, A.S., 2008, Northern Hemisphere Controls on Tropical Southeast African Climate During the Past 60,000 Years: Science, v. 322, p. 252–255.

Tierney, J.E., Russell, J.M., and Huang, Y., 2010, A molecular perspective on Late Quaternary climate and vegetation change in the Lake Tanganyika basin, East Africa: Quaternary Science Reviews, v. 29, no. 5-6, p. 787–800, doi: 10.1016/j.quascirev.2009.11.030.

Tierney, J.E., Russell, J.M., Sinninghe Damsté, J.S., Huang, Y., and Verschuren, D., 2011, Late Quaternary behavior of the East African monsoon and the importance of the Congo Air Boundary: Quaternary Science Reviews, v. 30, no. 7-8, p. 798–807, doi: 10.1016/j.quascirev.2011.01.017.

Tierney, J.E., Smerdon, J.E., Anchukaitis, K.J., and Seager, R., 2013, Multidecadal variability in East African hydroclimate controlled by the Indian Ocean: Nature, v. 493, no. 7432, p. 389–92, doi: 10.1038/nature11785.

Tierney, J.E. and deMenocal, P.B., 2013, Abrupt shifts in the Horn of Africa hydroclimate since the Last Glacial Maximum: Science, v. 342, p. 843-846.

Timmermann, A., An, S.-I., Krebs, U., and Goosse, H., 2005, ENSO Suppression due to Weakening of the North Atlantic Thermohaline Circulation: Journal of Climate, v. 18, p. 3122–3139.

Timmermann, a., Okumura, Y., An, S.-I., Clement, a., Dong, B., Guilyardi, E., Hu, a., Jungclaus, J.H., Renold, M., Stocker, T.F., Stouffer, R.J., Sutton, R., Xie, S.-P., and Yin, J., 2007, The Influence of a Weakening of the Atlantic Meridional Overturning Circulation on ENSO: Journal of Climate, v. 20, no. 19, p. 4899–4919, doi: 10.1175/JCLI4283.1.

Vincens, A., 1982, Palynologie, Environments Actuels et Plio-Pléistocènes à l'Est du Lac Turkana (Kenya). Thesis. Univ. Aix-Marseille 2, 244 p.

Verschuren, D., Sinninghe Damsté, J.S., Moernaut, J., Kristen, I., Blaauw, M., Fagot, M., and Haug, G.H., 2009, Half-precessional dynamics of monsoon rainfall near the East African Equator.: Nature, v. 462, no. 7273, p. 637–41, doi: 10.1038/nature08520.

Yuretich, R.F., 1979, Modern sediments and sedimentary processes in Lake Rudolf (Lake Turkana) eastern Rift Valley, Kenya: Sedimentology, v. 26, p. 313–331.

Figures

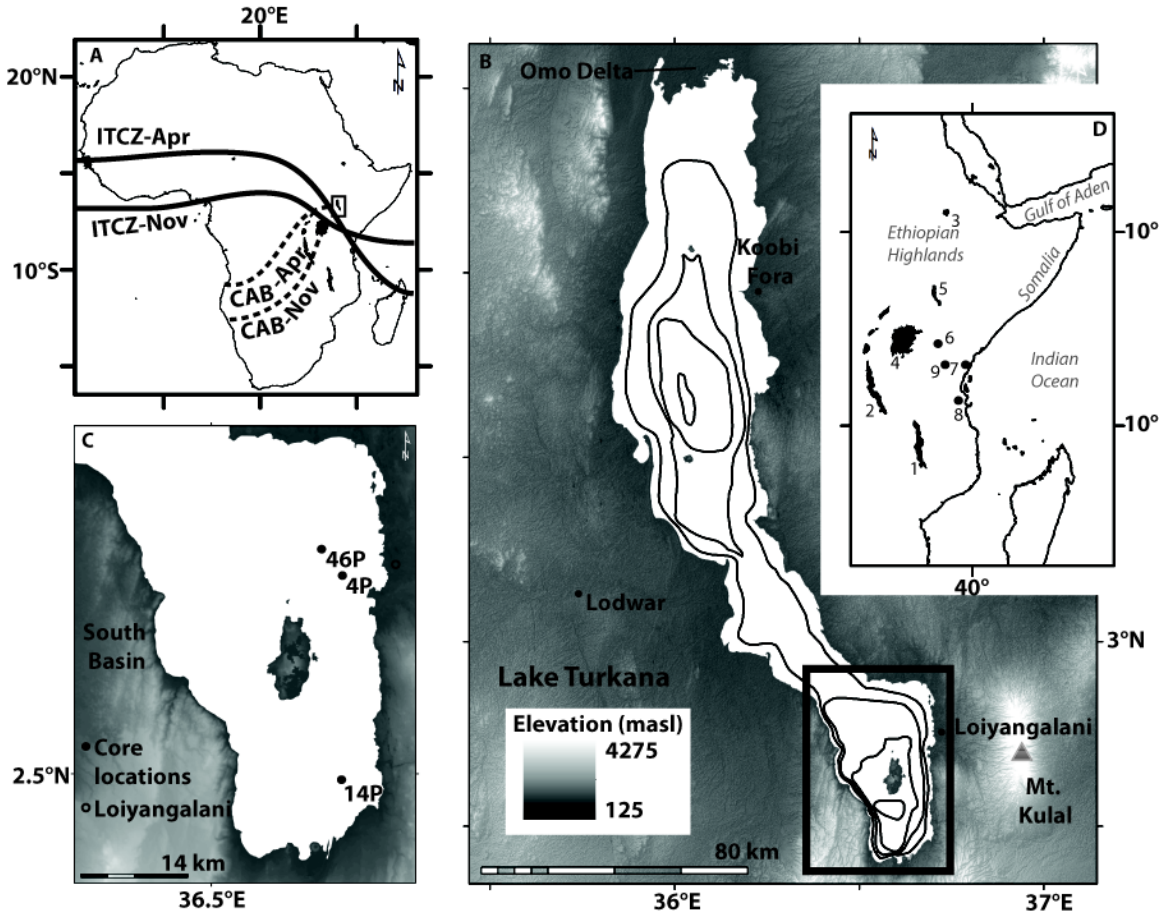

Fig 1. Location Map. (**A**) Africa with rainy season (April and November) locations of the ITCZ and the CAB. Black box locates Lake Turkana. (**B**) Lake Turkana and the surrounding topography. Bathymetry contour interval is 20 m. Black box locates the South Basin. (**C**) South Basin of Lake Turkana with core locations marked by black circles. (**D**) East Africa regional map with relevant locations identified: 1. Lake Malawi, 2. Lake Tanganyika, 3. Lake Tana, 4. Lake Victoria, 5. Lake Turkana, 6. Muguga, Kenya, 7. Mombasa, Kenya 8. Dar es Salaam, Tanzania, 9. Lake Challa.

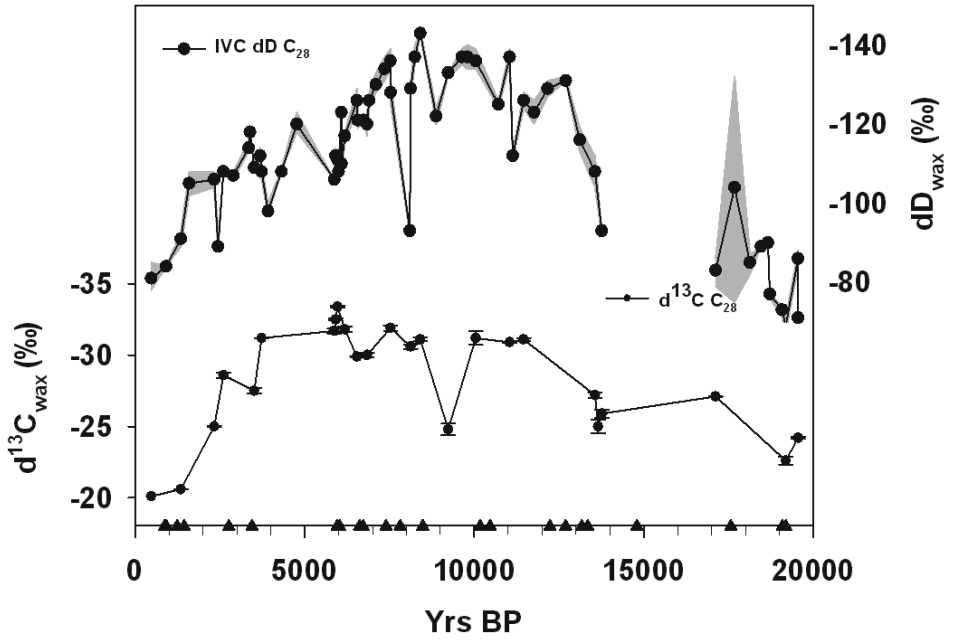

Fig. 2. Isotope data. Upper panel: Mean values of δD_{wax} values of the C_{28} homologue (black circles) from the composite sediment record. Gray error envelope is 1σ for samples run in triplicate and the range of values for samples run in duplicate. Lower panel: Mean $\delta^{13}C_{wax}$ values (black circles) of a subset of samples from the composite sediment record; all were run in duplicate. Error bars span the range of values. The $\delta^{13}C_{wax}$ measurements of the C_{26} and C_{30} homologues are in gray. Black triangles denote locations of samples utilized for ^{14}C dating.

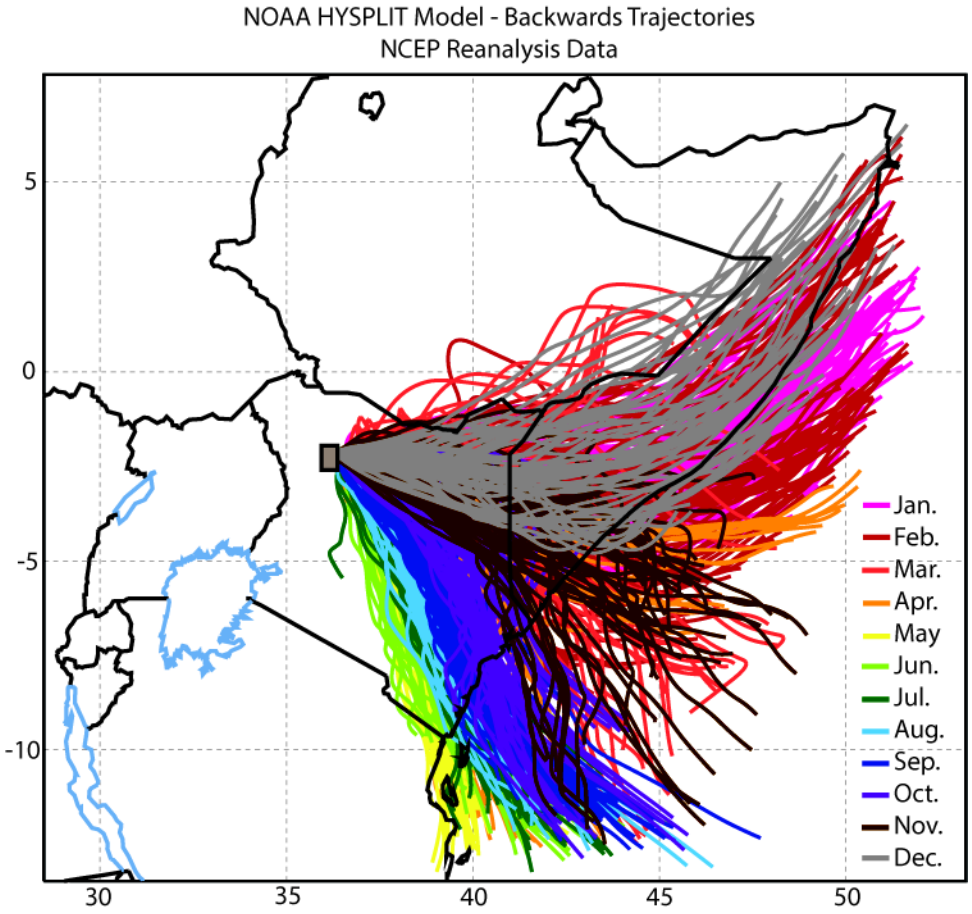

Fig. 3. Backwards trajectory models. NOAA HYSPLIT backward trajectory models for Lake Turkana using NCEP Reanalysis data between 2003-2008. Trajectories are color-coded by month. Lake location indicated by rectangle. Lake Turkana presently receives all of its moisture from Indian Ocean sources, and not from the Atlantic Ocean/Congo Basin.

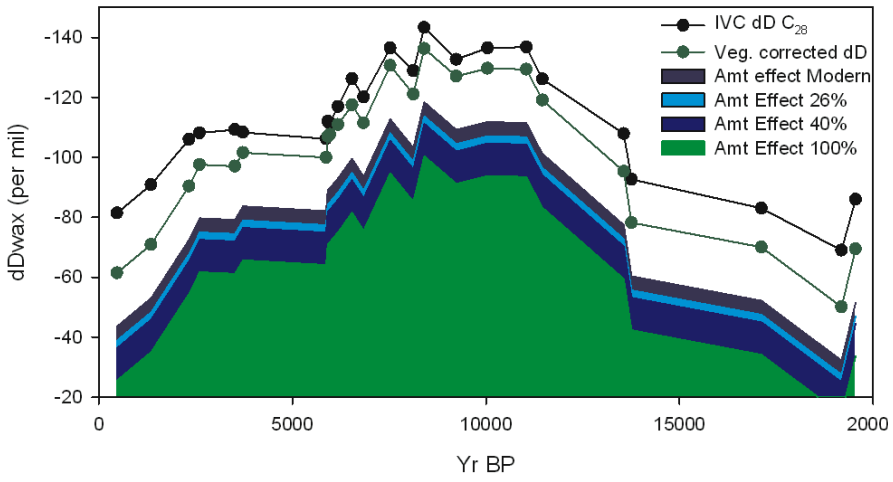

Fig. 4. Isotope corrections. Black data points and line represent ice volume corrected δD_{wax} values that correspond to $\delta^{13}C_{wax}$. Dark green data points and lines represent δD_{wax} values corrected for vegetation type based on $\delta^{13}C_{wax}$ values. The four areas represent the amount effect estimated by four different percentages of increased rainfall and modern isotope data. The darkest blue represents modern rainfall (0% increase), light blue represents the amount effect for a 26% increase in rainfall, medium blue represents the amount effect for a 40% increase in rainfall, and green represents 100% increase in rainfall.

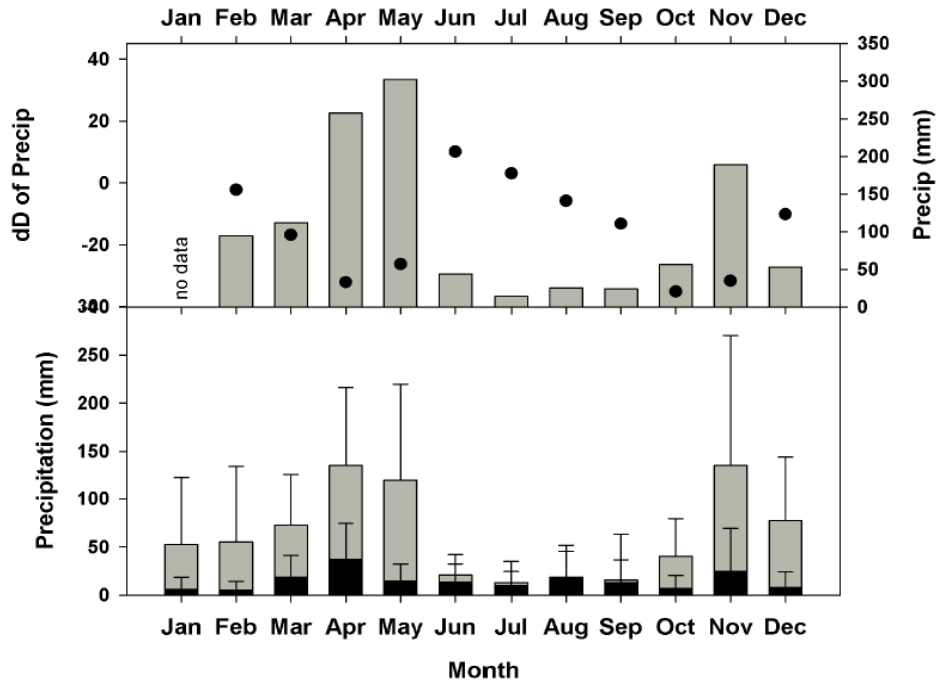

Fig. 5. Kenya rainfall data. Upper panel: Monthly average δD of precipitation at Muguga (Nairobi), Kenya during 1967 and 1968 (black dots) and rainfall amounts (grey bars) (IAEA/WMO, 2013). Lower panel: Mean precipitation amount and 1σ errors (NOAA/NCDC, 2014) at the Jomo-Kenyatta International Airport in Nairobi between 1960-2013 (light gray bars), and at Lodwar, a town west of Lake Turkana, between 1960-2013 (black bars); error bars are 1σ.

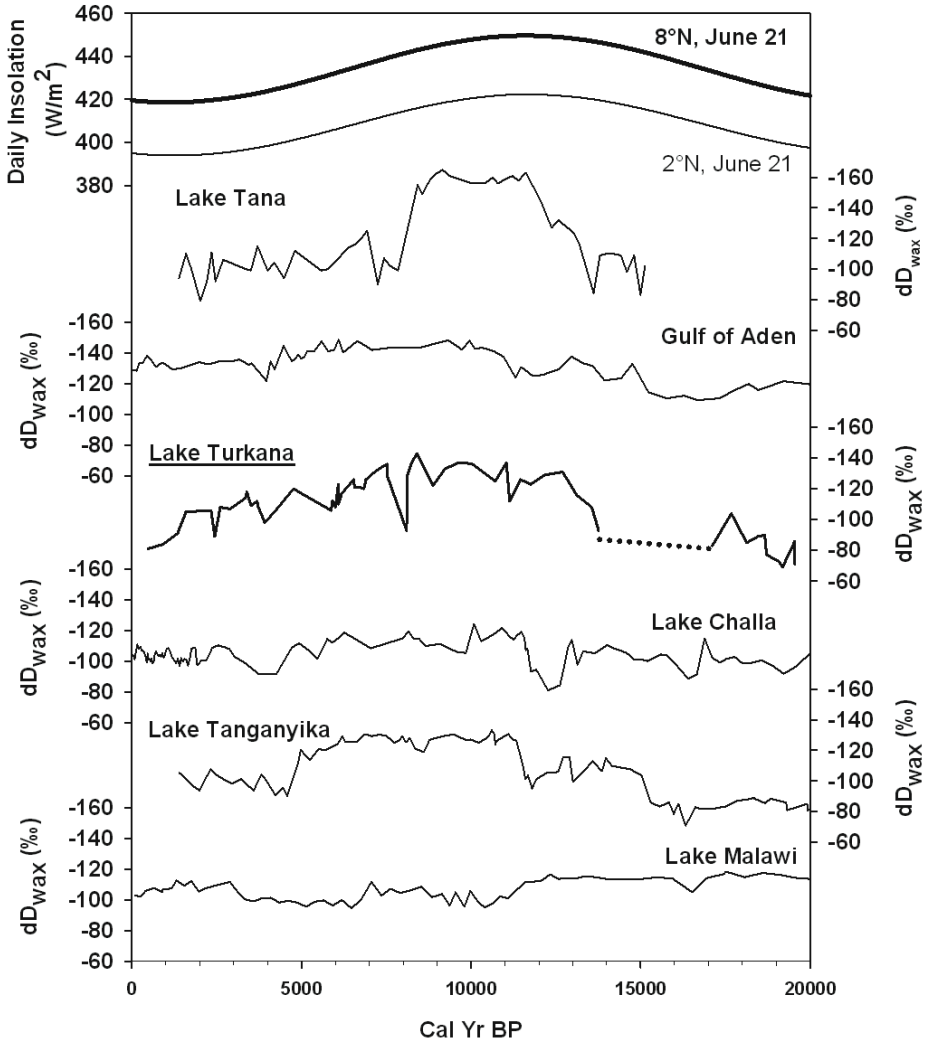

Fig. 6. African δD_{wax} records. δD_{wax} records from East African lakes; all data plotted at the same scale, and arranged from north to south; data from: Lake Tana (Costa et al., 2014), Gulf of Aden (Tierney and deMenocal, 2013), Lake Turkana (this study), Lake Challa (Tierney et al., 2011), Lake Tanganyika (Tierney et al., 2008), and Lake Malawi (Konecky et al., 2011)

8 Supplementary info

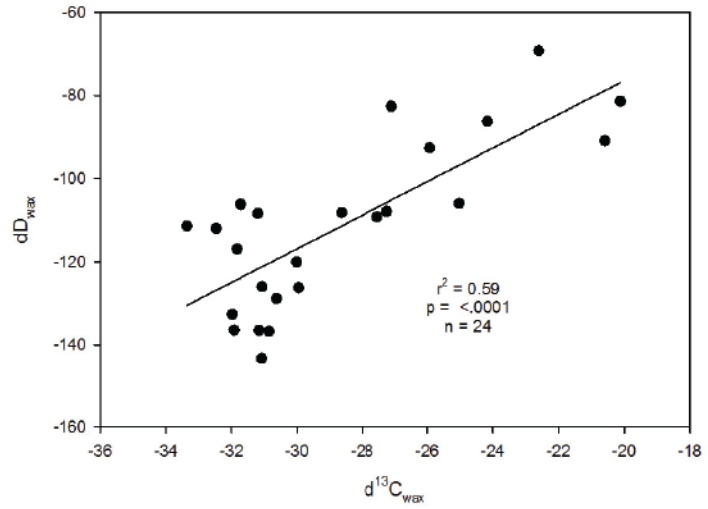

Supplementary Figure 1. Linear correlation of isotopes. Linear correlation between δD_{wax} and $\delta^{13}C_{wax}$.

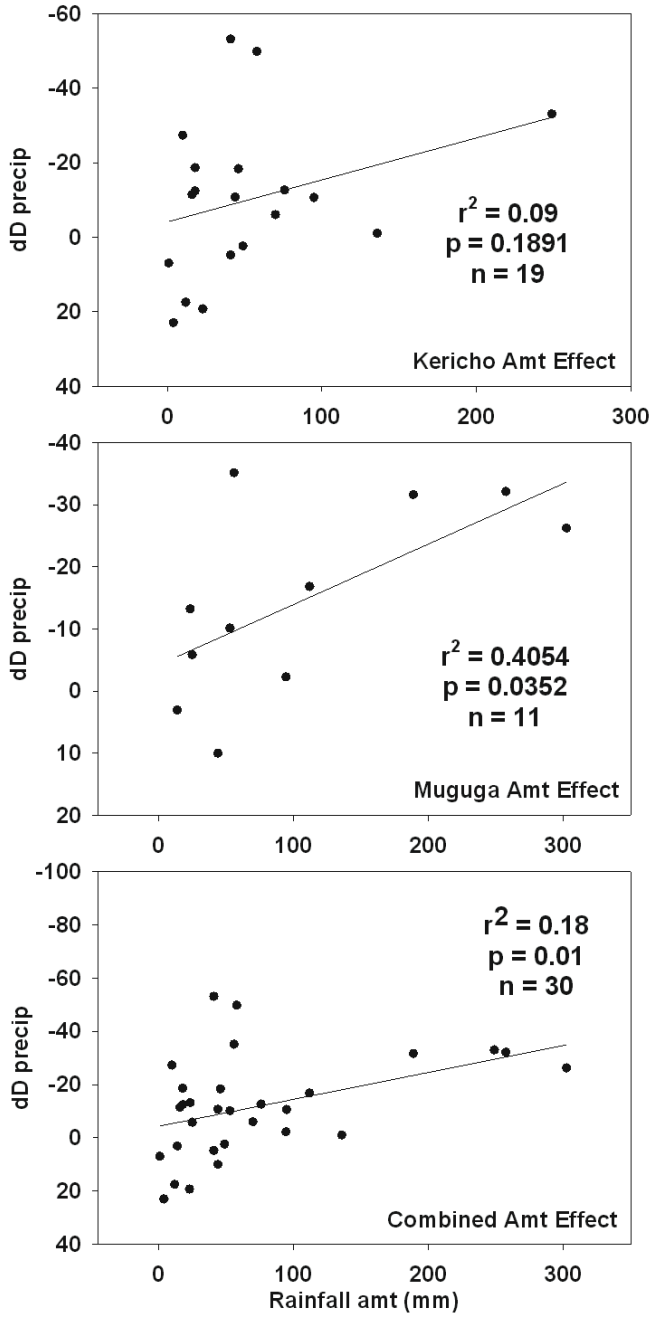

Supplementary Figure 2. Amount effect correlations. Linear correlations of the observed amount effects at Muguga, Kenya and Kericho, Kenya based on modern isotope and precipitation data. Upper most plot is data from Kericho. Middle plot is data from Muguga. Lower plot is both locations plotted together.

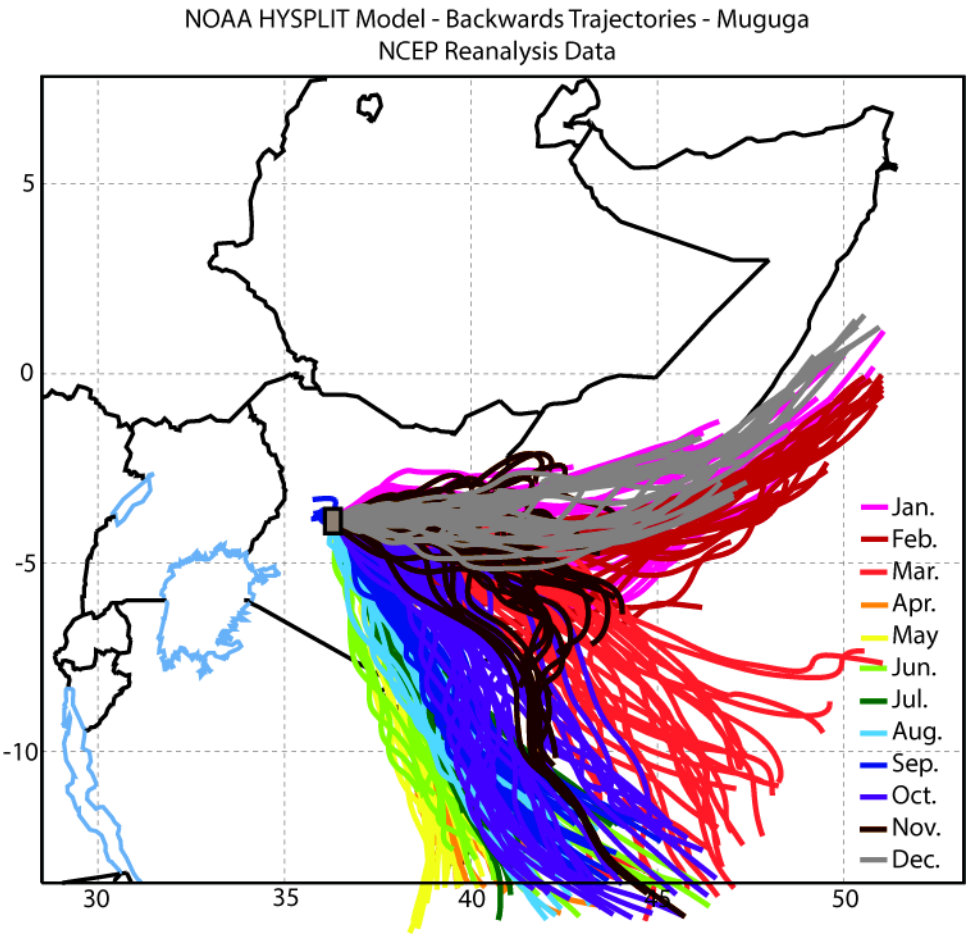

Supplementary Figure 3. Backwards trajectory models. NOAA HYSPLIT backward trajectory models for Muguga, Kenya using NCEP Reanalysis data between 2003-2008. Trajectories are color-coded by month.. This location is Location indicated by rectangle. Like Lake Turkana, Muguga, Kenya presently receives all of its moisture from Indian Ocean sources, and not from the Atlantic Ocean/Congo Basin. Precipitation isotope values are used from this location to extrapolate information about Lake Turkana

Supplementary Figure 4. Mean values of δDwax values of the C_{28} homologue from the composite sediment record highlighted by core from which they were derived.

Supplementary Table 1 Calculations for Amount Effect

Measured Data

	Rain (mm)	dD per mil	%Total Rain	Weighted dD
Feb	94.5	-13.9	0.08	-1.12
Mar	112.0	-15.7	0.10	-1.50
Apr	257.5	-30.4	0.22	-6.68
May	302.5	-34.9	0.26	-9.02
Jun	44.0	-8.8	0.04	-0.33
Jul	14.0	-5.8	0.01	-0.07
Aug	25.0	-6.9	0.02	-0.15
Sep	23.5	-6.7	0.02	-0.14
Oct	56.0	-10.0	0.05	-0.48
Nov	189.0	-23.5	0.16	-3.79
Dec	53.0	-9.7	0.05	-0.44
Total	1171.0	-166.3		-23.7
Average		-15.1		

Calculated Amt Effect = -17.9

26% increase

	Rain (mm)	dD per mil	%Total Rain	Weighted dD
Feb	119.1	-16.4	0.08	-1.32
Mar	141.1	-18.6	0.10	-1.78
Apr	324.5	-37.2	0.22	-8.17
May	381.2	-42.9	0.26	-11.08
Jun	55.4	-10.0	0.04	-0.37
Jul	17.6	-6.1	0.01	-0.07
Aug	31.5	-7.5	0.02	-0.16
Sep	29.6	-7.3	0.02	-0.15
Oct	70.6	-11.5	0.05	-0.55
Nov	238.1	-28.4	0.16	-4.59
Dec	66.8	-11.1	0.05	-0.50
Total	1475.5	-197.0		-28.7
Average		-17.9		

Calculated Amt Effect = -22.6

40% increase

	Rain (mm)	dD per mil	%Total Rain	Weighted dD
Feb	132.3	-17.7	0.08	-1.43
Mar	156.8	-20.2	0.10	-1.93
Apr	360.5	-40.8	0.22	-8.97
May	423.5	-47.2	0.26	-12.18
Jun	61.6	-10.6	0.04	-0.40
Jul	19.6	-6.3	0.01	-0.08
Aug	35.0	-7.9	0.02	-0.17
Sep	32.9	-7.7	0.02	-0.15
Oct	78.4	-12.3	0.05	-0.59
Nov	264.6	-31.1	0.16	-5.02
Dec	74.2	-11.9	0.05	-0.54
Total	1639.4	-213.6		-31.5
Average		-19.4		

Calculated Amt Effect = -25.1

100% increase

	Rain (mm)	dD per mil	%Total Rain	Weighted dD
Feb	189.0	-23.5	0.08	-1.89
Mar	224.0	-27.0	0.10	-2.58
Apr	515.0	-56.4	0.22	-12.41
May	605.0	-65.5	0.26	-16.93
Jun	88.0	-13.2	0.04	-0.50
Jul	28.0	-7.2	0.01	-0.09
Aug	50.0	-9.4	0.02	-0.20
Sep	47.0	-9.1	0.02	-0.18
Oct	112.0	-15.7	0.05	-0.75
Nov	378.0	-42.6	0.16	-6.87
Dec	106.0	-15.1	0.05	-0.68
Total	2342.0	-284.7		-43.1
Average		-25.9		

Calculated Amt Effect = -35.9

Chapter 3:

Late-Quaternary TEX_{86} paleotemperatures from the world's largest desert lake, Lake Turkana, Kenya

Amy Morrissey[1*], Christopher A. Scholz[1], James M. Russell[2]

[1]Dept of Earth Sciences, Syracuse University, Syracuse, NY 13244, USA

[2]Dept of Geological Sciences, Brown University, Box 1846, Providence, RI 02912, USA

*corresponding author, Dept of Earth Sciences, Syracuse University, Syracuse, NY 13244, USA, amorriss@syr.edu, +1-315-443-4334

Abstract

The precipitation-evaporation balance of a lake system is closely related to its heat budget. To attempt to quantify changes in temperature through the onset and termination of the African Humid Period, the paleotemperature proxy TEX_{86} was used to generate a 14-kyr record of lake surface temperatures for Lake Turkana. This biomarker and related measures are now routinely used to reconstruct regional and high-latitude paleotemperatures from the oceans and other continental systems, including other large African lakes. TEX_{86} temperatures from Lake Turkana from 14 to 0.4 ka are variable and range from 24.3 °C to 28.6 °C, with a mean of 25.9 °C. There is a long-term trend within the temperature record that follows mean northern hemisphere peak summer insolation, and a mean temperature of 26.2 °C during the early Holocene decreases to 25.7 °C during the late Holocene. A decade-to-century scale fluctuation of ~1 °C persists throughout most of the record; analyses of elemental ratios from the sediment cores suggest this high-frequency

variation is likely related to lake mixing processes that overprint the regional climate signal. While this was an unexpected result from this analysis, it shows that this proxy may have limitations in its application to well-mixed, arid-land lake systems. High-frequency variation in temperatures remains close to the mean for duration of the record, which may partially be attributed to the evaporation response of this lake system.

1 Introduction

Much of the world's freshwater is located in the watersheds of large lakes, and several of the largest lakes are located in tropical East Africa. Lake water volumes fluctuated significantly during times of changing climate, in some instances leading to complete lake desiccation (Johnson et al., 1996; Scholz et al., 2007; Lamb et al., 2007; Morrissey and Scholz, 2014). In a time of accelerating climate change, and with the likelihood of future temperature increases, analyses of the past temperature and evaporation changes and links to large lake hydrology are particularly important for the riparian populations of the desert region of Turkana. The paleotemperature proxy TEX_{86} quantifies the relative abundances of glycerol dialkyl glycerol tetraethers (GDGTs) preserved in sediments, and helps evaluate changes in temperature of the lake surface waters.

Lake surface paleotemperature reconstructions from East African lakes reveal significant variations in the amount of warming since the Last Glacial Maximum (LGM), as well as warming associated with the early Holocene African Humid Period (AHP) (Powers et al., 2005; Tierney et al., 2008; Berke et al., 2012a), a time when the East African tropics experienced increases in rainfall and relative humidity. Lakes Tanganyika and Victoria show ~2 °C of warming at the onset of the AHP, following northern hemisphere peak summer insolation trends (Tierney et al., 2008; Berke et al., 2012b). Lake Malawi however, does not display a temperature increase at the onset of the AHP (Powers et al., 2005) because at its location at 12° S of the equator it did not experience more humid conditions in the early Holocene as did much of North Africa. Earlier studies from Lake Turkana suggest a thermal maximum during the mid-Holocene (Berke et al., 2012a). The lake

surface temperatures in Lakes Malawi and Tanganyika respond to high latitude climate shifts such as the Younger Dryas (YD) and Heinrich Event 1 (Powers et al., 2005; Tierney et al., 2008), whereas the YD response at Lake Victoria is comparatively short-lived (Berke et al., 2012b). The events and trends captured within lake surface temperature reconstructions are variable and may represent high latitude teleconnections or capture local atmospheric and paleohydrological changes.

The environment at Lake Turkana is unique, as it is one of the largest lakes in the world but it is situated in a low elevation, near-equatorial desert. It receives 200 mm yr^{-1} of precipitation onto its surface, in contrast to other African Great Lakes such as Lake Tanganyika or Malawi, which receive upwards of 1000 mm yr^{-1} (Nicholson, 1996). Its fluctuation in annual temperature is minimal, and the annual evaporation amount is extremely high at 2300 mm yr^{-1} (Ferguson and Harbott, 1982). Additionally, the water column of Lake Turkana is well-mixed, setting it apart from the deep, stratified lakes of the Western Branch of the East African Rift System. Whereas the modern Turkana rift valley is hyper-arid, and the lake is slightly saline and hydrologically closed, the climate at Lake Turkana fluctuated significantly in the past. During the early Holocene, the lake level was high and overflowed to the White Nile River system (Owen et al., 1982; Halfman et al., 1988; Garcin et al., 2012; Morrissey and Scholz, 2014). When analyzing changes in precipitation and paleohydrology, the timing and duration of temperature changes are also important considerations, especially in an extreme environment such as the Turkana region where the riparian population of >700,000 relies on lake fishing as a key food source, and the water for grazing and watering of livestock as well as for irrigation. A new, 14-kyr lake surface temperature record for Lake Turkana is presented here, developed

using the TEX86 technique, in order to analyze fluctuations in regional temperature and hydrology in an area of extreme climate and over an interval that experienced dramatic regional climate change.

2 Geologic Background

Lake Turkana (2-5° N, 36-36.5° E, 360 m asl; Fig. 1) is the largest lake in the Eastern Branch of the East African Rift System at ~250 km long and ~30 km wide, and is a hydrologically closed basin in an arid environment. Precipitation at Lake Turkana occurs during the twice a year passing of the Intertropical Convergence Zone (ITCZ) in ~April and ~November. The lake is well-mixed due to strong diurnal winds from the southeast driven by cooling of high topography adjacent to the lake (Ferguson and Harbott, 1982), from a persistent unidirectional wind from the northeast with an average wind speed of 11 m s^{-1} (Burlando et al., 2010), and because the relatively shallow mean depth of 35 m (Yuretich, 1979). The Turkana area in northern Kenya is one of the hottest regions on the planet (Passey et al., 2010) with mean annual air temperatures at Lake Turkana of more than 29 °C (Fig. 2). Monthly average maximum temperatures in 2013 were at least 33.5 °C, and monthly average minimum temperatures were no lower than 23.8 °C (Fig. 2).

The Omo River provides a large amount of the sediment load, especially in the northern part of the lake (Yuretich, 1979). The South Basin, where these samples were collected, is 120 m at the deepest point and receives minimal sediment input directly from the Omo River (Yuretich, 1979, Cerling, 1986) (Fig. 1). The Omo River provides 80-90% of the hydrological input to the lake from the Ethiopian Highlands (Yuretich, 1979) and enters Lake Turkana at the northern shore of the lake at the Ethiopian border. The area of the

drainage basin is ~148,000 km^2 (Ferguson and Harbott, 1982; Garcin et al., 2012), and includes the Kerio and Turkwel Rivers to the west of the lake, as well as ephemeral rainy-season streams (Fig. 1).

Water temperature in Lake Turkana varies throughout the year both laterally and with depth (Fig. 3) (Ferguson and Harbott, 1982). Due to strong, persistent winds in the area and the straight shoreline morphology created by E-W structural deformation, surface currents develop and contribute to the mixing of the water column (Yuretich, 1979). Surface temperatures in the South Basin are generally lower than temperatures in the North Basin (Fig. 3), and temperatures are 1-3.5 °C lower in the peak northern hemisphere summer months than in the spring or fall (Ferguson and Harbott, 1982). The seasonal water temperature trends are similar to the trends observed in monthly air temperatures recorded at the lakeshore (Ferguson and Harbott, 1982; NOAA/NCDC, 2014) (Fig. 2).

3 Materials and Methods

3.1 Sample collection and sediment core chronology

Fifty-three paleotemperatures that span the period ~14 ka to 0.4 ka were produced using organic rich sediments (1-6% Total Organic Carbon) from Lake Turkana sediment cores (Fig. 4). Three Kullenberg piston cores, Turk10-4P, Turk10-14P, and Turk10-46P, were collected from the South Basin of Lake Turkana in water depths of 52, 56, and 58 m, and are 9.7, 8.5, and 10.6 m in length, respectively (Fig. 1). The cores were subsampled at an interval of ~240 years to generate a lake surface temperature record using the TEX_{86} paleotemperature proxy (Schouten et al., 2002). The three cores were stratigraphically correlated using magnetic susceptibility, gamma ray density, and total organic carbon

content, and together provide a continuous composite sediment record (Morrissey and Scholz, 2014).

The chronology for this record was developed using 24 AMS ^{14}C samples. Dated material consisted of bulk organic matter of mixed lacustrine and terrestrial origin, bulk carbonate from water column precipitation, and detrital carbonate from surface runoff, discrete macrophyte specimens, or ostracode and gastropod shells (Morrissey and Scholz, 2014). A flexible, Bayesian age-depth program, "Bacon" (Blaauw and Christen, 2011) was used to generate an age model for the composite core record. Morrissey and Scholz (2014) present detailed information on the stratigraphic framework, lithology, and geochemistry of the composite core record.

3.2 Lipid extraction and TEX_{86} Temperature proxy analysis

The total lipids (TLE) were extracted from individual freeze-dried and homogenized sediment samples via DIONEX™ accelerated solvent extraction, using Dichloromethane (DCM):Methanol (9:1). The polar and apolar fractions of the TLE were purified using activated alumina elution columns. Columns were precleaned with DCM:Methanol (1:1) and Hexane:DCM (9:1) solutions. The apolar fraction was then eluted using the Hexane:DCM (9:1) solution, and the polar fraction was eluted with the DCM:Methanol (1:1) solution, each into separate vials. The Glycerol Dialkyl Glycerol Tetraethers (GDGTs) quantification of the purified polar fraction of the TLE used for for TEX_{86} analysis was carried out using a high performance liquid chromatograph/positive ion atmospheric chemical ionization mass spectrometer (HPLC/APCI-MS) on an Agilent 1200 HPLC/MS

system. Replicate analyses produce results within ±0.1 ° C. Ratios of GDGTs I-IV were used to calculate the TEX_{86} temperatures (Schouten et al., 2002).

3.3 TEX_{86} Temperature proxy calibration

Multiple calibration equations have been developed for the application of TEX_{86} temperature reconstructions in different environments (i.e. Schouten et al., 2002; Powers et al., 2005, 2010; Kim et al., 2008, 2010; Tierney et al., 2010). Powers, et al. (2005, 2010) developed and later modified a calibration for the use of the TEX_{86} value for temperature reconstruction in large lakes. Tierney, et al. (2010) developed a proxy that used a larger dataset of African lakes of varying sizes, volumes and water chemistries. Kim et al. (2008) produced a global marine core top calibration study that includes 287 different samples. This calibration was later revised to include a subset of 255 core top samples specifically for a high temperature calibration, that is suggested for use in tropical environments (Kim et al., 2010). For this Lake Turkana study, several calibration equations were applied to the dataset (Fig. 5). The results from the large lake calibrations (Powers et al., 2005, 2010; Tierney et al., 2010) yield temperatures that are systematically low compared to modern Lake Turkana surface water temperatures (Fig. 5). There was minimal difference in the results between the Kim et al. (2008) and Kim et al. (2010) calibration equations. The temperatures that are produced using the open-marine core top calibrations (Kim et al., 2008, 2010) are most similar to modern temperature values (Fig. 5). Lake Turkana is well mixed and lacks a chemocline and permanent anoxic bottom waters that occur in many large tropical lakes. Accordingly, the populations of crenarchaeota present in Lake Turkana may be more similar to those of marine settings than of large lakes. Lake Turkana is also

slightly saline (1.5 ‰), which is more similar to marine settings than large freshwater lakes; however a study conducted by Wuchter et al. (2004) determined no difference in GDGT distributions in mesocosm experiments of salinities of 27‰ vs. 35‰. Thus, the mild salinity of the water in Lake Turkana is not likely a factor in calibration selection. Additionally, previous Lake Turkana TEX_{86} temperature studies carried out in different analytical facilities (Berke et al., 2012a) opted to use the calibration equation from Kim et al. (2010) for similar reasons.

3.4 Evaporation model parameters

Modern evaporation was calculated using an atmospheric stability model developed by Verburg and Antenucci (2010). This model was originally designed to evaluate seasonal atmospheric stability at Lake Tanganyika using measured parameters including lake surface temperature, air temperature, relative humidity, and air pressure; all were used as inputs to calculate sensible and latent heat flux between the lake surface and the air above the lake surface as well as to quantify evaporation (Verburg and Antenucci, 2010). Verburg and Antenucci (2010) assert that large tropical lakes like Lake Tanganyika are almost always unstable; that is the air temperature just above the lake surface is always higher than the lake surface temperature (Verburg and Antenucci, 2010). Here, we assume this is also true for Lake Turkana. The modern average lake surface temperature value (~26 °C), which is approximately equal to the average TEX_{86} value, is used as the water surface temperature input in the model. The difference between modern lake surface temperature and air temperature is ~3.5 °C. Modern relative humidity measurements at Lake Turkana vary between ~50-70% (NOAA/NCDC, 2014). Modern wind speeds at Lake Turkana are

~10 m s^{-1} on average (Burlando et al., 2010). The model was run three times using wind speeds of 5, 10, and 15 m s^{-1} and relative humidity was varied between 50 and 70%. Air pressure is held constant at 1013 mbar.

4 Results

4.1 Temperature proxy results and the BIT index

The TEX_{86} temperature record generated from Lake Turkana sediment cores varies from 24.3 °C to 28.6 °C with a mean of 25.9 °C and standard deviation of 1.1 °C (Fig. 4). There are two increases in temperature (near 27.5 °C) at ~9.2 and ~2.4 ka that exceed one standard deviation about the mean, and there are two significant increases (over 28 °C) that exceed two standard deviations about the mean, at ~11.7 and ~6.5 ka (Fig. 4), which occur near the onset and at the end of the AHP. Cooler temperatures, between 24.3 °C and 25 °C, occur between 12.7 and 12.3 ka, for short periods at 9.6 ka and 6.9 ka, for a sustained period between 5.8 and 4.5 ka, and briefly at 2.5 ka. All of the temperature decreases are near one standard deviation below the mean; none of the lowest temperatures approach two standard deviations below the mean (Fig. 4). For most of the duration of the record, the lake surface temperature fluctuates within one standard deviation of the mean on a centennial scale. The general trend of the dataset is slightly decreasing over time with an overall change of ~1.2°C.

The ratio of branched (soil-derived) to isoprenoid (aquatically-derived) tetraethers, or BIT index, is used as an evaluator of soil organic matter input (Hopmans et al., 2004) and the potential success of the TEX_{86} paleotemperature proxy. The TEX_{86} value is calculated using a ratio of isoprenoid tetraethers, but significant introduction of branched tetraethers

into an aquatic system suggest that terrestrially-derived isoprenoid tetraethers also influence the distributions of sedimentary isoprenoid tetraethers and the measured TEX_{86} ratio (Hopmans et al., 2004). Accordingly, a low BIT value (<0.3) is typically required for a valid TEX_{86} analysis. BIT values for this data set range from 0.09 to 0.25 with a mean of 0.16 and a standard deviation of 0.04. Consistently low values suggest minimal influence from soil-derived organic matter.

4.2 Model results

The model results using different wind speed and relative humidity inputs are displayed in table 2. The temperature input for each model run was 26 °C; wind speed was varied from 5 to 15 m s^{-1} using a 5 m s^{-1} interval. Relative humidity was varied from 50 to 70% by a 10% interval. Calculated evaporation rates vary from 750 to 7700 mm yr^{-1} (Table 2). The evaporation rate of ~5000 mm yr^{-1} is calculated using parameters most similar to modern conditions (wind speed of 10 ms^{-1} and humidity of 50%). This value is much higher than the accepted value of ~2300 mm yr^{-1} from past studies estimated from yearly lake level fall over the time period of 1945 to 1975 (Ferguson and Harbott, 1982).

5 Discussion

5.1 Long term temperature change

TEX_{86} paleotemperatures indicate relative temperature stability at Lake Turkana throughout the Holocene, with a long-term average of 26 °C (Fig. 4). The full range of temperatures in the Turkana record is not unlike the range of temperatures seen in other African lakes (Table 1), and temperatures were not constant over the time period studied

(24.3 – 28.6°C). The record does not contain consistent long-term trends in temperature; however, temperature fluctuates within one standard deviation (1.1 °C) about the mean. This suggests that there was relative, long-term temperature stability during a time when there were significant shifts in other climate parameters such as precipitation and evaporation, as well as insolation, greenhouse gas concentrations, and vegetation cover.

The temperature record from Turkana shares some characteristics with records from other lakes in East Africa. Temperatures increase between 12.7 and 11.7 ka at Turkana, a characteristic that is also seen at Lake Victoria and Lake Tanganyika (Tierney et al., 2008; Berke et al., 2012a). The 4 °C temperature increase at Turkana is greater in magnitude than the change over the same time period at Lakes Victoria and Tanganyika (Tierney et al., 2008; Berke et al., 2012a). This warming is associated with deglaciation and increasing northern hemisphere summer insolation. Temperatures at Lake Turkana, Lake Victoria, Lake Tanganyika and Lake Malawi all decrease slightly between ~5.5 and 4 ka (Powers et al., 2004; Tierney et al., 2008; Berke et al., 2012a).

Lake level at Turkana was not stable during much of the Holocene, due to precipitation changes associated with AHP moisture (i.e., Owen et al., 1982; Halfman et al., 1988; Garcin et al., 2012; Morrissey and Scholz, 2014) (Fig. 4). Many of the short-term temperature changes observed in this study correlate with times of pronounced shifts in lake level, however the relationship between lake level change and temperature is not consistent. Increases in temperature correlate to both rising and falling lake level. This suggests that changes in the paleohydrology and evaporation of Lake Turkana were probably closely related to resulting temperature changes at the lake surface at times, but they do not consistently explain fluctuations seen in the temperature record.

Lake surface temperatures decreased from the early Holocene to late Holocene by 0.5 °C from a mean of 26.2 °C to 25.7 °C. This is within the error of the TEX_{86} proxy, but follows the trend of decreasing summer insolation over the same time period (Fig. 4). While there is variation within the record, the mean value of temperatures during the AHP highstand is 0.5 °C higher than the mean value of the late Holocene lowstand temperatures (Fig. 4). By comparison of the temperature record to seasonal insolation curves, the long-term trend in the temperature record from Lake Turkana follows summer insolation (Fig. 2). The mean annual temperature at Lake Turkana is most similar to JJA and NDJ temperatures, which correspond to times of year when direct sunlight and possibly productivity are highest, potentially biasing the temperature being recorded by the TEX_{86} record.

5.2 Other Turkana temperature records

An earlier study generated a TEX_{86} paleotemperature record from mid-late Holocene sediments from the South Basin of Lake Turkana. Berke et al. (2012a) present a TEX_{86} temperature record from Lake Turkana that extends from ~1–6 ka, using samples from legacy 1980's sediment cores (Halfman et al., 1988, 1992) (Fig. 7) recovered from both the North and South Basin of Lake Turkana. Berke et al. (2012b) conclude that a mid-Holocene thermal maximum of 28.3 °C at 5 ka followed September-November insolation that also peaked at 5 ka. The thermal maximum indicated by Berke et al. (2012b) is not observed in the temperature record in this study. There are several explanations for different results between the two studies.

The first is a topic discussed in Berke et al. (2012b) to explain differences between temperature records generated for cores in the North and South basins of Lake Turkana. Wind mixing and upwelling in Lake Turkana create a spatially variable temperature water column cross section along the axis of the lake (Fig. 3). According to Berke et al. (2012a), the distance (~140 km) between the two cores, which were recovered from North Basin and South Basin from the previous study, is sufficient for an offset in temperature to persist over centuries. While the main cores from this study and the mid-Holocene record (LT84-2P) from Berke et al., (2012b) are both from the South Basin, they are ~15 km apart (Fig. 1). Additionally, the precise core location for LT84-2P is not known, as the cores were collected prior to the advent of the modern Global Positioning System and was located by periodic RADAR fixes and dead reckoning (Halfman, 1987). In addition to their distance, the upwelling in the South Basin (Fig. 3) is isolated to the easternmost shore, the area where all three cores from this study were recovered, while the surface circulation at the core location of LT84-2P is potentially less affected by upwelling deepwater. The differences between the two temperature records are difficult to explain as the lake is well mixed; however, lake circulation may account for some of the differences in the two records (Fig. 7).

Another possible explanation for the different results in the two studies is age model uncertainty. The material dated in Berke et al. (2012b) consisted of ostracode fractions, and core LT84-2P has only three dated samples. Other age constraints for core LT84-2P are correlated ages from other LT84 cores using marker horizons in downcore carbonate abundance and magnetic susceptibility. The age model from our study is constrained by a total of 24 radiocarbon dates from the three cores from the South Basin on material that

potentially records a more reliable age (Morrissey and Scholz, 2014). Because of the distance between LT84-2P and the cores from our study, it is not possible to correlate them stratigraphically using other proxies. Another possible explanation for differences between the two temperature records is the time elapsed between the recovery of the cores from the lake and sampling for TEX_{86} analysis. The cores from the previous study were collected in 1984 and sampled for TEX_{86} analysis more than two decades later, after the core was desiccated and had shrunk non-linearly by as much as ~20%. The potential for loss of precision in below-lake-floor-depth is high, and may contribute to additional offset between the two age models. All three explanations presented here together are likely responsible for differences in the records.

In figure 8, the record from LT84-2P was stretched by ~1.5 kyr to match the temperature high described in Berke et al. (2012a) with the temperature high at ~6 ka in the record from this study. It does not, however, reconcile most of the other features seen in the new temperature record. Neither the low temperatures from 5.8 ka to 4.5 nor the short-lived temperature high at 2.4 ka in the new record are replicated in the LT84-2P record (Fig. 7). The lack of correlation between these two records is best explained by differences in age models and the possibility of differential desiccation in the legacy cores from the previous study, in addition to naturally occurring variability in the temperature structure and wind mixing of Lake Turkana.

5.3 Ecological changes and TEX_{86}

The ratio of branched to isoprenoidal tetraethers, the BIT index, has been used to interpret paleoecological changes in tropical environments (Hopmans et al., 2004,

Verschuren et al., 2009; Sinninghe-Damsté et al., 2009). Branched tetraethers are mainly soil-derived, while isoprenoidal tetraethers are mainly aquatic, and increases in the ratio have been interpreted as an increase in terrestrial runoff during times of high rainfall (Verschuren et al., 2009; Sinninghe-Damsté et al., 2009).The persistent low values over the duration of the record (less than ~0.3), suggest that the soil-derived component of the sediment samples is sufficiently low to permit robust TEX_{86} temperature analysis, which is based solely on aquatic tetraethers. While there is variability in the BIT index over time, it does not contain the high-frequency variability observed in the temperature data. The correlation between BIT index and lake level change (Fig. 4) suggests that the BIT index is capturing large-scale ecological shifts within the lake basin. When lake level is stable, either high or moderately low, the BIT values from Turkana vary between ~0.1 and 0.15 (Fig. 4). When lake level is changing or low, observed BIT are slightly elevated to values between 0.2 and 0.25 (Fig. 4).

Additionally, the influence of other sources of GDGTs over time could explain anomalous temperatures in the TEX_{86} record (Schouten et al., 1998 2007; Blaga et al., 2009; Zhang et al., 2011). Methanotrophic archaea produce GDGTs that can influence the relative abundances of GDGTs in the ratio used in the TEX_{86} proxy. Zhang et al. (2011) describe the Methane Index (MI) to evaluate the possible influence of methane oxidizing *Euryarchaeota* on GDGT relative abundances. Methane oxidizing *Euryarchaeota* produce GDGT-1, -2, and -3, but they do not produce crenarchaeol and its regio isomer. Thus, this index consists of the ratio of GDGT-1, -2, and -3 to GDGT-1, -2, -3, crenarchaeol and its regio isomer (Zhang et al., 2011). An MI value above ~0.3 indicates substantial influence from methanotrophic organisms. The range of MI values from Lake Turkana samples analyzed for the TEX_{86}

proxy is 0.14–0.32 with a mean of 0.21 and a standard deviation of 0.03 (Fig. 8). These consistently low values suggest that, in general, there was minimal influence of methanotrophic organisms at Lake Turkana over the study period. However, there is a short interval at ~4 ka that correlates to relatively high temperatures in the TEX_{86} record that were possibly influenced by an increase in methanotrophic organisms (Fig. 8).

Another explanation for variation within the TEX_{86} record is the presence of methanogenic archaea, which also produce GDGTs and can affect the relative abundances of GDGTs that contribute to the TEX_{86} value (Schouten et al., 2007). The ratio of GDGT-0 to crenarchaeol (Cren) can be used to assess the influence of methanogenic organisms on the abundances of GDGTs (Schouten et al., 1998; Blaga et al., 2009). The range of GDGT-0:Cren for the Turkana record is 0.06 – 0.2 with a mean of 0.13 and a standard deviation of 0.03 (Fig. 8). All of the samples from Turkana have a ratio of 0.2 or lower, suggesting there is no other significant source for GDGT-0 other than Crenarchaeota. The high-frequency variability in the TEX_{86} temperature record is not a product of shifts in the source of tetraethers, but rather must be a product of water column temperature variation, lake mixing and sediment preservation.

5.4 High-frequency temperature variability

The long-term temperature decrease observed in the Turkana TEX_{86}record is over-printed with high-frequency variability. Temperatures fluctuate by ~0.5–1.5 °C on decadal to centennial timescales between 14 ka and 0.4 ka (Fig. 4). This is unlike most of the other TEX_{86} temperature records from large African lakes, where temperatures remain relatively constant over long periods of time (Powers et al., 2005; Berke et al., 2012a; Tierney et al.,

2008). The persistent winds, mechanical heat transfer, and lake mixing are possible climatological influences on TEX_{86} temperatures.

The temperature profile of Lake Turkana is complex due to persistent winds and substantial lake mixing (Fig. 3). Due to upwelling, the north-south temperature gradient ranges from 1–3.5 °C annually. It is broadly accepted that TEX_{86} records the temperature of water from the upper water column (Tierney et al., 2008; Schouten et al., 2012), however the constant wave action and mixing in Turkana, particularly the South Basin, may exert an influence here. The vigorous mixing of the water column influences the distribution of tetraethers that are deposited on the lake floor. This is likely a source for variation in the temperatures that are recorded at a core location. Redox indicators from high-resolution scanning X-ray fluorescence data show significant variations between different elemental ratios (Fig. 9), and the fluctuations within these datasets correlate to fluctuations within the TEX_{86} temperatures. The Fe:Ti and Mn:Ti ratios covary with temperature for much of the record, suggesting that preserved temperatures are related to the redox state of the lake; in this case, wind-driven mixing probably controls the redox state.

5.5 Short-lived temperature events and lake level change

There are several significant, decadal and centennial scale temperature increases (over 28 °C) that exceed two standard deviations about the mean at ~11.7 and ~6.5 ka, as well as significant variations between 3 and 2.2 ka. The temperature increases at 11.7 and 6.5 ka correlate approximately to shifts in lake level associated with the onset and termination of the AHP. Fluctuations in temperature during these intervals could be related to shifts in the precipitation-evaporation ratio and the amount of cloud cover during

changing climate. Temperatures vary between 24 °C and 27 °C (Fig. 4 and 11) between 3 and 2.2 ka. This increase in temperature occurs just before a moderate lowstand that is interpreted at 2.2 ka (Morrissey and Scholz, 2014). These temperature changes may indicate a perturbation in the regional climate at this location, as they roughly correlate to slight (<1 °C) temperature decreases at ~3 ka at Lakes Tanganyika and Malawi (Powers et al., 2005; Tierney et al., 2010).

5.6 Regional temperature change correlations

Climate records from large lakes in East Africa indicate that along with increased precipitation, many areas also experienced changes in temperatures during the African Humid Period (Tierney et al., 2010; Powers et al., 2005), an interval of increased northern hemisphere summer insolation (Fig. 4). In other TEX_{86} records from East African lakes, the highest lake surface temperatures do not occur during the peak of the AHP, but are observed during the onset and during the termination of the AHP. In Lake Tanganyika (6–9 °S), temperatures as high as 28 °C occur between 11.5 and 10.7 ka and as high as 26 °C between 7 and 6.5 ka, while during the AHP temperatures ranged between 23 °C and 25 °C (Tierney et al., 2010) (Fig. 10). At Lake Malawi (10–14 °S), temperatures increased (27–28 °C) from 14–13 ka and remain over 27 °C from 6.7–4.2 ka while temperatures during the AHP were ~25 °C (Powers et al., 2005) (Fig. 10). Lake Turkana displays a similar record, with ~2 °C increases in temperatures at ~11.7 ka and ~6.5 ka, with temperatures near 26 °C (Fig. 10).

Lakes Tanganyika and Malawi are both south of the equator, and during the AHP, they both experienced summer insolation minima. Lake Tanganyika responded

hydrologically however, to peak northern hemisphere summer insolation (Tierney et al., 2008) whereas Lake Malawi did not (Powers et al., 2005). Lake Turkana is north of the equator and experienced high summer insolation during the AHP. This would suggest that lake surface temperatures should be highest at the time of peak insolation. Increased insolation, however, probably also produced a shift in the ITCZ, causing increased atmospheric convergence over the Turkana region. Increased convergence would promote increased rainfall in the area, accompanied by more cloud cover and associated increases in relative humidity. Additionally, an increase in relative humidity would limit heat loss from the lake surface from a decrease in evaporation.

5.7 Modeled evaporation changes and relative humidity

The model run using a wind speed of 10 m s^{-1} is most similar to the modern climatic and environmental conditions at Lake Turkana (Table 2). Calculated evaporation rates using modern model parameters are ~5000 mm yr^{-1}. That is more than twice the amount of evaporation as the 2300 mm yr^{-1} value that is well cited in the literature (Ferguson and Harbott, 1982). Annual lake level declines recorded over several decades were used to calculate that evaporation value (Ferguson and Harbott, 1982). In the same study, workers report attempts to use a number of evaporation tank experiments and determined that abnormally high measures of evaporation were unreliable (Ferguson and Harbott, 1982). The model used here suggests extremely high evaporation may be possible under current climate conditions. Evaporation is an efficient means by which to dissipate heat from a lake system, and varying evaporation may be an explanation for the high-frequency, low-

amplitude temperature variation at Lake Turkana during a time of extreme global climate change.

Model results for paleotemperature and relative humidity proxies suggest extreme changes in evaporation (Table 2). Evaporation amounts are highly sensitive to wind speed according to model results. Wind speed at Lake Turkana today is ~10 m s^{-1}, but there are no definitive proxies for ancient wind speeds. Redox sensitive elemental ratios can be used as a qualitative wind speed and degree of lake mixing, however the proxy is not precise enough to determine exact wind speed. The nightly cooling of high topography adjacent to the South Basin creates strong winds at Lake Turkana. Since the same topography persisted over the time interval of this study, the winds of today likely persisted in the past. If this is the case, then the evaporation reduction modeled during the AHP is most sensitive to the amount of relative humidity. Increases in relative humidity would be coupled with increases in precipitation and cloud cover. Past studies of Lake Turkana have reported that during infrequent thunderstorms over the lake surface, air temperature rapidly decreases, which is possibly due to a decrease in direct sunlight, as an increase in humidity should reduce heat loss from the lake surface (Ferguson and Harbott, 1982). Monthly means of measured insolation also indicate that cloud cover reduces solar insolation by up to 28% (Griffiths, 1972), which affects surface water temperature. During the AHP, evaporation decreased due to an increase in relative humidity, and temperature likely did not increase due to a decrease in direct sunlight on the lake surfaceIn the late Holocene, when relative humidity and cloud cover decreased, evaporation aided in the dissipation of heat that prevented an increase in surface water temperatures from increased direct sunlight.

6 Conclusions

- Lake surface temperatures determined from TEX_{86} at Lake Turkana between 14 ka and 0.4 ka indicate a long-term climate trend of slightly decreasing temperature that was likely controlled by changes in summer insolation.
- Apparent increases in temperature correspond approximately to large-scale fluctuations in lake level. This may be due to increases in soil-derived tetraethers influencing the tetraether composition in the lake and biasing the tetraether distribution.
- Significant fluctuations (+/-1–3 °C) in lake surface temperature are short-lived, decade-to-century scale events imprinted over insolation-driven temperature change. The short-term events are attributed to significant lake mixing and the complex temperature profile that persists year-around at Lake Turkana.
- Lake Turkana's low elevation, near-equatorial position, arid climate, well-mixed water column, closed basin, and relatively small size are unique compared to other large African Great Lakes. The physical mixing of the water column distorts regional or high latitude climate signals in the temperature record.
- The surface water mean temperature during the late Holocene decreased by 0.5 °C as peak NH summer insolation decreased in conjunction with the termination of the AHP. This was coeval with the lowering of lake level and the onset of regional hyperaridity.
- The range of relative humidity and wind speeds present at modern Lake Turkana likely produce highly variable evaporation rates at Lake Turkana. The range of possible evaporation rates likely contributes to the high-frequency, low-amplitude

variability in the TEX_{86} temperature record, however precise estimates on paleo-humidity and paleo-wind speeds are difficult to constrain quantitatively.

7 Acknowledgments

We thank the government of Kenya for research permissions. Financial support was provided by the sponsors of the Syracuse University Lacustrine Rift Basins Research Program. We also thank the National Oil Corporation of Kenya for assistance during field operations. The authors thank the people of Loiyangalani and the Turkana Rift Valley, for their cooperation, assistance, and hospitality during multiple field seasons at Lake Turkana. We would also like to thank Dr. Shannon Loomis, Dr. Rafael Tarozo, and Lily Cohen for assistance with sample preparations and laboratory procedures at Brown University. The authors would like to thank P. Verburg and J. Antenucci for the public availability of their model. We also thank Dr. Bruce Wilkinson for his comments and suggestions on early versions this manuscript.

8 References

Berke, M. a., Johnson, T.C., Werne, J.P., Schouten, S., and Sinninghe Damsté, J.S., 2012a, A mid-Holocene thermal maximum at the end of the African Humid Period: Earth and Planetary Science Letters, v. 351-352, p. 95–104.

Berke, M.A., Johnson, T.C., Werne, J.P., Grice, K., Schouten, S., and Sinninghe, J.S., 2012b, Molecular records of climate variability and vegetation response since the Late Pleistocene in the Lake Victoria basin, East Africa: Quaternary Science Reviews, v. 55, p. 59–74.

Blaauw, M., and Christen, J.A., 2011, Flexible Paleoclimate Age-Depth Models Using an Autoregressive Gamma Process: Bayesian Analysis, v. 6, no. 3, p. 457–474, doi: 10.1214/11-BA618.

Blaga, C.I., Reichart, G.-J., Heiri, O., and Sinninghe Damsté, J.S., 2008, Tetraether membrane lipid distributions in water-column particulate matter and sediments: a study of 47 European lakes along a north–south transect: Journal of Paleolimnology, v. 41, no. 3, p. 523–540, doi: 10.1007/s10933-008-9242-2.

Burlando, M., Durante, F., and Claveri, L., 2010, The Lake Turkana Wind Farm Project: DEWI Magazin, v. 37, p. 6–15.

Cerling, T.E., 1986, A Mass-balance approach to basin sedimentation: Constraints on the recent history of the Turkana Basin: Palaeogeography, Palaeoclimatology, Palaeoecology, v. 54, p. 63–86.

Ferguson, A.J.D. and Harbott, B.J., 1982, Geographical, physical, and chemical aspects of Lake Turkana, in: Hopson, A.J. (Ed.), Lake Turkana: A Report on the Findings of the

Lake Turkana Project, 1972-1975. Overseas Development Administration, London, pp. 1–108.

Garcin, Y., Melnick, D., Strecker, M.R., Olago, D., and Tiercelin, J.-J., 2012, East African mid-Holocene wet–dry transition recorded in palaeo-shorelines of Lake Turkana, northern Kenya Rift: Earth and Planetary Science Letters,, p. 322–334, doi: 10.1016/j.epsl.2012.03.016.

Griffiths, J.F., 1972, Eastern Africa, Ethiopian Highlands. In: World Survey of Climatology: Climates of Africa, H.E. Lansberg, Ed., Elsevier, Amsterdam, v. 10, p. 369-381.

Halfman, J.D., 1987, High-resolution sedimentology and paleoclimatology of Lake Turkana, Kenya [Ph.D. Thesis]: Durham, North Carolina, Duke University, 180 p.

Halfman, J.D., and Johnson, T.C., 1988, High-resolution record of cyclic climatic change during the past 4 ka from Lake Turkana, Kenya: Geology, v. 16, p. 496–500, doi: 10.1130/0091-7613(1988)016<0496.

Halfman, J.D., Jacobson, D.F., Cannella, C.M., Haberyan, K.A., and Finney, B.P., 1992, Fossil diatoms and the mid to late Holocene paleolimnology of Lake Turkana, Kenya: a reconnaissance study: Journal of Paleolimnology, v. 7, p. 23–35.

Hopmans, E.C., Weijers, J.W.., Schefuß, E., Herfort, L., Sinninghe Damsté, J.S., and Schouten, S., 2004, A novel proxy for terrestrial organic matter in sediments based on branched and isoprenoid tetraether lipids: Earth and Planetary Science Letters, v. 224, no. 1-2, p. 107–116, doi: 10.1016/j.epsl.2004.05.012.

Johnson, T.C., Halfman, J.D., Rosendahl, B.R., and Lister, G.S., 1987, Climatic and tectonic effects on sedimentation in a rift-valley lake : Evidence from high-resolution seismic

profiles, Lake Turkana, Kenya: GSA Bulletin, v. 98, p. 439–447, doi: 10.1130/0016-7606(1987)98<439.

Johnson, T.C., Scholz, C., Talbot, M., Kelts, K., Ricketts, R., Ngobi, G., Beuning, K., Ssemmanda, I., and McGill, J., 1996, Late Pleistocene Desiccation of Lake Victoria and Rapid Evolution of Cichlid Fishes: Science (New York, N.Y.), v. 273, no. 5278, p. 1091–3.

Kim, J.-H., Schouten, S., Hopmans, E.C., Donner, B., and Sinninghe Damsté, J.S., 2008, Global sediment core-top calibration of the TEX86 paleothermometer in the ocean: Geochimica et Cosmochimica Acta, v. 72, no. 4, p. 1154–1173, doi: 10.1016/j.gca.2007.12.010.

Kim, J.-H., van der Meer, J., Schouten, S., Helmke, P., Willmott, V., Sangiorgi, F., Koç, N., Hopmans, E.C., and Damsté, J.S.S., 2010, New indices and calibrations derived from the distribution of crenarchaeal isoprenoid tetraether lipids: Implications for past sea surface temperature reconstructions: Geochimica et Cosmochimica Acta, v. 74, no. 16, p. 4639–4654, doi: 10.1016/j.gca.2010.05.027.

Lamb, H.F., Bates, C.R., Coombes, P. V., Marshall, M.H., Umer, M., Davies, S.J., and Dejen, E., 2007, Late Pleistocene desiccation of Lake Tana, source of the Blue Nile: Quaternary Science Reviews, v. 26, no. 3-4, p. 287–299, doi: 10.1016/j.quascirev.2006.11.020.

Morrissey, A., and Scholz, C. A., 2014, Paleohydrology of Lake Turkana and its influence on the Nile River System: Palaeogeography, Palaeoclimatology, Palaeoecology, in press, doi: 10.1016/j.palaeo.2014.03.029.

Morrissey, A., Scholz, C.A., and Russell, J.M., in prep., Late Quaternary atmospheric circulation over the Turkana Rift, East Africa.

Nicholson, S.E., 1996, A review of climate dynamics and variability in East Africa. In: Johnson, T.C., Odada, E.O. (Eds.), The Limnology, Climatology and Paleoclimatology of the East African Lakes. Gordon and Breach, Amerstam, pp. 25-56.

NOAA/NCDC, National Climate Data Center, accessed 9 Feb 2014, http://www.ncdc.noaa.gov/cdo-web/datasets#GHCNDMS.

Owen, R.B., Barthelme, J.W., Renaut, R.W., and Vincens, A., 1982, Palaeolimnology and archaeology of Holocene deposits north-east of Lake Turkana, Kenya: Nature, v. 298, p. 523–529.

Passey, B.H., Levin, N.E., Cerling, T.E., Brown, F.H., and Eiler, J.M., 2010, High-temperature environments of human evolution in East Africa based on bond ordering in paleosol carbonates.: Proceedings of the National Academy of Sciences of the United States of America, v. 107, no. 25, p. 11245–11249, doi: 10.1073/pnas.1001824107.

Powers, Lindsay A., Johnson, T.C., Werne, Josef P., Castañeda, Isla A., Hopmans, Ellen C., Sinninghe Damsté, J. S., Schouten, S., 2005, Large temperature variability in the southern African tropics since the Last Glacial Maximum: Geophysical Research Letters, v. 32, no. 8, p. L08706, doi: 10.1029/2004GL022014.

Powers, L., Werne, J.P., Vanderwoude, A.J., Sinninghe Damsté, J.S., Hopmans, E.C., and Schouten, S., 2010, Applicability and calibration of the TEX86 paleothermometer in lakes: Organic Geochemistry, v. 41, no. 4, p. 404–413, doi: 10.1016/j.orggeochem.2009.11.009.

Scholz, C. a, Johnson, T.C., Cohen, A.S., King, J.W., Peck, J. a, Overpeck, J.T., Talbot, M.R., Brown, E.T., Kalindekafe, L., Amoako, P.Y.O., Lyons, R.P., Shanahan, T.M., Castañeda, I.S., Heil, C.W., et al., 2007, East African megadroughts between 135 and 75 thousand years

ago and bearing on early-modern human origins.: Proceedings of the National Academy of Sciences of the United States of America, v. 104, no. 42, p. 16416–21, doi: 10.1073/pnas.0703874104.

Schouten, S., Hoefs, M.J.L., Koopmans, M.P., Bosch, H-J., Sinninghe Damste, J.S., 1998 Structural identification, occurrence and fate of archael ether-bound acyclic and cyclic biphytanes and corresponding diols in sediments, Organic Geochemistry, v. 29, p. 1305-1319.

Schouten, S., Hopmans, E.C., Schefuss, E., and Sinninghe Damsté, J.S., 2002, Distributional variations in marine crenarchaeotal membrane lipids : a new tool for reconstructing ancient sea water temperatures?: Earth and Planetary Science Letters, v. 204, p. 265–274.

Schouten, S., Forster, A., Panoto, F.E., Sinninghe Damsté, J.S., 2007, Towards calibration of the TEX_{86} palaeothermometer for tropical sea surface temperatures in ancient greenhouse worlds: Organic Geochemistry, v. 38, p. 1537-1546.

Schouten, S., Rijpstra, W.I.C., Durisch-Kaiser, E., Schubert, C.J., and Sinninghe Damsté, J.S., 2012, Distribution of glycerol dialkyl glycerol tetraether lipids in the water column of Lake Tanganyika: Organic Geochemistry, v. 53, p. 34–37, doi: 10.1016/j.orggeochem.2012.01.009.

Sinninghe Damsté, J.S., Ossebaar, J., Abbas, B., Schouten, S., and Verschuren, D., 2009, Fluxes and distribution of tetraether lipids in an equatorial African lake: Constraints on the application of the TEX86 palaeothermometer and BIT index in lacustrine settings: Geochimica et Cosmochimica Acta, v. 73, no. 14, p. 4232–4249, doi: 10.1016/j.gca.2009.04.022.

Tierney, J.E., Russell, J.M., Huang, Y., Damsté, J.S.S., Hopmans, E.C., and Cohen, A.S., 2008, Northern Hemisphere Controls on Tropical Southeast African Climate During the Past 60,000 Years: Science, v. 322, p. 252–255.

Tierney, J.E., Russell, J.M., Eggermont, H., Hopmans, E.C., Verschuren, D., and Sinninghe Damsté, J.S., 2010, Environmental controls on branched tetraether lipid distributions in tropical East African lake sediments: Geochimica et Cosmochimica Acta, v. 74, no. 17, p. 4902–4918, doi: 10.1016/j.gca.2010.06.002.

Verburg, P., and Antenucci, J.P., 2010, Persistent unstable atmospheric boundary layer enhances sensible and latent heat loss in a tropical great lake: Lake Tanganyika: Journal of Geophysical Research, v. 115, no. D11, p. D11109, doi: 10.1029/2009JD012839.

Verschuren, D., Sinninghe Damsté, J.S., Moernaut, J., Kristen, I., Blaauw, M., Fagot, M., and Haug, G.H., 2009, Half-precessional dynamics of monsoon rainfall near the East African Equator.: Nature, v. 462, no. 7273, p. 637–41, doi: 10.1038/nature08520.

Wuchter, C., 2004, Temperature-dependent variation in the distribution of tetraether membrane lipids of marine Crenarchaeota: Implications for TEX 86 paleothermometry: Paleoceanography, v. 19, no. 4, p. 1537–1546, doi: 10.1029/2004PA001041.

Yuretich, R.F., 1979, Modern sediments and sedimentary processes in Lake Rudolf (Lake Turkana) eastern Rift Valley, Kenya: Sedimentology, v. 26, p. 313–331.

Zhang, Y.G., Zhang, C.L., Liu, X.-L., Li, L., Hinrichs, K.-U., and Noakes, J.E., 2011, Methane Index: A tetraether archaeal lipid biomarker indicator for detecting the instability of

marine gas hydrates: Earth and Planetary Science Letters, v. 307, no. 3-4, p. 525–534, doi: 10.1016/j.epsl.2011.05.031.

9 Figures

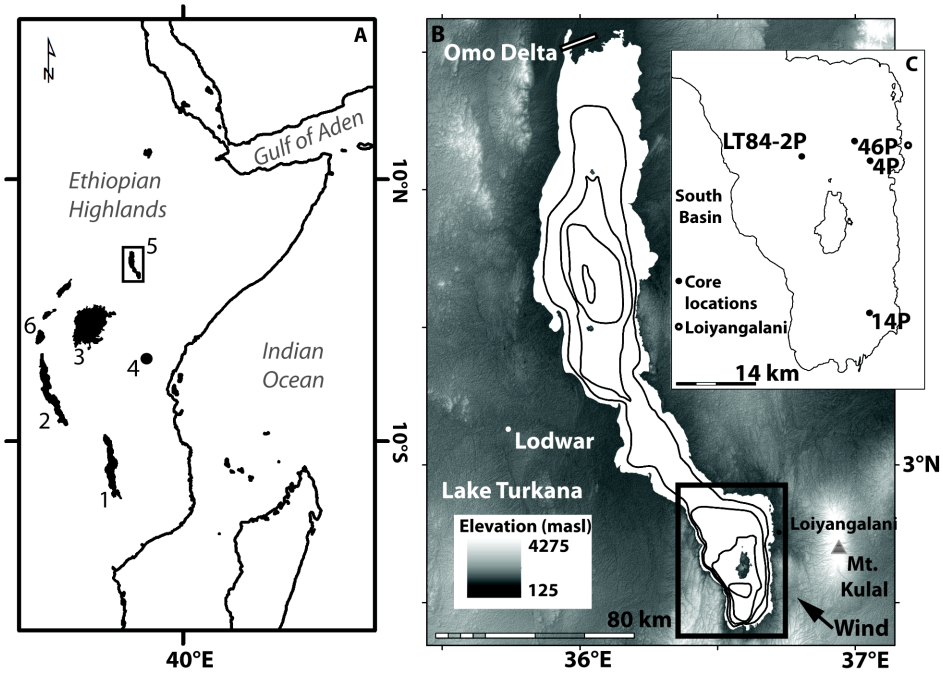

Fig. 1. Map of study area. A. Regional map of East Africa. 1. Lake Malawi. 2. Lake Tanganyika. 3. Lake Victoria. 4. Lake Challa. 5. Lake Turkana. 6. Lake Kivu. B. Elevation and bathymetric map of Lake Turkana, bathymetric contours are 20 m. C. Map of core locations from this study and past TEX_{86} records from the South Basin (Halfman et al., 1988; Berke et al., 2012a).

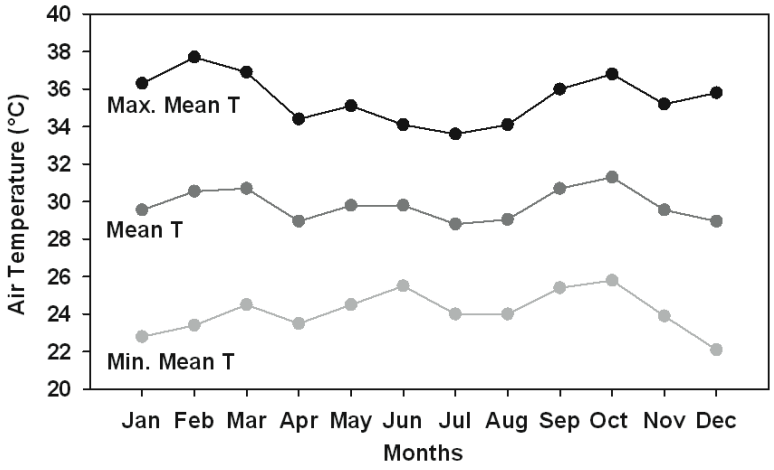

Fig. 2. Monthly temperatures. Temperature from weather station at Lodwar, Kenya. Upper curve is monthly average maximum temperatures, middle curve is monthly average temperature, and the lower curve is monthly average minimum temperature.

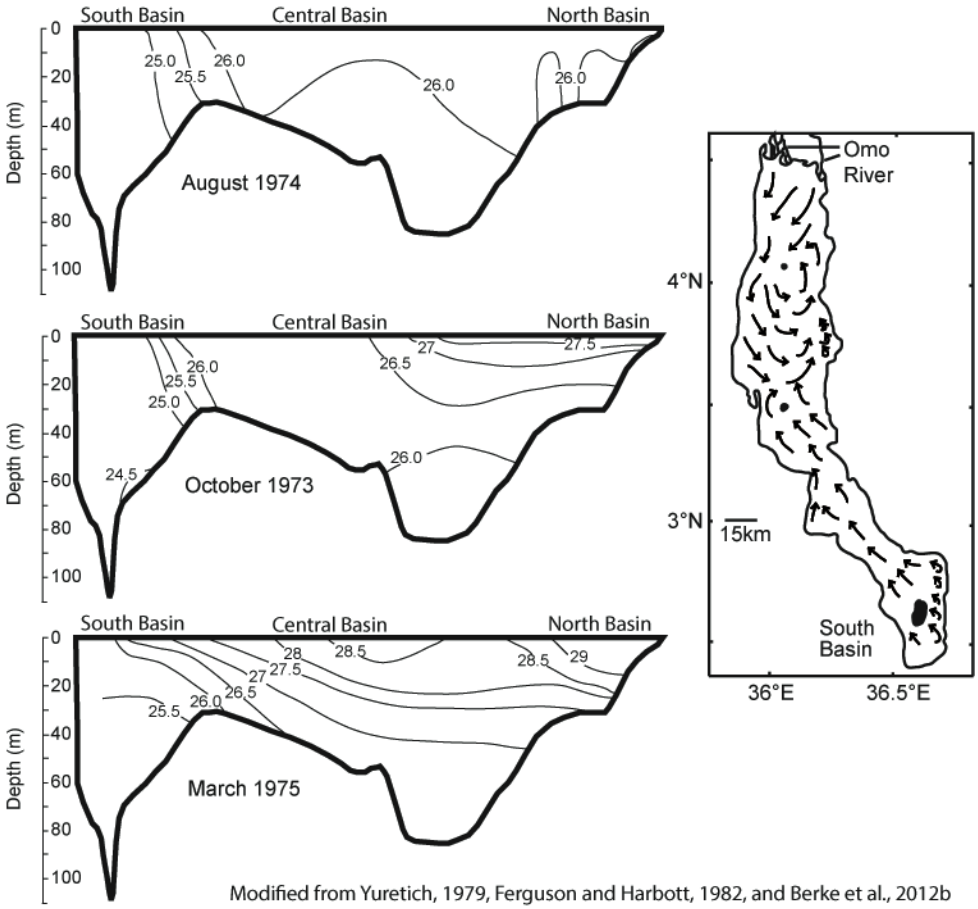

Fig. 3. Temperature profiles and surface currents. Temperature profiles for Lake Turkana in the summer (August) and the rainy seasons (October and March), figure modified from Berke, et al., 2012b; original data from Ferguson and Harbott, 1982. Map shows surface current directions as derived by Yuretich, 1979.

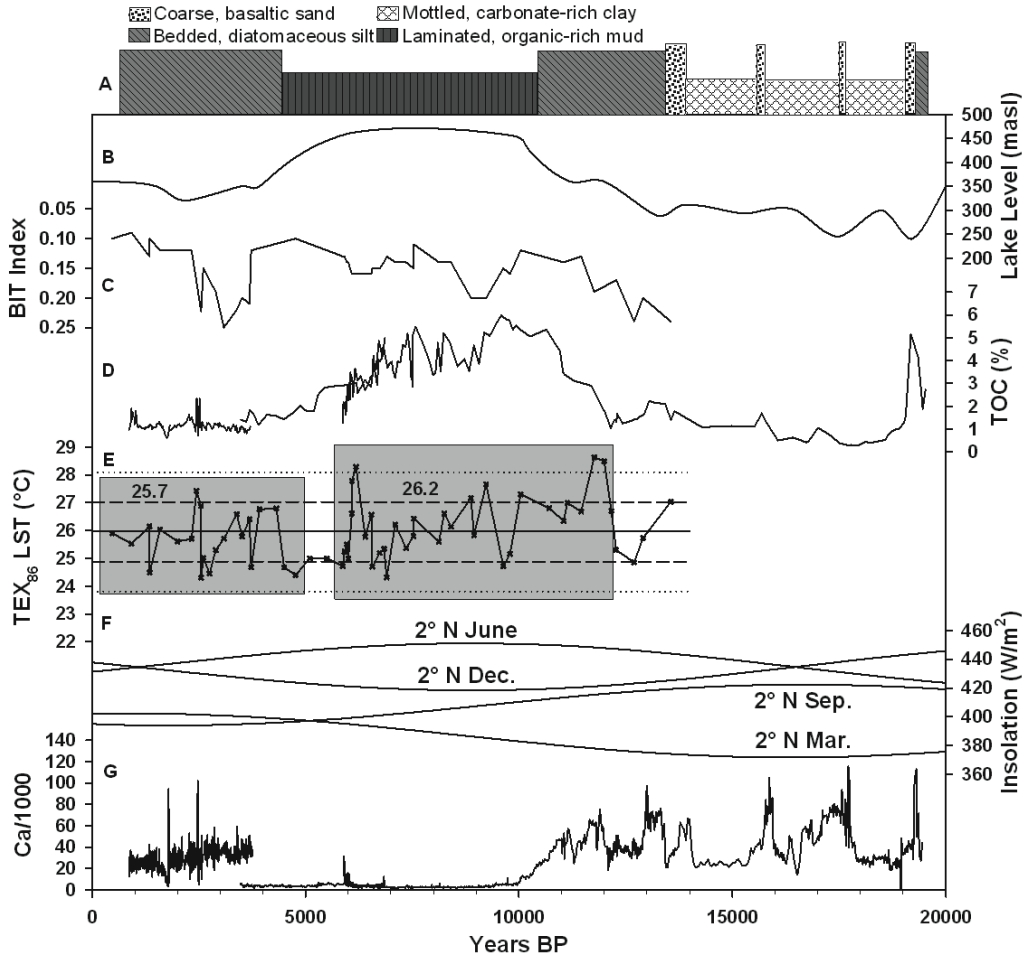

Fig. 4. TEX_{86} with ancillary datasets. A. Simplified lithology of composite sediment core record from Lake Turkana. B. Multiproxy deepwater lake level curve for Lake Turkana (Morrissey and Scholz, 2014). C. BIT index. D. Total organic carbon from composite sediment record; sampled at 8-cm interval. E. TEX_{86} record. Solid line represents mean of dataset, dashed lines are one standard deviation from the mean and the dotted lines are two standard deviations about the mean. Two shaded boxes separate (I) African Humid Period temperatures from (II) late Holocene temperatures. Mean of box I is 26.2 °C and mean of box II is 25.7 °C. F. Mean insolation curves for21 March, 21 June, 21 September, and 21 December daily insolation curves for 2 °N. G. Calcium abundance from composite

core record.

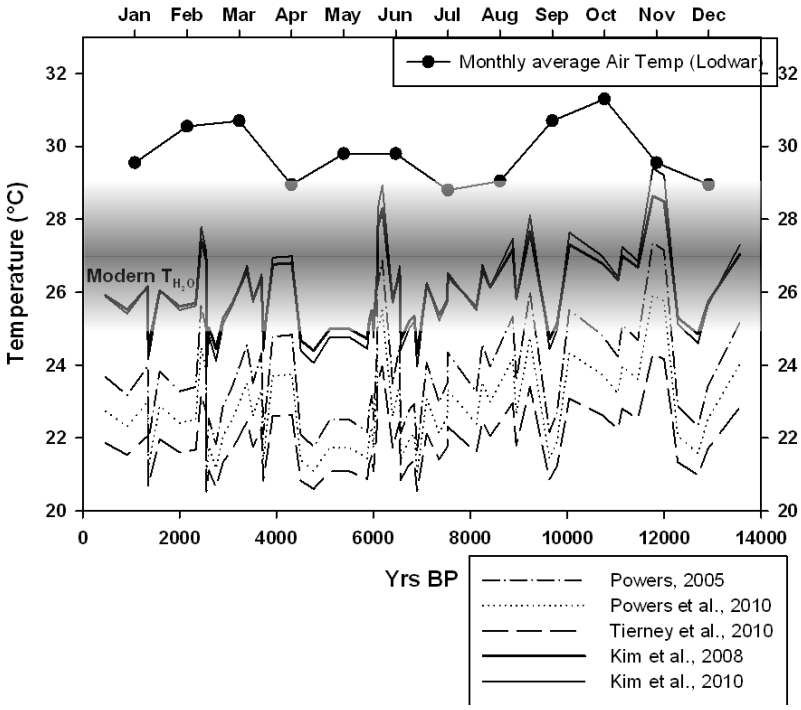

Fig. 5. Calibrations. Filled black circles are modern monthly average air temperatures from Lodwar, Kenya. Lower panel contains the three calibration equations developed for large lakes from Powers et al., 2005 and 2010 and Tierney et al., 2010, and the two marine core top calibrations from Kim et al., 2008 and 2010. Shaded box indicates range of surface water temperatures recorded in the South Basin in 2010.

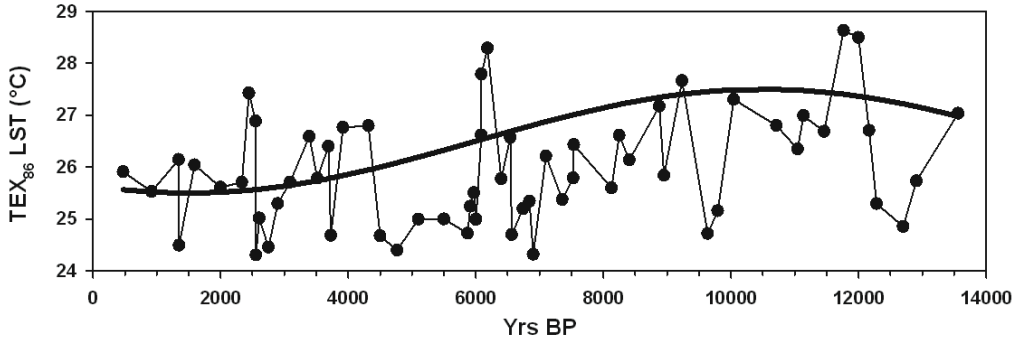

Fig. 6. Curve fits. Visual best fit of a sine wave with the same statistical parameters as the TEX_{86} data.

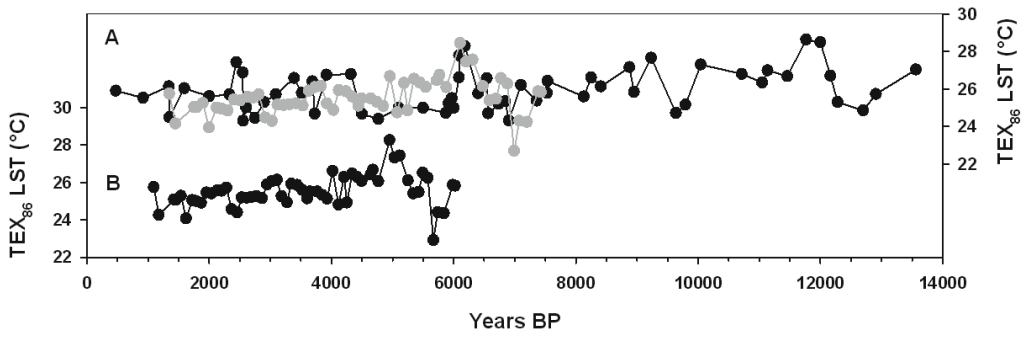

Fig. 7. New and previous TEX_{86} records. Direct comparison of the TEX_{86} records from Lake Turkana. Upper curve is record from this study with temperatures from Berke et al., 2012a overlaid with the data stretched by ~1500 years for a best fit to new temperature data. Lower curve is TEX_{86} data from previous study as published in Berke et al., 2012a.

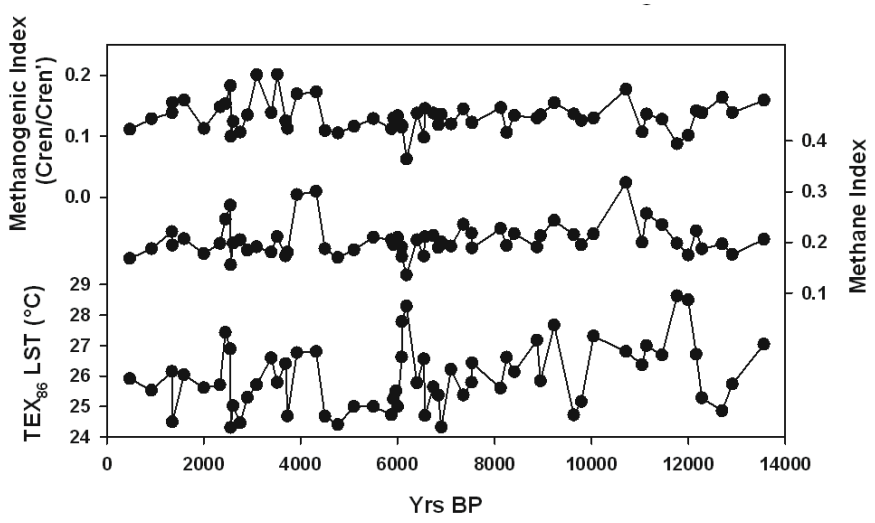

Fig. 8. Methane indicators compared to TEX_{86}. Top: Indicator ratio for methanogenesis, GDGT-0 to Crenarchaeota. Center: Methane index, indicator ratio for Methanotrophic Archaea, GDGT-1, -2, -3 to GDGT-1, -2, -3, Crenarchaeota and its regio isomer. Lower: TEX_{86} record.

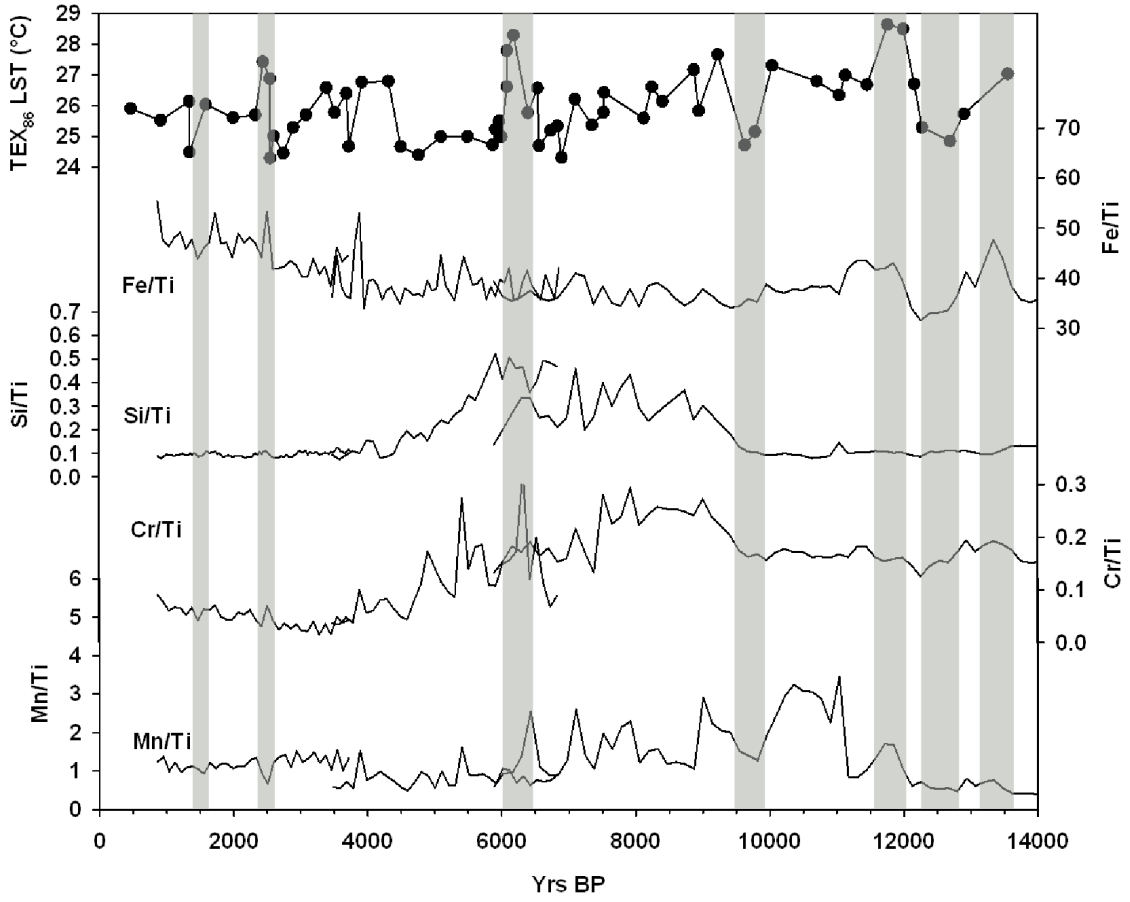

Fig. 9. Lake mixing indicators. TEX_{86} record compared to lake mixing and redox indicators derived from scanning X-ray fluorescence data on the same cores used for TEX_{86} sampling. Gray bars indicate intervals where there is visual correlation between the TEX86 record and one or more redox indicator.

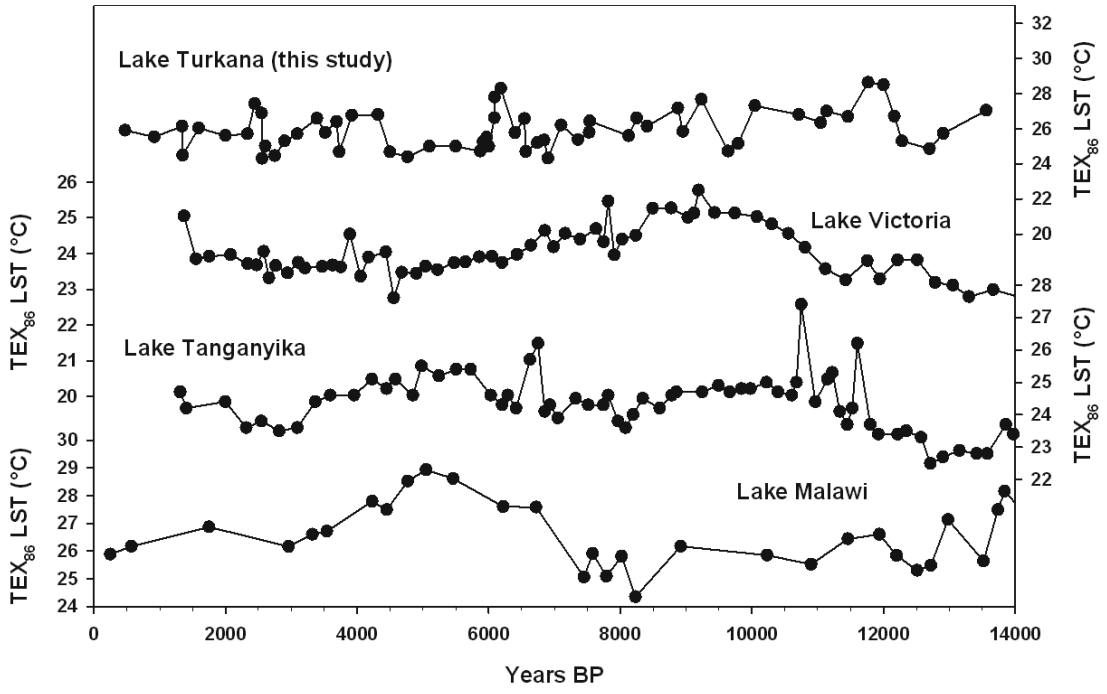

Fig. 10. Regional TEX_{86} records. TEX_{86} paleotemperature records from across East Africa by latitude. From north to south: Lake Turkana (this study), Lake Victoria (Berke et al., 2012b), Lake Tanganyika (Tierney et al., 2008), Lake Malawi (Powers et al., 2005).

Table 1. Regional TEX_{86} Lake Surface Temperatures (14 ka to present)

Lake	**Max TEX_{86} T (°C)**	**Min TEX_{86} T (°C)**	**Range of T (°C)**
Turkana	28.6	24.3	4.2
Tanganyika	27.4	22.5	4.9
Malawi	28.9	24.4	4.5
Victoria	25.8	22.8	3.0

Table 2. Evaporation model inputs and results

Relative humidity/Wind speed	**5 m s^{-1}**	**10 m s^{-1}**	**15 m s^{-1}**
50%	2100 mm yr^{-1}	5000 mm yr^{-1}	7700 mm yr^{-1}
60%	1425 mm yr^{-1}	3400 mm yr^{-1}	5250 mm yr^{-1}
70%	750 mm yr^{-1}	1800 mm yr^{-1}	2800 mm yr^{-1}

Project summary

Lakes sediments are one of the best archives of continental climate change, particularly in the tropical latitudes where continental records are otherwise poorly preserved. The Great Lakes of the East African Rift System are some of the largest and deepest lakes on Earth and contain millions of years of climate and tectonic history. Lake Turkana is the largest lake in the Eastern Branch of the East African Rift System and the largest lake in the world in a desert. It is markedly smaller, however, in length, depth, and volume compared to analogous half-graben lake basins located in the Western Branch. The Turkana region is subject to the twice annual passing of the Intertropical Convergence Zone (ITCZ) due to its near-equatorial position in northwestern Kenya. This low-elevation desert receives less than 200 mm yr^{-1} of cumulative precipitation, and the evaporation is over 2300 mm yr^{-1}. Wind speeds measured at Lake Turkana are upwards of 10 m s^{-1}, which produces a well-mixed water column. This highly evaporative environment creates a hydrologically closed lake with moderately alkaline and slightly saline water.

Prior to this study, the knowledge of the sedimentary framework and paleolimnology of Lake Turkana was relatively limited. The acquisition of high-resolution compressed high intensity radar pulse (CHIRP) seismic reflection data in conjunction with ~10 m Kullenberg piston cores allowed for the recovery of a nearly 20 kyr paleolimnologic record. Sediment core lithology was described, and the cores analyzed for basic geochemical and geophysical parameters including total organic carbon, total inorganic carbon, water content, gamma ray attenuated porosity evaluation bulk density, and whole-core magnetic susceptibility. Sediment chronology is constrained by 24 radiocarbon dates from three sediment cores. Downcore density curves were used for correlation to CHIRP

seismic data, which was used to interpret seismic sequences based on stratigraphic relationships and seismic character.

With these data in hand, a multiproxy lake level history was derived for the last 20 kyr. After the Last Glacial Maximum, Lake Turkana experienced at least two desiccation events at 18.5 and 17 ka when the lake was at least 100 m lower than modern, as evidenced by basin-wide, high amplitude reflections correlated to sand intervals in the sediment cores. Lake level rose abruptly at ~11 ka as interpreted from an increase in organic carbon content and abrupt shift to silt and clay-sized sediment. It was after this shift when Lake Turkana overflowed and became part of the White Nile River System via the now relict Turkana-Nile River. Highstand conditions lasted until ~5 ka when the lake once again became a closed basin. The loss of Lake Turkana as a White Nile input likely had significant repercussions to nascent communities living along the Nile as well as the Turkana-Nile River. Lake level has remained at a moderate lowstand since its mid Holocene closure. Lake level fluctuations in this region loosely follow trends in mean solar insolation, however, onset of lake level extremes are much more abrupt than rates of insolation change.

Lake Turkana is not the only lake in East Africa with evidence for increased precipitation between ~13 and ~5 ka. This time interval is often referred to as the African Humid Period (AHP) due to the fact that many lakes where at highstand and much of the Sahara Desert was green. Increased northern hemisphere summer insolation is often invoked as a forcing for increased atmospheric convergence over much of northern Africa during this period of increased precipitation. More recently, an easterly shift of moisture derived from the Congo Basin has been proposed as an additional moisture source for

environments in East Africa during the AHP. Much of this evidence comes from an expanding number of hydrogen isotope records from different lake basins in East Africa that have allowed workers to begin to understand the zonal moisture sources in the region and how they may have changed over time.

The hydrogen isotope values of different moisture sources vary based on its transport history. The two main sources of moisture for East Africa are the Indian and Atlantic Oceans, however Lake Turkana presently receives 100% of its moisture from the Indian Ocean via the African Monsoons. Congo derived moisture is typically more depleted in deuterium than Indian Ocean moisture because it has a more complex transport history and has been subjected to more over land processes that lead to depletion. To determine the possibility of Atlantic derived moisture via the Congo Basin reaching Lake Turkana in the past, compound specific (C_{28} *n*-alkanoic acids) hydrogen isotopes (δD_{wax}) were measured from the composite sediment core record from Lake Turkana.

The record revealed that hydrogen isotope values were depleted by as much as -60‰ during the AHP. Isotope depletion occurs abruptly at 13.7 ka and is sustained throughout the AHP, and values slowly become more enriched after 7 ka. This depletion suggests that Congo derived moisture had a significant influence on Turkana precipitation during the AHP, but depletion of that magnitude cannot be explained solely by a change in moisture source. An explanation for the remainder of the depletion is a significant increase in the amount affect, a fractionation process described to occur during tropical rainstorms whereas raindrops produced during thunderstorms generated by convective processes are more depleted than the moisture source. Finally, because the hydrogen isotopes where measure on leaf waxes, the vegetation type change through time must also be considered

as significant differences exist between the fractionation processes in C_3 vs. C_4 plant metabolic processes.

These three possible effects were quantified using stable carbon isotopes ($\delta^{13}C_{wax}$), modern Kenyan amount effect estimations coupled with a published basin fill model, and a previously published study on the quantification of modern isotope effects caused by Congo-derived moisture for Lake Tana, a lake in the Ethiopian Highlands. It was determined that vegetation can account for up to -17‰ of the total AHP depletion, amount effect estimations range from -17‰ to - 24‰ of the total depletion. After accounting for these effects, precipitation during the AHP is depleted relative to a 100% change in precipitation amount, which we suggest is driven by an influx of moisture derived from the Congo Basin. Our calculations suggest that at least 45% of the moisture supplied to this part of East Africa during the AHP was Congo-derived.

The precipitation-evaporation balance of a lake system is closely related to its heat budget. This is especially true in Lake Turkana, where evaporations rates are extremely high and precipitation changes over time have been dramatic. To attempt to quantify changes in temperature through the onset and termination of the AHP, a paleotemperature proxy originally developed for the marine system called TEX_{86} was used to generate a 14-kyr record of lake surface temperatures for Lake Turkana. This proxy uses the relative abundance of organic compounds called Glycerol Dialkyl Glycerol Tetraethers (GDGTs) produced by temperature-sensitive aquatic bacteria (Group I crenarchaeota) that live in surface waters and are deposited on the lake floor to calculate a lake surface temperature. This proxy has recently been shown to successfully reconstruct regional and high-latitude climate events in the paleotemperatures from other large African lakes.

TEX_{86} temperatures from 14 to 0.4 ka are highly variable and range from 24.3 °C to 28.6 °C with a mean of 25.9 °C. There is a long-term trend within the temperature record that follows mean northern hemisphere peak summer insolation. The mean temperature of 26.2 °C during the early Holocene is 0.5 °C warmer than the late Holocene mean temperature of 25.7 °C. The temperature record generated from Lake Turkana sediments, however, appears to be sensitive to lake evaporation and lake mixing processes that overprint the regional climate signal. A decade-to-century scale fluctuation of ~1 °C persists throughout most of the record. While this was an unexpected result from this analysis, it has shown that this proxy may have limitations in its application to well-mixed lake systems.

Lake Turkana has experienced dramatic climatic and limnologic changes over the past 20 kyr. The timing and magnitude of change during the African Humid Period varies between proxies, but it is clear that the landscape of Lake Turkana was affected by more humid conditions for several thousand years in the early Holocene. After the time of high rainfall, the area became hyper arid, and this environment persists to present day. Lake level has dropped ~10 m since the 1970s and continued water loss may negatively affect the hydrologic budget and water chemistry of the lake. Further concentration of ions would lead to increased salinity and alkalinity making water unsuitable for livestock watering and irrigation purposes. A negative response from fish populations would eliminate a food source for the riparian communities surrounding the lake. The future of Lake Turkana is unclear as ongoing plans to implement an 1800 MW dam on the Omo River may further deprive the lake of its main water source.

Recommendations for future work

The results of this project provided a long-term overview of climate and limnologic change in the Turkana region, however the variability of climate on short timescales in the area is still not well understood. TEX_{86} temperatures were highly variable on decadal to century scales, and late Holocene δD_{wax} values show significant variation with enhanced aridity. As today's climate continues to change, a super high-resolution, recent climate record would benefit the understanding the climate processes that occur in Lake Turkana and how they might respond to future climate change.

In conjunction with the seismic reflection data and Kullenberg sediment cores acquired for this project, several short gravity cores were collected to capture the shallowest sediments as well as the intact sediment-water interface. Sedimentation rates in these cores have been constrained by Pb-210 dating and were determined to be ~1 cm yr^{-1}. A sampling strategy could be designed to generate a record of quasi-annual climate change for the past century in effort to identify the true scale of temperature and precipitation variability. High-resolution XRF scans are recommended prior to intense sampling for organic proxy analysis, as performed in this study, to evaluate changes in sediment source and distinct changes in water chemistry over time. An entire half-core sample would likely be required to acquire sufficient quantities of sediment to perform $\delta D_{wax,}$ $\delta^{13}C_{wax}$, and TEX_{86} analysis.

If sediment could be collected on an interannual basis, these proxies could be applied on the interannual scale to assess true seasonal climate variability. Seasonal sediment trap studies could further enhance the understanding of annual variability in the regional climate system. However, this would require additional fieldwork. The potential

success of long-term sediment trap studies in Lake Turkana is questionable due to the deep wave base of the lake. An additional approach to determining annual variability is analysis of satellite photos and other remote sensing data to quantify changes in wind patterns on the lake surface as well as seasonal changes in vegetation cover.

Finally, a specific issue that was encountered in this project was the quantitative analysis of the amount effect at Lake Turkana. The quantification of precipitation on a per-event scale coupled with isotope measurements of water from the same events would greatly enhance the understanding of the amount effect in the region today. These data simply do not exist at present, and assumptions must be made when extrapolating these data from other regions. The acquisition of these data would also lend additional insight into the different fractionation components of the δD_{wax} record analyzed in this study.

Appendix A

Output from Bacon flexible Bayesian Age Model

Turk10-46P

depth	Age
0	5839
1	5840
2	5841
3	5842
4	5843
5	5844
6	5845
7	5846
8	5847
9	5848
10	5849
11	5850
12	5851
13	5852
14	5853
15	5854
16	5855
17	5856
18	5857
19	5858
20	5859
21	5860
22	5861
23	5862
24	5864
25	5865
26	5866
27	5867
28	5868
29	5869
30	5870
31	5871
32	5872
33	5873
34	5874
35	5875
36	5876
37	5877
38	5878
39	5879
40	5880
41	5881
42	5882
43	5883

Turk10-14P

depth	Age
0	380
1	399
2	417
3	436
4	455
5	473
6	492
7	511
8	529
9	548
10	567
11	585
12	604
13	623
14	641
15	660
16	679
17	697
18	716
19	735
20	753
21	772
22	791
23	809
24	828
25	847
26	865
27	884
28	903
29	921
30	940
31	959
32	977
33	996
34	1015
35	1033
36	1052
37	1071
38	1089
39	1108
40	1127
41	1145
42	1164
43	1183

Turk10-4P

depth	Age
0	864
1	865
2	866
3	868
4	869
5	870
6	871
7	873
8	874
9	875
10	877
11	878
12	879
13	881
14	882
15	883
16	884
17	886
18	887
19	888
20	890
21	891
22	892
23	894
24	895
25	896
26	897
27	899
28	900
29	901
30	903
31	904
32	905
33	907
34	908
35	909
36	910
37	912
38	913
39	914
40	916
41	917
42	918
43	920

44	5884
45	5885
46	5886
47	5887
48	5888
49	5889
50	5890
51	5891
52	5892
53	5893
54	5894
55	5895
56	5896
57	5897
58	5898
59	5899
60	5900
61	5901
62	5902
63	5903
64	5904
65	5905
66	5906
67	5907
68	5908
69	5909
70	5910
71	5911
72	5912
73	5913
74	5914
75	5915
76	5916
77	5917
78	5918
79	5919
80	5920
81	5921
82	5922
83	5923
84	5924
85	5925
86	5926
87	5927
88	5928
89	5929
90	5930
91	5931
92	5932

44	1201
45	1220
46	1229
47	1238
48	1246
49	1255
50	1264
51	1273
52	1282
53	1290
54	1299
55	1308
56	1317
57	1325
58	1334
59	1343
60	1352
61	1361
62	1369
63	1378
64	1387
65	1396
66	1430
67	1465
68	1500
69	1534
70	1569
71	1604
72	1638
73	1673
74	1708
75	1743
76	1777
77	1812
78	1847
79	1881
80	1916
81	1951
82	1985
83	2020
84	2055
85	2089
86	2101
87	2112
88	2123
89	2134
90	2146
91	2157
92	2168

44	921
45	922
46	923
47	925
48	926
49	927
50	928
51	928
52	929
53	930
54	930
55	931
56	931
57	932
58	933
59	933
60	934
61	935
62	935
63	936
64	937
65	937
66	942
67	946
68	950
69	955
70	959
71	963
72	968
73	972
74	974
75	976
76	979
77	981
78	983
79	986
80	988
81	990
82	995
83	999
84	1004
85	1008
86	1013
87	1018
88	1022
89	1027
90	1030
91	1034
92	1037

93	5933
94	5934
95	5935
96	5936
97	5937
98	5938
99	5939
100	5940
101	5941
102	5942
103	5943
104	5944
105	5945
106	5947
107	5948
108	5949
109	5950
110	5951
111	5952
112	5953
113	5954
114	5955
115	5956
116	5957
117	5958
118	5959
119	5960
120	5961
121	5962
122	5963
123	5964
124	5965
125	5966
126	5967
127	5968
128	5969
129	5970
130	5971
131	5972
132	5973
133	5974
134	5975
135	5976
136	5977
137	5978
138	5979
139	5980
140	5981
141	5982

93	2179
94	2191
95	2202
96	2213
97	2224
98	2236
99	2247
100	2258
101	2269
102	2281
103	2292
104	2303
105	2315
106	2322
107	2330
108	2337
109	2345
110	2352
111	2360
112	2368
113	2375
114	2383
115	2390
116	2398
117	2405
118	2413
119	2421
120	2428
121	2436
122	2443
123	2451
124	2458
125	2466
126	2478
127	2489
128	2500
129	2512
130	2523
131	2535
132	2546
133	2558
134	2569
135	2581
136	2592
137	2603
138	2615
139	2626
140	2638
141	2649

93	1040
94	1044
95	1047
96	1051
97	1054
98	1056
99	1059
100	1061
101	1063
102	1065
103	1067
104	1070
105	1072
106	1078
107	1083
108	1089
109	1095
110	1100
111	1106
112	1112
113	1117
114	1120
115	1123
116	1125
117	1128
118	1130
119	1133
120	1135
121	1138
122	1143
123	1149
124	1154
125	1159
126	1165
127	1170
128	1176
129	1181
130	1188
131	1195
132	1201
133	1208
134	1215
135	1221
136	1228
137	1235
138	1235
139	1236
140	1236
141	1237

142	5983
143	5984
144	5985
145	5986
146	5987
147	5988
148	5989
149	5990
150	5991
151	5992
152	5993
153	5994
154	5995
155	5996
156	5997
157	5998
158	5999
159	6000
160	6001
161	6002
162	6003
163	6004
164	6005
165	6006
166	6007
167	6008
168	6009
169	6010
170	6011
171	6012
172	6013
173	6015
174	6016
175	6018
176	6019
177	6021
178	6022
179	6023
180	6025
181	6026
182	6028
183	6029
184	6031
185	6032
186	6034
187	6035
188	6036
189	6038
190	6039

142	2661
143	2672
144	2684
145	2695
146	2726
147	2757
148	2788
149	2818
150	2849
151	2880
152	2911
153	2942
154	2973
155	3004
156	3034
157	3065
158	3096
159	3127
160	3158
161	3189
162	3219
163	3250
164	3281
165	3312
166	3328
167	3344
168	3360
169	3376
170	3393
171	3409
172	3425
173	3441
174	3457
175	3473
176	3489
177	3505
178	3521
179	3537
180	3554
181	3570
182	3586
183	3602
184	3618
185	3634
186	3643
187	3653
188	3662
189	3672
190	3681

142	1237
143	1238
144	1238
145	1239
146	1242
147	1244
148	1247
149	1250
150	1253
151	1256
152	1258
153	1261
154	1267
155	1273
156	1279
157	1284
158	1290
159	1296
160	1302
161	1307
162	1308
163	1309
164	1309
165	1310
166	1311
167	1311
168	1312
169	1313
170	1315
171	1317
172	1319
173	1321
174	1323
175	1325
176	1327
177	1329
178	1330
179	1332
180	1333
181	1334
182	1336
183	1337
184	1339
185	1340
186	1343
187	1345
188	1348
189	1351
190	1353

191	6041
192	6042
193	6044
194	6045
195	6046
196	6048
197	6049
198	6050
199	6052
200	6053
201	6054
202	6056
203	6057
204	6058
205	6060
206	6061
207	6062
208	6064
209	6065
210	6066
211	6068
212	6069
213	6071
214	6074
215	6076
216	6078
217	6080
218	6083
219	6085
220	6087
221	6089
222	6091
223	6094
224	6096
225	6098
226	6100
227	6103
228	6105
229	6107
230	6109
231	6112
232	6114
233	6121
234	6128
235	6135
236	6142
237	6149
238	6156
239	6163

191	3690
192	3700
193	3709
194	3719
195	3728
196	3737
197	3747
198	3756
199	3766
200	3775
201	3784
202	3794
203	3803
204	3813
205	3822
206	3847
207	3872
208	3896
209	3921
210	3946
211	3971
212	3996
213	4021
214	4045
215	4070
216	4095
217	4120
218	4145
219	4169
220	4194
221	4219
222	4244
223	4269
224	4294
225	4318
226	4343
227	4368
228	4393
229	4418
230	4443
231	4468
232	4493
233	4518
234	4543
235	4568
236	4593
237	4617
238	4642
239	4667

191	1356
192	1359
193	1361
194	1366
195	1370
196	1375
197	1379
198	1384
199	1388
200	1393
201	1397
202	1397
203	1398
204	1398
205	1398
206	1398
207	1398
208	1399
209	1399
210	1400
211	1402
212	1404
213	1406
214	1407
215	1409
216	1411
217	1413
218	1413
219	1414
220	1415
221	1416
222	1416
223	1417
224	1418
225	1419
226	1422
227	1425
228	1428
229	1431
230	1434
231	1438
232	1441
233	1444
234	1452
235	1460
236	1468
237	1476
238	1484
239	1492

240	6170
241	6177
242	6184
243	6191
244	6198
245	6205
246	6212
247	6220
248	6227
249	6234
250	6241
251	6248
252	6255
253	6268
254	6281
255	6293
256	6306
257	6319
258	6332
259	6345
260	6358
261	6371
262	6383
263	6396
264	6409
265	6422
266	6435
267	6448
268	6461
269	6474
270	6486
271	6499
272	6512
273	6514
274	6515
275	6517
276	6518
277	6520
278	6522
279	6523
280	6525
281	6526
282	6528
283	6529
284	6531
285	6533
286	6534
287	6536
288	6537

240	4692
241	4717
242	4742
243	4767
244	4792
245	4817
246	4839
247	4862
248	4884
249	4906
250	4929
251	4951
252	4973
253	4996
254	5018
255	5041
256	5063
257	5085
258	5108
259	5130
260	5152
261	5175
262	5197
263	5219
264	5242
265	5264
266	5270
267	5277
268	5283
269	5289
270	5295
271	5301
272	5308
273	5314
274	5320
275	5326
276	5333
277	5339
278	5345
279	5351
280	5357
281	5364
282	5370
283	5376
284	5382
285	5389
286	5423
287	5458
288	5493

240	1500
241	1508
242	1509
243	1511
244	1512
245	1514
246	1515
247	1517
248	1518
249	1519
250	1526
251	1533
252	1539
253	1546
254	1552
255	1559
256	1565
257	1572
258	1573
259	1573
260	1574
261	1575
262	1575
263	1576
264	1577
265	1577
266	1579
267	1581
268	1583
269	1584
270	1586
271	1588
272	1589
273	1591
274	1592
275	1593
276	1593
277	1594
278	1595
279	1596
280	1596
281	1597
282	1602
283	1608
284	1613
285	1618
286	1623
287	1629
288	1634

289	6539
290	6541
291	6542
292	6544
293	6545
294	6546
295	6547
296	6548
297	6549
298	6551
299	6552
300	6553
301	6554
302	6555
303	6556
304	6558
305	6559
306	6560
307	6561
308	6562
309	6563
310	6565
311	6566
312	6567
313	6573
314	6578
315	6584
316	6590
317	6596
318	6602
319	6607
320	6613
321	6619
322	6625
323	6630
324	6636
325	6642
326	6648
327	6653
328	6659
329	6665
330	6671
331	6677
332	6682
333	6686
334	6690
335	6695
336	6699
337	6703

289	5528
290	5563
291	5598
292	5633
293	5668
294	5703
295	5737
296	5772
297	5807
298	5842
299	5877
300	5912
301	5947
302	5982
303	6017
304	6051
305	6086
306	6108
307	6130
308	6152
309	6174
310	6197
311	6219
312	6241
313	6263
314	6285
315	6307
316	6329
317	6351
318	6373
319	6395
320	6417
321	6439
322	6461
323	6483
324	6505
325	6527
326	6534
327	6541
328	6548
329	6555
330	6562
331	6569
332	6576
333	6582
334	6589
335	6596
336	6603
337	6610

289	1639
290	1641
291	1643
292	1645
293	1647
294	1649
295	1651
296	1653
297	1655
298	1657
299	1658
300	1660
301	1661
302	1663
303	1664
304	1666
305	1667
306	1670
307	1673
308	1676
309	1680
310	1683
311	1686
312	1689
313	1692
314	1693
315	1694
316	1695
317	1696
318	1697
319	1698
320	1699
321	1700
322	1707
323	1715
324	1722
325	1729
326	1737
327	1744
328	1751
329	1759
330	1762
331	1765
332	1768
333	1772
334	1775
335	1778
336	1781
337	1784

338	6707
339	6711
340	6715
341	6719
342	6723
343	6727
344	6731
345	6735
346	6739
347	6743
348	6747
349	6751
350	6755
351	6759
352	6763
353	6769
354	6774
355	6779
356	6785
357	6790
358	6795
359	6801
360	6806
361	6811
362	6816
363	6822
364	6827
365	6832
366	6838
367	6843
368	6848
369	6854
370	6859
371	6864
372	6869
373	6876
374	6883
375	6890
376	6896
377	6903
378	6910
379	6916
380	6923
381	6930
382	6937
383	6943
384	6950
385	6957
386	6963

338	6617
339	6624
340	6631
341	6638
342	6645
343	6652
344	6659
345	6666
346	6675
347	6685
348	6694
349	6704
350	6713
351	6722
352	6732
353	6741
354	6751
355	6760
356	6770
357	6779
358	6789
359	6798
360	6808
361	6817
362	6827
363	6836
364	6845
365	6855
366	6859
367	6862
368	6866
369	6870
370	6873
371	6877
372	6881
373	6884
374	6888
375	6892
376	6895
377	6899
378	6903
379	6906
380	6910
381	6914
382	6917
383	6921
384	6925
385	6928
386	6942

338	1786
339	1787
340	1788
341	1789
342	1790
343	1791
344	1793
345	1794
346	1794
347	1795
348	1796
349	1796
350	1797
351	1797
352	1798
353	1798
354	1803
355	1807
356	1811
357	1815
358	1819
359	1824
360	1828
361	1832
362	1833
363	1834
364	1835
365	1837
366	1838
367	1839
368	1840
369	1841
370	1850
371	1858
372	1867
373	1876
374	1884
375	1893
376	1902
377	1910
378	1914
379	1918
380	1922
381	1926
382	1931
383	1935
384	1939
385	1943
386	1947

387	6970
388	6977
389	6983
390	6990
391	6997
392	7004
393	7008
394	7013
395	7017
396	7022
397	7026
398	7031
399	7036
400	7040
401	7045
402	7049
403	7054
404	7058
405	7063
406	7067
407	7072
408	7077
409	7081
410	7086
411	7090
412	7095
413	7103
414	7111
415	7119
416	7127
417	7135
418	7143
419	7151
420	7159
421	7168
422	7176
423	7184
424	7192
425	7200
426	7208
427	7216
428	7224
429	7232
430	7240
431	7248
432	7256
433	7264
434	7271
435	7278

387	6955
388	6968
389	6981
390	6995
391	7008
392	7021
393	7035
394	7048
395	7061
396	7074
397	7088
398	7101
399	7114
400	7127
401	7141
402	7154
403	7167
404	7181
405	7194
406	7205
407	7215
408	7226
409	7236
410	7247
411	7258
412	7268
413	7279
414	7289
415	7300
416	7311
417	7321
418	7332
419	7342
420	7353
421	7364
422	7374
423	7385
424	7395
425	7406
426	7411
427	7415
428	7420
429	7424
430	7429
431	7433
432	7438
433	7443
434	7447
435	7452

387	1952
388	1956
389	1960
390	1965
391	1969
392	1973
393	1978
394	1982
395	1986
396	1991
397	1995
398	1999
399	2004
400	2008
401	2012
402	2016
403	2020
404	2025
405	2029
406	2033
407	2037
408	2041
409	2045
410	2050
411	2056
412	2061
413	2066
414	2072
415	2077
416	2082
417	2087
418	2093
419	2100
420	2106
421	2112
422	2118
423	2124
424	2130
425	2136
426	2147
427	2158
428	2169
429	2181
430	2192
431	2203
432	2214
433	2226
434	2233
435	2239

436	7285
437	7293
438	7300
439	7307
440	7314
441	7322
442	7329
443	7336
444	7343
445	7351
446	7358
447	7365
448	7372
449	7380
450	7387
451	7394
452	7401
453	7405
454	7409
455	7413
456	7417
457	7421
458	7425
459	7429
460	7433
461	7437
462	7441
463	7445
464	7449
465	7453
466	7457
467	7461
468	7465
469	7469
470	7473
471	7477
472	7481
473	7483
474	7486
475	7489
476	7491
477	7494
478	7497
479	7499
480	7502
481	7504
482	7507
483	7510
484	7512

436	7456
437	7461
438	7465
439	7470
440	7475
441	7479
442	7484
443	7488
444	7493
445	7497
446	7507
447	7518
448	7528
449	7538
450	7548
451	7558
452	7568
453	7578
454	7588
455	7599
456	7609
457	7619
458	7629
459	7639
460	7649
461	7659
462	7669
463	7679
464	7690
465	7700
466	7704
467	7708
468	7713
469	7717
470	7721
471	7725
472	7730
473	7734
474	7738
475	7742
476	7747
477	7751
478	7755
479	7759
480	7764
481	7768
482	7772
483	7777
484	7781

436	2246
437	2253
438	2260
439	2267
440	2273
441	2280
442	2282
443	2284
444	2286
445	2288
446	2290
447	2292
448	2293
449	2295
450	2302
451	2308
452	2315
453	2321
454	2327
455	2334
456	2340
457	2346
458	2350
459	2353
460	2357
461	2360
462	2364
463	2367
464	2371
465	2374
466	2377
467	2380
468	2384
469	2387
470	2390
471	2393
472	2396
473	2399
474	2401
475	2403
476	2404
477	2406
478	2408
479	2410
480	2411
481	2413
482	2415
483	2417
484	2419

485	7515
486	7518
487	7520
488	7523
489	7525
490	7528
491	7531
492	7533
493	7554
494	7575
495	7596
496	7617
497	7639
498	7660
499	7681
500	7702
501	7723
502	7744
503	7765
504	7786
505	7807
506	7828
507	7849
508	7870
509	7891
510	7912
511	7933
512	7954
513	7961
514	7967
515	7974
516	7981
517	7987
518	7994
519	8001
520	8007
521	8014
522	8021
523	8027
524	8034
525	8041
526	8048
527	8054
528	8061
529	8068
530	8074
531	8081
532	8088
533	8096

485	7785
486	7812
487	7840
488	7867
489	7895
490	7922
491	7950
492	7977
493	8004
494	8032
495	8059
496	8087
497	8114
498	8141
499	8169
500	8196
501	8224
502	8251
503	8278
504	8306
505	8333
506	8338
507	8343
508	8349
509	8354
510	8359
511	8364
512	8369
513	8374
514	8379
515	8384
516	8389
517	8394
518	8399
519	8404
520	8409
521	8414
522	8420
523	8425
524	8430
525	8435
526	8448
527	8460
528	8473
529	8486
530	8499
531	8511
532	8524
533	8537

485	2421
486	2424
487	2426
488	2428
489	2430
490	2433
491	2436
492	2439
493	2442
494	2445
495	2448
496	2451
497	2454
498	2459
499	2463
500	2468
501	2472
502	2477
503	2481
504	2485
505	2490
506	2495
507	2500
508	2505
509	2510
510	2515
511	2520
512	2525
513	2530
514	2531
515	2531
516	2531
517	2532
518	2532
519	2532
520	2533
521	2533
522	2536
523	2538
524	2541
525	2543
526	2546
527	2548
528	2551
529	2554
530	2555
531	2557
532	2559
533	2561

534	8104
535	8112
536	8120
537	8128
538	8136
539	8144
540	8152
541	8160
542	8168
543	8176
544	8185
545	8193
546	8201
547	8209
548	8217
549	8225
550	8233
551	8241
552	8249
553	8272
554	8294
555	8316
556	8339
557	8361
558	8384
559	8406
560	8428
561	8451
562	8473
563	8496
564	8518
565	8540
566	8563
567	8585
568	8608
569	8630
570	8652
571	8675
572	8697
573	8711
574	8725
575	8738
576	8752
577	8766
578	8780
579	8794
580	8808
581	8821
582	8835

534	8550
535	8563
536	8575
537	8588
538	8601
539	8614
540	8627
541	8639
542	8652
543	8665
544	8678
545	8690
546	8702
547	8714
548	8726
549	8738
550	8750
551	8762
552	8773
553	8785
554	8797
555	8809
556	8821
557	8833
558	8844
559	8856
560	8868
561	8880
562	8892
563	8904
564	8916
565	8927
566	8961
567	8995
568	9028
569	9062
570	9096
571	9129
572	9163
573	9197
574	9230
575	9264
576	9298
577	9331
578	9365
579	9399
580	9432
581	9466
582	9500

534	2563
535	2564
536	2566
537	2568
538	2568
539	2569
540	2569
541	2569
542	2569
543	2570
544	2570
545	2570
546	2571
547	2573
548	2574
549	2575
550	2576
551	2577
552	2579
553	2580
554	2581
555	2582
556	2583
557	2584
558	2585
559	2586
560	2587
561	2588
562	2593
563	2597
564	2601
565	2606
566	2610
567	2614
568	2619
569	2623
570	2631
571	2639
572	2646
573	2654
574	2662
575	2670
576	2678
577	2686
578	2686
579	2687
580	2688
581	2689
582	2690

583	8849
584	8863
585	8877
586	8890
587	8904
588	8918
589	8932
590	8946
591	8959
592	8973
593	8988
594	9004
595	9019
596	9034
597	9050
598	9065
599	9080
600	9095
601	9111
602	9126
603	9141
604	9157
605	9172
606	9187
607	9202
608	9218
609	9233
610	9248
611	9264
612	9279
613	9298
614	9317
615	9335
616	9354
617	9373
618	9392
619	9411
620	9430
621	9449
622	9467
623	9486
624	9505
625	9524
626	9543
627	9562
628	9580
629	9599
630	9618
631	9637

583	9533
584	9567
585	9601
586	9610
587	9619
588	9628
589	9637
590	9646
591	9655
592	9664
593	9673
594	9682
595	9691
596	9700
597	9710
598	9719
599	9728
600	9737
601	9746
602	9755
603	9764
604	9773
605	9782
606	9793
607	9803
608	9814
609	9825
610	9835
611	9846
612	9856
613	9867
614	9878
615	9888
616	9899
617	9910
618	9920
619	9931
620	9941
621	9952
622	9963
623	9973
624	9984
625	9995
626	10019
627	10043
628	10067
629	10092
630	10116
631	10140

583	2691
584	2692
585	2692
586	2694
587	2696
588	2698
589	2700
590	2702
591	2704
592	2706
593	2708
594	2711
595	2714
596	2716
597	2719
598	2722
599	2724
600	2727
601	2730
602	2732
603	2734
604	2737
605	2739
606	2742
607	2744
608	2746
609	2749
610	2756
611	2764
612	2772
613	2779
614	2787
615	2795
616	2802
617	2810
618	2811
619	2812
620	2813
621	2813
622	2814
623	2815
624	2816
625	2817
626	2821
627	2825
628	2829
629	2833
630	2837
631	2841

632	9656
633	9666
634	9676
635	9685
636	9695
637	9705
638	9715
639	9725
640	9735
641	9745
642	9755
643	9764
644	9774
645	9784
646	9794
647	9804
648	9814
649	9824
650	9834
651	9843
652	9853
653	9863
654	9873
655	9884
656	9894
657	9904
658	9914
659	9924
660	9934
661	9944
662	9954
663	9964
664	9974
665	9984
666	9994
667	10005
668	10015
669	10025
670	10035
671	10045
672	10055
673	10102
674	10149
675	10196
676	10243
677	10290
678	10337
679	10384
680	10431

632	10164
633	10189
634	10213
635	10237
636	10261
637	10286
638	10310
639	10334
640	10358
641	10383
642	10407
643	10431
644	10456
645	10480
646	10485
647	10490
648	10495
649	10500
650	10506
651	10511
652	10516
653	10521
654	10526
655	10531
656	10536
657	10542
658	10547
659	10552
660	10557
661	10562
662	10567
663	10572
664	10578
665	10583
666	10608
667	10634
668	10660
669	10685
670	10711
671	10737
672	10762
673	10788
674	10814
675	10840
676	10865
677	10891
678	10917
679	10942
680	10968

632	2845
633	2849
634	2853
635	2856
636	2860
637	2863
638	2867
639	2870
640	2874
641	2877
642	2879
643	2880
644	2882
645	2883
646	2885
647	2886
648	2888
649	2889
650	2891
651	2892
652	2894
653	2895
654	2897
655	2899
656	2900
657	2902
658	2904
659	2906
660	2908
661	2910
662	2912
663	2914
664	2916
665	2918
666	2922
667	2926
668	2930
669	2934
670	2938
671	2943
672	2947
673	2951
674	2953
675	2955
676	2956
677	2958
678	2960
679	2962
680	2964

681	10479
682	10526
683	10573
684	10620
685	10667
686	10714
687	10761
688	10808
689	10855
690	10902
691	10949
692	10996
693	11001
694	11005
695	11010
696	11015
697	11019
698	11024
699	11028
700	11033
701	11037
702	11042
703	11047
704	11051
705	11056
706	11060
707	11065
708	11069
709	11074
710	11079
711	11083
712	11088
713	11136
714	11185
715	11233
716	11282
717	11330
718	11379
719	11427
720	11476
721	11524
722	11573
723	11621
724	11670
725	11718
726	11767
727	11815
728	11864
729	11912

681	10994
682	11019
683	11045
684	11071
685	11096
686	11118
687	11139
688	11161
689	11182
690	11203
691	11225
692	11246
693	11267
694	11289
695	11310
696	11332
697	11353
698	11374
699	11396
700	11417
701	11438
702	11460
703	11481
704	11503
705	11524
706	11566
707	11608
708	11649
709	11691
710	11733
711	11775
712	11817
713	11859
714	11901
715	11943
716	11984
717	12026
718	12068
719	12110
720	12152
721	12194
722	12236
723	12277
724	12319
725	12361
726	12384
727	12407
728	12429
729	12452

681	2966
682	2969
683	2972
684	2975
685	2979
686	2982
687	2985
688	2988
689	2991
690	2997
691	3002
692	3008
693	3013
694	3018
695	3024
696	3029
697	3035
698	3042
699	3050
700	3058
701	3066
702	3074
703	3082
704	3090
705	3098
706	3099
707	3100
708	3101
709	3101
710	3102
711	3103
712	3104
713	3105
714	3108
715	3111
716	3114
717	3117
718	3120
719	3123
720	3126
721	3128
722	3132
723	3135
724	3139
725	3142
726	3145
727	3149
728	3152
729	3155

730	11961
731	12009
732	12058
733	12069
734	12079
735	12090
736	12101
737	12112
738	12122
739	12133
740	12144
741	12155
742	12166
743	12176
744	12187
745	12198
746	12209
747	12219
748	12230
749	12241
750	12252
751	12262
752	12273
753	12274
754	12275
755	12276
756	12277
757	12278
758	12279
759	12280
760	12281
761	12282
762	12283
763	12284
764	12285
765	12286
766	12287
767	12288
768	12289
769	12290
770	12291
771	12292
772	12293
773	12312
774	12331
775	12350
776	12368
777	12387
778	12406

730	12475
731	12497
732	12520
733	12543
734	12566
735	12588
736	12611
737	12634
738	12657
739	12679
740	12702
741	12725
742	12747
743	12770
744	12793
745	12816
746	12823
747	12831
748	12839
749	12847
750	12855
751	12863
752	12871
753	12878
754	12886
755	12894
756	12902
757	12910
758	12918
759	12925
760	12933
761	12941
762	12949
763	12957
764	12965
765	12973
766	12979
767	12986
768	12992
769	12999
770	13005
771	13012
772	13018
773	13025
774	13031
775	13038
776	13044
777	13051
778	13057

730	3159
731	3163
732	3168
733	3172
734	3176
735	3180
736	3184
737	3188
738	3188
739	3189
740	3190
741	3190
742	3191
743	3192
744	3192
745	3193
746	3195
747	3198
748	3200
749	3203
750	3205
751	3208
752	3210
753	3213
754	3217
755	3221
756	3225
757	3229
758	3233
759	3237
760	3241
761	3245
762	3246
763	3247
764	3248
765	3249
766	3250
767	3251
768	3252
769	3253
770	3262
771	3271
772	3279
773	3288
774	3297
775	3306
776	3314
777	3323
778	3326

779	12425
780	12444
781	12462
782	12481
783	12500
784	12519
785	12538
786	12556
787	12575
788	12594
789	12613
790	12632
791	12650
792	12669
793	12677
794	12685
795	12693
796	12700
797	12708
798	12716
799	12724
800	12732
801	12740
802	12747
803	12755
804	12763
805	12771
806	12779
807	12786
808	12794
809	12802
810	12810
811	12818
812	12825
813	12841
814	12856
815	12871
816	12886
817	12901
818	12916
819	12932
820	12947
821	12962
822	12977
823	12992
824	13008
825	13023
826	13038
827	13053

779	13064
780	13070
781	13077
782	13083
783	13090
784	13096
785	13103
786	13110
787	13117
788	13124
789	13130
790	13137
791	13144
792	13151
793	13158
794	13165
795	13172
796	13179
797	13185
798	13192
799	13199
800	13206
801	13213
802	13220
803	13227
804	13234
805	13240
806	13253
807	13265
808	13277
809	13289
810	13301
811	13314
812	13326
813	13338
814	13350
815	13362
816	13374
817	13387
818	13399
819	13411
820	13423
821	13435
822	13448
823	13460
824	13472
825	13484

779	3330
780	3333
781	3336
782	3339
783	3342
784	3345
785	3348
786	3349
787	3350
788	3351
789	3351
790	3352
791	3353
792	3354
793	3354
794	3356
795	3358
796	3360
797	3362
798	3364
799	3366
800	3368
801	3369
802	3371
803	3372
804	3374
805	3375
806	3377
807	3378
808	3380
809	3381
810	3383
811	3385
812	3387
813	3389
814	3391
815	3393
816	3395
817	3397
818	3399
819	3402
820	3404
821	3406
822	3409
823	3411
824	3413
825	3416
826	3417
827	3420

828	13068
829	13083
830	13099
831	13114
832	13129
833	13156
834	13183
835	13211
836	13238
837	13265
838	13292
839	13320
840	13347
841	13374
842	13401
843	13429
844	13456
845	13483
846	13510
847	13538
848	13565
849	13592
850	13619
851	13647
852	13674
853	13762
854	13849
855	13937
856	14025
857	14113
858	14200
859	14288
860	14376
861	14464
862	14551
863	14639
864	14727
865	14814
866	14902
867	14990
868	15078
869	15165
870	15253
871	15341
872	15429
873	15462
874	15495
875	15529
876	15562

828	3422
829	3424
830	3426
831	3429
832	3431
833	3433
834	3435
835	3437
836	3440
837	3442
838	3444
839	3446
840	3449
841	3451
842	3453
843	3455
844	3457
845	3460
846	3462
847	3464
848	3466
849	3469
850	3471
851	3473
852	3475
853	3477
854	3480
855	3482
856	3484
857	3486
858	3489
859	3491
860	3493
861	3495
862	3497
863	3500
864	3502
865	3504
866	3506
867	3509
868	3511
869	3513
870	3515
871	3517
872	3520
873	3522
874	3524
875	3526
876	3529

877	15595
878	15629
879	15662
880	15695
881	15729
882	15762
883	15796
884	15829
885	15862
886	15896
887	15929
888	15962
889	15996
890	16029
891	16062
892	16096
893	16142
894	16189
895	16235
896	16282
897	16328
898	16375
899	16421
900	16468
901	16514
902	16561
903	16607
904	16654
905	16700
906	16747
907	16793
908	16840
909	16886
910	16933
911	16979
912	17026
913	17057
914	17088
915	17119
916	17150
917	17182
918	17213
919	17244
920	17275
921	17306
922	17337
923	17369
924	17400
925	17431

877	3531
878	3533
879	3535
880	3537
881	3540
882	3542
883	3544
884	3546
885	3549
886	3551
887	3553
888	3555
889	3557
890	3560
891	3562
892	3564
893	3566
894	3568
895	3571
896	3573
897	3575
898	3577
899	3580
900	3582
901	3584
902	3586
903	3588
904	3591
905	3593
906	3595
907	3597
908	3600
909	3602
910	3604
911	3606
912	3608
913	3611
914	3613
915	3615
916	3617
917	3620
918	3622
919	3624
920	3626
921	3628
922	3631
923	3633
924	3635
925	3637

926	17462
927	17493
928	17525
929	17556
930	17587
931	17618
932	17649
933	17655
934	17661
935	17667
936	17673
937	17678
938	17684
939	17690
940	17696
941	17701
942	17707
943	17713
944	17719
945	17725
946	17730
947	17736
948	17742
949	17748
950	17753
951	17759
952	17765
953	17786
954	17808
955	17829
956	17851
957	17872
958	17894
959	17915
960	17936
961	17958
962	17979
963	18001
964	18022
965	18044
966	18065
967	18086
968	18108
969	18129
970	18151
971	18172
972	18194
973	18214
974	18234

926	3640
927	3642
928	3644
929	3646
930	3648
931	3651
932	3653
933	3655
934	3657
935	3660
936	3662
937	3664
938	3666
939	3668
940	3671
941	3673
942	3675
943	3677
944	3680
945	3682
946	3684
947	3686
948	3688
949	3691
950	3693
951	3695
952	3697
953	3700
954	3702
955	3704
956	3706
957	3708
958	3711
959	3713
960	3715
961	3717
962	3720
963	3722
964	3724
965	3726
966	3728
967	3731
968	3733

975	18255
976	18275
977	18296
978	18316
979	18336
980	18357
981	18377
982	18398
983	18418
984	18438
985	18459
986	18479
987	18500
988	18520
989	18541
990	18561
991	18581
992	18602
993	18609
994	18616
995	18622
996	18629
997	18636
998	18643
999	18650
1000	18657
1001	18664
1002	18671
1003	18678
1004	18685
1005	18692
1006	18699
1007	18705
1008	18712
1009	18719
1010	18726
1011	18733
1012	18740
1013	18754
1014	18767
1015	18781
1016	18795
1017	18808
1018	18822
1019	18836
1020	18849
1021	18863
1022	18877
1023	18890

1024	18904
1025	18918
1026	18931
1027	18945
1028	18959
1029	18972
1030	18986
1031	19000
1032	19013
1033	19035
1034	19056
1035	19078
1036	19099
1037	19121
1038	19142
1039	19164
1040	19185
1041	19207
1042	19228
1043	19250
1044	19271
1045	19293
1046	19314
1047	19336
1048	19357
1049	19379
1050	19400
1051	19422
1052	19443
1053	19465
1054	19486
1055	19508
1056	19529
1057	19551
1058	19572
1059	19594
1060	19615
1061	19637
1062	19658
1063	19680
1064	19701

Appendix B

4P Downcore Geochemistry and Geophysical Data

Age(ya)	Depth (cm)	TIC (%)	TOC (%)
864	0	1.81	0.97
874	8	1.60	1.05
884	16	1.98	1.09
895	24	2.33	1.12
905	32	2.12	1.28
916	40	2.37	1.90
926	48	1.92	1.80
931	56	2.15	1.73
939	64	1.97	1.46
966	72	2.25	1.71
	73	2.23	1.53
989	81	2.05	1.19
1022	89	1.30	1.79
1050	97	2.01	1.27
1072	105	2.16	1.08
1110	113	1.84	1.14
1137	121	1.70	1.10
1177	129	2.04	1.04
1225	137	1.89	1.05
1240	145	1.86	1.00
1260	153	1.79	1.09
1299	161	1.91	1.07
1313	169	1.58	1.14
1326	177	1.58	1.08
1339	185	1.90	1.16
1360	193	2.22	1.22
1390	201	2.18	1.16
1399	209	2.03	1.02
1410	217	1.67	1.01
	222	1.82	1.10
1419	230	2.18	1.06
1443	238	2.14	1.08
1496	246	1.73	1.07
1521	254	1.62	1.24
1562	262	1.76	1.26
1577	270	1.64	1.33
1589	278	1.76	1.20
1599	286	1.47	1.25
1632	294	1.60	1.08
1653	302	1.85	1.12
1667	310	1.51	1.02
1687	318	1.07	0.95
1702	326	1.28	0.79
1749	334	0.81	0.62
1780	342	0.56	0.70

46P Downcore Geochemistry and

Age(ya)	Depth (cm)	TOC (%)
5872	32	1.27
5880	40	1.65
5888	48	2.17
5896	56	2.07
5904	64	1.92
5912	72	
5920	80	1.91
5928	88	2.18
5936	96	1.63
5944	104	1.75
5953	112	1.93
5961	120	1.81
5969	128	2.47
5977	136	2.46
5985	144	2.41
5992	151	2.94
6000	159	2.39
6008	167	2.27
6018	175	3.02
6029	183	2.65
6041	191	2.30
6052	199	3.49
6062	207	3.36
6076	215	3.32
6094	223	3.23
6114	231	2.42
6163	239	3.66
6219	247	3.12
6294	255	3.32
6396	263	2.71
6493	271	3.05
6523	279	3.30
6536	287	3.24
6547	295	3.16
6553	300	3.35
6562	308	3.20
6590	316	4.22
6636	324	3.42
6681	332	2.94
6715	340	4.05
6747	348	3.97
6785	356	4.09
6827	364	4.67
6871	372	4.17
6923	380	3.69

1792	350	3.62	0.79
1800	358	1.80	1.08
1826	366	1.50	1.17
	371	2.14	1.11
1844	379	1.53	0.97
1899	387	2.61	1.05
1939	395	1.93	1.17
1973	403	1.54	1.09
2008	411	2.57	1.20
2042	419	2.19	1.22
2083	427	2.44	1.11
2133	435	2.28	1.19
2212	443	2.14	1.32
2271	450	2.04	1.62
2296	458	2.81	1.39
2338	466	2.09	1.52
2371	474	2.40	1.25
2395	482	1.88	1.21
2412	490	1.57	1.02
2428	498	1.87	0.89
2452	505	2.57	2.34
2486	512	1.34	0.72
2523	519	2.11	2.34
2534	526	1.88	1.11
2551	533	1.93	1.10
2565	540	2.03	1.01
2570	546	1.77	0.97
2579	554	2.00	1.31
2589	562	2.49	1.20
2621	570	2.15	1.13
2674	578	1.85	0.96
2692	586	2.24	1.26
2707	594	2.27	1.20
2727	602	2.36	1.28
2749	610	2.51	1.23
2798	618	2.45	1.03
2818	626	2.94	1.01
2845	634	1.96	1.10
2873	642	2.30	1.25
2888	650	2.17	1.21
2900	657	1.99	1.23
2917	665	1.96	1.19
2945	673	2.16	1.26
2965	681	1.80	1.09
2989	689	2.09	1.26
3031	697	1.92	1.11
3086	705	1.99	1.15
3105	713	2.20	1.06
3126	721	2.17	1.01

6977	388	3.90
7022	396	3.95
7058	404	3.50
7098	412	3.25
7159	420	3.96
7224	428	3.94
7285	436	4.70
7343	444	4.60
7391	451	5.18
7449	459	4.39
7472	467	3.27
7496	470	3.24
7507	478	2.86
7518	486	5.15
7580	494	5.49
7744	502	4.78
7908	510	3.96
7994	518	3.36
8047	526	3.47
8104	534	4.78
8168	542	3.52
8237	550	5.21
8384	558	4.79
8563	566	3.74
8722	574	4.07
8835	582	3.55
8946	590	4.66
9065	598	3.85
9187	606	5.23
9317	614	5.08
9439	621	5.52
9590	629	5.99
9700	637	5.81
9779	645	5.77
9858	653	5.35
9939	661	5.55
10020	669	5.37
10267	677	5.06
10643	685	5.36
10966	693	4.41
11035	701	3.49
11072	709	3.39
11306	717	3.11
11694	725	2.90
12034	733	1.68
12149	741	1.04
12235	749	1.40
12278	757	1.42
12286	765	1.31

3152	729	1.96	0.93
3182	737	1.91	1.03
3193	745	1.63	1.10
3211	753	2.16	1.05
3239	761	1.62	0.91
3256	769	1.66	1.00
3311	777	1.86	1.21
3344	785	1.99	1.07
3354	793	1.85	0.97
3367	801	2.04	0.97
3380	806	2.33	1.14
3395	814	1.64	0.89
3413	822	1.64	0.84
3431	830	1.66	0.86
3449	838	1.36	0.89
3466	846	2.09	1.09
3484	854	2.06	1.02
3502	862	2.13	1.13
3520	870	2.24	1.11
3537	878	2.12	1.07
3555	886	1.92	0.97
3573	894	1.82	0.86
3591	902	1.83	1.00
3608	910	1.81	0.90
3626	918	1.99	0.81
3644	926	2.02	0.94
3662	934	2.02	0.98
3680	942	2.06	0.97
3711	950	1.98	1.11

12302	771	1.69
12425	779	1.25
12575	787	1.32
12692	795	1.42
12755	803	1.42
12822	811	1.54
12932	819	1.64
13053	827	2.23
13211	835	2.15
13429	843	2.11
13565	848	1.41
13647	851	1.79
14288	859	1.09
14990	867	1.14
15525	875	1.13
15695	880	1.70
15795	883	1.31
16070	891	0.51
16421	899	0.63
16747	906	0.42
16793	907	0.49
17010	912	1.06
17275	920	0.76
17525	928	0.38
17672	936	0.32
17719	944	0.28
17781	952	0.31
17936	960	0.27
18108	968	0.44
18275	976	0.41
18438	984	0.47
18588	992	0.54
18657	1000	0.76
18712	1008	0.86
18795	1016	0.97
18904	1024	1.01
19021	1032	1.27
19067	1035	1.61
19185	1040	5.17
19357	1048	4.14
19465	1053	1.88
19529	1056	2.73

Geophysical Data

TIC (%)
1.03
0.80
1.35
0.98
1.17
1.41
0.64
0.70
0.52
0.48
0.59
0.50
1.03
0.62
0.65
0.57
0.49
0.42
0.56
0.31
0.29
0.30
0.24
0.27
0.25
0.29
0.15
0.13
0.17
0.18
0.28
0.15
0.18
0.18
0.21
0.17
0.18
0.14
0.13
0.14
0.17
0.14
0.12
0.11
0.14

14P Downcore (overlapping with 4P and 46P) Geochemistry a

Age(ya)	Depth (cm)	TIC (%)	TOC (%)
3489	176	0.80	1.41
3614	184	0.97	1.33
3700	192	0.97	1.84
3775	200	1.14	1.68
3897	208	0.46	1.19
4095	216	0.89	1.63
4294	224	1.04	1.60
4493	232	0.63	1.43
4692	240	0.64	1.70
4884	248	0.67	2.02
5018	254	0.68	1.80
5196	262	0.61	1.78
5295	270	0.86	2.50
5345	278	0.61	2.62
5440	286	0.62	2.82
5703	294	0.26	2.89
5981	302	0.18	2.93
6196	310	0.19	3.04
6219	311	0.20	2.57
6395	319	0.33	3.15
6537	327	0.23	2.86
6596	335	0.39	3.77
6652	343	0.19	3.63
6722	351	0.17	4.87
6798	359	0.25	4.17
6861	367	0.18	4.99

0.14
0.13
0.11
0.08
0.17
0.09
0.08
0.14
0.08
0.13
0.15
0.11
0.07
0.08
0.14
0.11
0.07
0.33
0.12
0.07
0.10
0.14
0.12
0.11
0.10
0.11
0.11
0.15
0.15
0.13
0.12
0.13
0.12
0.13
0.17
0.18
0.18
0.19
0.24
0.59
1.06
2.04
1.82
2.74
2.07
2.33
3.47
1.82
2.13

2.07
2.69
2.39
2.45
1.92
2.10
2.46
2.06
2.34
3.62
3.36
3.43
2.75
1.63
2.46
1.73
1.85
2.02
2.16
3.89
1.94
1.71
1.76
2.36
1.96
2.69
2.86
2.64
3.53
1.87
1.71
1.49
1.59
1.47
1.21
1.37
1.43
2.70
2.17
2.61
6.97
3.22

nd Geophysical Data

Appendix C

GDGT and TEX86 data for composite record from 4P, 14P, and 46P

			GDGT-0	GDGT-1	GDGT-2	GDGT-3	CREN	CREN'
sample	Core	age (ya)	m/z 1302	*m/z 1300*	*m/z 1298*	*m/z 1296*	m/z 1292	*m/z 1292'*
3-17	14P	473	1731207	1203097	955853	1043307	15584026	257970
1_2	4P	919	2045237	1438692	1116460	1189260	15945759	296420
1_9	14P	1342	6466660	5004725	4095894	4447584	46743640	1064195
3-5	4P	1350	7578540	4898392	3572037	3545650	48906780	939874
3-7	4P	1592	7646995	4733577	4185857	3883391	48071044	925428
5-1	4P	2000	516012	393376	300284	320393	4593319	96463
3-9	4P	2333	8107146	5261356	4201219	4332121	54796640	1144764
4_14	4P	2445	8720123	6903013	6303926	6194162	56994992	2618350
4_2	4P	2550	14964016	11705773	10335743	10160734	81987992	3717573
3-21	14P	2555	942205	746542	529877	503697	9484675	174121
3-20	4P	2605	5561810	4491779	3414388	3412812	44799116	924595
5-9	14P	2750	582912	590546	481323	370625	5480267	116440
1_3	4P	2898	961034	633665	488968	516947	7142705	115086
3-14	4P	3089	5516969	2515538	2082220	2026325	27514072	520402
3-15	4P	3391	3859182	2262623	2217253	1781311	27878358	541604
1_5	4P	3515	7383912	3822002	3184518	3052097	36721412	850034
3-16	4P	3690	3338863	2110254	1782143	1825133	26742278	548401
3-4	14P	3728	3215815	2624101	1947041	1862706	28637956	580983
4_1	14P	3921	17286096	16585066	15265816	13046207	102285432	5564720
4_9	14P	4318	19496586	19705550	17415594	14924144	113174088	8058398
5-7	14P	4500	713316	636484	464831	443734	6549585	155602
3-18	14P	4767	2668896	2249286	1493490	1592355	25443282	583355
5-3	14P	5100	1103477	889027	724517	599095	9522680	206725
5-6	14P	5500	964534	818899	639715	585877	7507105	184478
3-1	46P	5873	3845856	3752759	2795067	2570213	34354956	937345
3-3	46P	5915	6114913	4730127	3657869	3420567	47333564	1251912
1_4	46P	5969	4892330	4284250	3346628	3171344	40827776	1215686
2-17	46P	6003	8608222	7130251	5343207	5093745	64512660	1834238
1_6	14P	6086	1405205	1123765	919620	941494	12282306	400734
1_8	46P	6088	678632	419973	415228	388901	5762023	151748
2-23	46P	6184	5282683	4967099	3857268	5026961	85174368	3089540
5-8	14P	6400	1976746	1452929	1279178	1066035	14380641	345457
3-8	46P	6542	4360920	3621632	2795665	3142940	44520900	1305563
2-19	46P	6564	9846341	7853692	5763507	5116221	67899680	2279863

2-9	46P	6739	10752999	8739470	6756141	6456823	78253048	2762904
1_10	46P	6842	1584700	1312628	1061424	857276	13375406	419774
3-19	14P	6902	6504648	5234789	3598376	3540625	48015716	1339700
2-8	46P	7102	4508551	3506636	3106254	2614298	37681692	1054586
2-14	46P	7357	12301175	10851226	8812458	7464126	85058040	3068480
2-16	46P	7528	10359867	9691277	7651002	7083042	84478720	3237258
3-22	14P	7537	5157233	3823104	3356320	2968527	42435548	1225570
2-20	46P	8127	14393932	11991790	9567426	8435277	98205600	3831568
2-5	46P	8249	8326620	7398299	5957866	6155531	78561184	2765801
3-12	14P	8409	10369622	8577421	7254935	6465966	77569456	2734446
1_11	46P	8876	2151935	1457796	1377083	1194809	16600013	534283
5-5	46P	8950	1934053	1528323	1344070	1112807	14351852	391484
2-3	46P	9233	16573425	12280462	12601043	10851618	107080200	4151315
2-13	46P	9636	10079706	8840729	6360498	5835501	74088320	2645285
3-13	14P	9792	8257351	6732900	4711079	4994278	65770620	2060444
2-2	46P	10044	11582298	9409735	8456069	7977339	89461552	3905540
4_12	46P	10713	21755828	23192518	20601030	17801362	123137992	9153142
2-11	46P	11046	4956754	4407899	3706532	3811095	46538496	1130134
4_11	46P	11136	6862446	6609972	6270972	5300134	50396092	2253341
1_1	14P	11459	8876132	8083365	7379270	6636780	69621352	2364510
2-7	46P	11766	2658545	2338335	3603192	1717785	30501110	540814
5-4	46P	12000	175442	119056	142538	114033	1734908	37238
4_13	46P	12165	6427171	5093820	4090154	4364912	45445284	1890429
1_7	46P	12282	356364	233555	164491	205314	2578715	42835
2-10	46P	12700	5443509	3284171	2454163	2546607	33285638	581102
3-11	14P	12909	4477685	2722917	2103283	2236301	32326476	683218
3-2	14P	13562	2611245	1498196	1489144	1357974	16439626	300767

V	VI	VII								
m/z 1050	m/z 1036	m/z 1022	Tex 86	T(tex)	BIT-Index	LST (°C, Powers 2005)	LST (°C, Powers et al. 2010)	LST (°C, Tierney et al. 2010-Hot)	LST (°C, Kim et al. 2008)	Kim et al 2010
198656	736687	707346	0.65	23.27	0.10	23.67	22.74	21.86	25.88	25.91
136080	576870	813218	0.64	22.75	0.09	23.17	22.31	21.53	25.41	25.53
692055	2768775	3409778	0.66	23.59	0.13	23.97	23.00	22.06	26.17	26.14
438117	2068965	3098363	0.62	21.37	0.10	21.88	21.19	20.68	24.17	24.49
449982	2268769	3584452	0.66	23.45	0.12	23.83	22.88	21.97	26.04	26.04
			0.65	22.86	0.00	23.28	22.41	21.60	25.51	25.61
584139	2842261	4164124	0.65	22.99	0.12	23.40	22.51	21.68	25.63	25.70
			0.69	25.41		25.68	24.47	23.19	27.80	27.43
			0.67	24.63		24.95	23.84	22.71	27.11	26.89
228038	1174444	1322932	0.62	21.12	0.22	21.65	20.99	20.52	23.95	24.30
662419	2916030	4143339	0.63	22.07	0.15	22.54	21.76	21.11	24.80	25.02
			0.62	21.32	0.00	21.83	21.16	20.65	24.13	24.46
104438	556846	961527	0.64	22.43	0.19	22.87	22.05	21.34	25.12	25.29
588130	3274807	5404242	0.65	22.99	0.25	23.41	22.51	21.69	25.63	25.71
584599	2876812	4323980	0.67	24.21	0.22	24.55	23.50	22.45	26.73	26.59
704192	3435133	4890779	0.65	23.10	0.20	23.51	22.60	21.75	25.73	25.79
468961	2400084	4118698	0.66	23.95	0.21	24.31	23.29	22.28	26.49	26.40
264143	1830279	1728592	0.63	21.62	0.12	22.11	21.40	20.83	24.40	24.68
			0.67	24.46		24.78	23.70	22.60	26.95	26.76
			0.67	24.51		24.83	23.74	22.63	26.99	26.80
			0.63	21.61	0.00	22.10	21.39	20.83	24.39	24.67
196612	1494263	1292998	0.62	21.25	0.10	21.76	21.09	20.60	24.06	24.40
			0.63	22.03	0.00	22.50	21.73	21.09	24.77	24.99
			0.63	22.04	0.00	22.51	21.74	21.09	24.77	25.00
348769	2438464	2217654	0.63	21.67	0.13	22.16	21.44	20.87	24.45	24.72
458983	3372635	2943096	0.64	22.36	0.13	22.81	22.00	21.30	25.07	25.24
416666	3053936	3085585	0.64	22.72	0.14	23.15	22.29	21.52	25.39	25.51
735178	4908562	4797068	0.63	22.03	0.14	22.50	21.73	21.09	24.77	24.99
116528	1046225	1171115	0.67	24.25	0.16	24.59	23.54	22.47	26.77	26.62
59071	470139	536715	0.69	25.92	0.16	26.16	24.89	23.51	28.27	27.78
882728	6961727	7975758	0.71	26.67	0.16	26.87	25.51	23.98	28.94	28.29
			0.65	23.08	0.00	23.49	22.59	21.74	25.71	25.77
483613	3804382	4473107	0.67	24.17	0.16	24.51	23.47	22.42	26.69	26.56
706170	5506622	6031406	0.63	21.64	0.15	22.13	21.41	20.85	24.42	24.70

725326	6179395	6836518	0.65	22.90	0.15	23.32	22.44	21.63	25.55	25.64
119554	927845	1136727	0.64	22.53	0.14	22.97	22.14	21.40	25.22	25.37
419782	3192273	3716558	0.62	21.14	0.13	21.66	21.01	20.54	23.97	24.32
402568	2894658	3086918	0.66	23.68	0.14	24.06	23.07	22.12	26.25	26.21
720094	5617948	7062680	0.64	22.54	0.14	22.98	22.14	21.41	25.22	25.37
860919	6437158	7084095	0.65	23.10	0.15	23.51	22.60	21.76	25.73	25.79
324837	2372234	2565028	0.66	23.99	0.11	24.34	23.32	22.31	26.53	26.43
929258	7319864	8005392	0.65	22.84	0.14	23.26	22.39	21.59	25.50	25.60
874873	6380615	5019605	0.67	24.24	0.14	24.58	23.53	22.46	26.76	26.61
811268	5832726	6396406	0.66	23.58	0.14	23.96	22.99	22.05	26.16	26.14
219599	1750031	2059142	0.68	25.04	0.20	25.33	24.17	22.96	27.47	27.17
			0.65	23.18	0.00	23.58	22.66	21.80	25.80	25.84
1577486	######	12361900	0.69	25.76	0.20	26.01	24.76	23.41	28.12	27.67
749803	6316147	6272748	0.63	21.67	0.15	22.16	21.44	20.86	24.44	24.72
662457	5554795	6262917	0.64	22.25	0.16	22.71	21.91	21.23	24.97	25.16
646948	6203266	5152348	0.68	25.23	0.12	25.51	24.33	23.08	27.64	27.30
			0.67	24.51		24.83	23.75	22.63	27.00	26.80
386062	3081581	3836174	0.66	23.90	0.14	24.26	23.25	22.25	26.45	26.36
			0.68	24.78		25.09	23.97	22.80	27.24	26.99
555272	4328675	5237352	0.67	24.35	0.13	24.68	23.61	22.53	26.85	26.68
650056	2846680	3201532	0.71	27.18	0.18	27.34	25.91	24.29	29.39	28.63
			0.71	26.98	0.00	27.15	25.75	24.16	29.21	28.49
			0.67	24.38		24.71	23.64	22.55	26.88	26.71
31422	195564	298173	0.64	22.41	0.17	22.86	22.04	21.32	25.11	25.28
703581	4124880	5604869	0.63	21.85	0.24	22.33	21.58	20.98	24.60	24.86
908194	2507408	4544416	0.65	23.03	0.20	23.44	22.54	21.71	25.66	25.73
411410	2212852	2486157	0.68	24.85	0.24	25.15	24.02	22.84	27.30	27.04

Appendix D

Composite compound-specific (C28 alkanoic acids) hydrogen and carbon isotope records from 4P, 14P, 46P

Age (ya)	IVC dD C28
473	-81
919	-84
1350	-91
1592	-105
2333	-106
2445	-89
2605	-108
2898	-107
3348	-114
3391	-118
3515	-109
3690	-112
3728	-108
3921	-98
4318	-108
4767	-120
5873	-106
5915	-112
5969	-111
6003	-108
6086	-123
6088	-110
6184	-117
6542	-126
6564	-121
6739	-121
6842	-120
6902	-126
7102	-130
7357	-134
7528	-136
7537	-128
8103	-93
8127	-129
8249	-137
8409	-143
8876	-122
9233	-133
9636	-137
9792	-137

Age (ya)	Methylation Corrected d13C C28
473	-20.1
1350	-20.6
2333	-25.0
2605	-28.6
3515	-27.5
3728	-31.2
5873	-31.7
5915	-32.5
5969	-33.4
6184	-31.8
6542	-29.9
6842	-30.0
7528	-31.9
8127	-30.6
8409	-31.1
9233	-24.8
9233	-32.0
10044	-31.2
11046	-30.9
11459	-31.1
13562	-27.2
13654	-25.0
13761	-25.9
17119	-27.1
19185	-22.6
19550	-24.2

10044	-136
10713	-125
11046	-137
11136	-112
11459	-126
11766	-123
12165	-129
12700	-131
13113	-116
13562	-108
13761	-93
17119	-83
17678	-104
18129	-85
18458	-89
18663	-90
18719	-77
19077	-73
19185	-69
19550	-86
19550	-71

Biographical Data

Name of Author: Amy Jo Morrissey

Place of Birth: Branson, Missouri

Date of Birth: September 22, 1986

Undergraduate schools attended:

- University of Missouri, Columbia, Missouri

Degrees awarded:

- Bachelor of Science, 2009, Geological Sciences, *magna cum laude*, with honors in
- Bachelor of Arts, 2009, Anthropology, *magna cum laude*

Professional experience:

- Teaching and research assistant, Department of Earth Sciences, Syracuse University, 2009–2014
- Geologist Intern, Newfield Exploration Company, Houston, Texas, 2009
- Science Peer Tutor, Success Center, University of Missouri 2008–2009